UNIVERSITÄT BERN

Graduate School for Cellular and Biomedical Sciences

University of Bern

Multimodal MRI of motor impairment and inhibition: Functional connectivity and neurometabolic profiles in spinal cord injury and functional paralysis

PhD Thesis submitted by

Vanessa Vallesi

for the degree of

PhD in Neuroscience

Supervisor
Prof. Dr. Johannes Slotboom
Institute for Diagnostic and Interventional Neuroradiology
Faculty of Medicine of the University of Bern

Co-advisor
Prof. Dr. med. Rajeev Kumar Verma
Swiss Paraplegic Research
Faculty of Health Sciences and Medicine of the University of Lucerne

Accepted by the Faculty of Medicine, the Faculty of Science and the Vetsuisse Faculty of the University of Bern at the request of the Graduate School for Cellular and Biomedical Sciences

Bern, Dean of the Faculty of Medicine

Bern, Dean of the Faculty of Science

Bern, Dean of the Vetsuisse Faculty Bern

This thesis is dedicated to Josh, who left this world on my first day of my PhD journey but stayed with me in every half-formed idea and quiet breakthrough.

Acknowledgements

What a journey. Despite the inevitable challenges of a PhD, I remain deeply grateful for this experience—not just for the science, but for the profound lesson it taught me: we are only as strong as the people around us. Research is never truly solitary; it thrives on mentorship, camaraderie, and the shared pursuit of understanding. To those who shaped this work and my growth, I owe endless thanks:

To Hans (Johannes Slotboom), you are a rare kind of deeply caring, fiercely encouraging mentor, and a spectroscopist with the profoundest knowledge. Thank you for having the patience to introduce me to the spectroscopy universe (it felt that immense to me) and for supporting me through every single difficulty. I am convinced the only reason I finished my PhD was knowing you were at my back. The scientific community needs more Hanses. After this, I wish one day I become a mentor to someone as you were for me.

To my co-advisor Rajeev Verma, you were always here—from the first to the last day of my PhD—even though you did not have to be, even during the busiest days in clinical life, but you still were. Thank you for keeping your calmness and humour through every difficult moment.

To my (unofficial) mentor Andrea Federspiel, I had the honour to learn on Tuesdays from probably the most experienced scientist I have ever met. I wish I could have transferred your almost infinite knowledge to me. Thank you for every single piece of advice.

To Anke Scheel-Sailer, whose extraordinary compassion in patient care and positivity taught me the profound impact of kindness in medicine and research. To Jürg Schwarz, for countless hours spent discussing statistical concepts—you paved the way for my deep fascination with statistics. To Cécile Galléa, to have had the awesome opportunity to spend a year in your research group in Paris, where I grew as a scientist and as a person. To my Post-Doc friends, Samantha Weber and Raphaela Muri, my academic older sisters I look up to. To all my PhD colleagues, especially, Jothini Sritharan, Nga Chau My Ha, Nicola Brunello, Vridhi Rohira, and Thai-Moc Tram Tran who became close friends of mine. I consider myself truly lucky. To my family, especially my older sisters Angela and Marilisa, my friends and my partner Timothy for cheering me on through even the smallest milestones. To the radiology department of the Swiss Paraplegic Centre and to the Swiss Paraplegic Research Institute—thank you for making this possible.

Abstract

Spinal cord injury (SCI) disrupts ascending and descending neural pathways, leading to motor and/or sensory dysfunction, with severity depending on lesion height and extent. In functional paralysis (FP), a subtype of functional neurological disorder, similar symptoms occur without yet detectable structural damage. While SCI primarily disrupts spinal signalling, how its supraspinal effects on motor networks evolve from the subacute to chronic phase remains unclear. In FP, symptom generation is presumed to originate from the brain, as suggested by functional neuroimaging studies, yet the underlying mechanism and the meaning of these brain activity alterations remain debated. Additionally, dysfunctional motor inhibitory control, as evidenced by cognitive studies, may further contribute to FP's pathophysiology.

This thesis investigates functional and metabolic correlates of paralysis in SCI and FP using magnetic resonance-based approaches. First, resting-state functional magnetic resonance imaging (fMRI) was used to compare functional connectivity (FC) and spontaneous activity in subacute vs. chronic SCI and healthy controls (HC). Second, fMRI during a motor-inhibition task was used to assess potential differences in the motor-inhibition network between individuals with FP, SCI and HC. Third, proton magnetic resonance spectroscopy was used to compare metabolic profiles in key FP regions among individuals with FP, SCI and HC.

Individuals with SCI (both in chronic and subacute phase) exhibited reduced FC in the cerebellar vermis IX, right superior frontal gyrus, and right lateral occipital cortex versus HC. Individuals with chronic SCI showed lower FC in bilateral cerebellar crus I, left precentral gyrus, and middle frontal gyrus than individuals with SCI in the subacute phase and HC, suggesting chronic phase adaptation. Altered spontaneous activity in the left thalamus was unique to individuals with subacute SCI, possibly reflecting early reorganisation. During motor inhibition, both FP and SCI groups showed intact behavioural performance but higher FC in the right precentral gyrus and left insula compared to HC, suggesting compensatory plasticity. Metabolically, both individuals with FP and SCI exhibited lower anterior cingulate total N-acetyl-aspartate to total creatine ratios (tNAA/tCr) compared to HC. As lower tNAA is generally considered a marker of reduced neuronal viability, this finding points to neuronal compromise in both conditions. However, tNAA/tCr correlated significantly with motor strength in SCI but not in FP, suggesting that in FP, the reduction in tNAA/tCr may reflect the presence of paralysis itself rather than its severity.

Paralysis alters brain networks, with shared and distinct patterns between SCI phases and between FP and SCI, implying adaptive plasticity. Both conditions showed altered inhibitory network connectivity and reduced anterior cingulate tNAA/tCr, suggesting a relevant contribution of condition-unspecific neural adaptation due to motor dysfunction. Clarifying whether FP-specific functional and metabolic alterations represent mechanistic contributors to symptom generation or reflect non-specific consequences of paralysis will be an important focus for future research.

Table of content

1. Introduction

1.2 Spinal cord injury

1.2.1 Characteristics

Spinal cord injury (SCI) involves damage to the nerve fibres in the spinal cord, resulting from either non-traumatic causes (e.g., tumours or infections) or traumatic causes (e.g., external physical forces such as accidents) (Ahuja et al., 2017). The immediate mechanical damage of traumatic SCI is typically described as the *primary injury*, which may include compression, shearing, or laceration, leading to bleeding from ruptured blood vessels (haemorrhage), swelling (oedema), and acute inflammation (Ahuja et al., 2017; Anjum et al., 2020). Within minutes to hours, this progresses to the delayed cascade of damage, namely the *secondary injury*, where disrupted blood flow (ischemia), excessive glutamate release (excitotoxicity), and calcium overload (mitochondrial dysfunction) collectively drive oxidative stress and apoptosis (programmed cell death) (Crowe et al., 1997; Li & Stys, 2000; Schanne et al., 1979). Over time, cystic cavities form from merged cysts, surrounded by reactive astrocytes, creating a glial scar that inhibits axon regeneration but also isolates the injury site to prevent further damage (Hill et al., 2001; Silva et al., 2014).

Clinically, this manifests as either a complete loss of motor and sensory function below the level of the injury or an incomplete dysfunction, where partial voluntary movement and/or sensation persists (Alizadeh et al., 2019). Secondary complications may include autonomic dysreflexia (in injuries at or above the sixth thoracic vertebra), neurogenic bladder and bowel dysfunction, sexual dysfunction, and pressure sores (Karlsson, 2006). The clinical presentation depends on both the injury level (tetraplegia = cervical; paraplegia = thoracic/lumbar) and its completeness (Karlsson, 2006).

The phases after SCI are continuous and highly variable in terms of recovery. Even though there is no clear cutoff, these categories are often used: acute (first 48 hours), subacute (first 2-14 days) (Witiw & Fehlings, 2015), intermediate (< 6 months), and chronic (> 6 months) (Alizadeh et al., 2019). Rehabilitation outcomes are generally more favourable in incomplete SCI (Waters et al., 1991). Most individuals with SCI experience the greatest recovery within the first 3 months, though some may continue to show improvement for up to 18 months post-injury (Fawcett et al., 2007).

SCI is considered a rare condition, with an annual incidence in Switzerland of 18.0 per million inhabitants, aligning with global estimates from the World Health Organization

(Chamberlain et al., 2015). While exact frequencies vary by country (Barbiellini Amidei et al., 2022; DeVivo, 2012), traumatic SCI occurs more frequently in males (74.5%) than in females (25.6%), with the most common age range at the time of injury being 16–30 years (Chamberlain et al., 2015). The leading causes include falls, sports/leisure activities, and transport-related injuries (Chamberlain et al., 2015).

1.2.2 Neurochemical changes

To investigate tissue degeneration in the spinal cord, in vivo proton magnetic resonance spectroscopy (^{1}H-MRS, see more in chapter 1.4.2) was performed in traumatically injured rats, showing dynamic metabolic changes in the epicentre and adjacent regions. N-acetylaspartate (NAA), a marker of neuronal viability, and total creatine (Cr), reflecting energy metabolism, both showed significant decreases at the lesion epicentre and in both rostral and caudal regions at 14 days post-injury, with these reductions persisting at 56 days after SCI (Qian et al., 2010). In contrast, total choline (Cho) levels, which indicate inflammatory activity, displayed an inverse pattern: Cho concentrations increased during the first 14 days before decreasing by 56 days in both the epicentre and caudal regions, while remaining unchanged in the rostral region throughout the observation period (Qian et al., 2010).

Expanding beyond the spinal cord, Erschbamer et al. (2011) included the brain using the same ^{1}H-MRS method in a rat model. Their results showed opposing trends for the combined glutamate and glutamine signal (Glx), a marker of excitatory neurotransmission: while Glx increased in the spinal cord during the first few days post-injury, it decreased in the cortex. Both changes normalised by 4 months post-injury. In contrast, myo-inositol (mI) levels in the spinal cord increased by approximately one-third after SCI and remained elevated even at 4 months, reflecting astrogliosis, an abnormal proliferation of astrocytes triggered by neuronal damage (Erschbamer et al., 2011).

In humans with chronic SCI, similar patterns were observed, with lower total NAA/mI and Cho/mI ratios found in the spine. Individuals with tetraplegia showed more pronounced reductions than those with paraplegia, and the atrophy, measured as spinal cord area, was associated with these changes (Wyss et al., 2019). Notably, metabolic changes extended beyond the spinal cord, as individuals with cervical myelopathy, a condition

causing motor impairments due to compression of the cervical spinal cord, showed lower NAA/Cr ratios in the motor cortex distal to the lesion site (Kowalczyk et al., 2012).

1.2.3 Structural and functional brain changes

SCI alters the entire motor pathway, including the motor cortex. In individuals with SCI compared to healthy controls (HC), a 30% reduction in the spinal cord area was found, along with smaller white matter volume in the medullary pyramids and left cerebellar peduncles, as well as reduced grey matter volume and cortical thinning in the sensorimotor cortex (Freund et al., 2011). This motor cortex atrophy was associated with a score for motor impairments (Hou et al., 2014). Furthermore, it was shown that individuals with poor recovery after SCI had lower cortical thickness in the right premotor cortex compared to individuals with good recovery (Hou et al., 2016). Individuals with tetraplegia had more pronounced white matter microstructural alterations in the brain, reflected by lower fractional anisotropy and higher radial diffusivity (indicative of demyelination) in the left posterior thalamic radiation compared to individuals with paraplegia (Guo et al., 2019).

Cortical functional reorganisation begins within minutes after SCI, as demonstrated in a rat model where spontaneous cortical activity immediately slowed to a state of slow-wave activity compared to pre-injury levels (Aguilar et al., 2010). After a thoracic SCI in rats resulting in hindlimb paralysis, some of the severed corticospinal neurons sprouted new connections to the forelimb region in the cervical spinal cord. The forelimb sensory map in the cortex expanded into the former hindlimb sensory map, and these rewired neurons became responsive to forelimb stimulation, suggesting functional integration into forelimb circuits (Ghosh et al., 2010). In humans, the synchrony of activity (functional connectivity, see more in chapter 1.4.1) within the sensorimotor cortex was reduced in individuals with SCI compared to HC (Pan et al., 2017). Furthermore, how the motor cortex and premotor cortex show synchrony in terms of activity indicates favourable vs unfavourable recovery after SCI, with greater synchrony associated with better recovery outcomes (Hou et al., 2016).

Beyond the sensorimotor cortex, altered brain activity in SCI also involves regions such as the paracentral lobule, vermis, and right cerebellar hemispheric lobules III–VI, as reported in a meta-analysis by Wang et al. (2019). Meta-regression further showed that more severe and lower-level injuries were associated with stronger cerebellar activation, suggesting compensatory overactivation in response to impaired spinal pathways.

1.3 Functional paralysis

1.3.1 Characteristics

Functional paralysis (FP), a subtype of the broader functional neurological disorder (FND), affects the function of the nervous system while its structure remains intact. Depending on the subtype of FND, symptoms may be motor-related (e.g., paralysis, tremor, gait disorder), sensory-related (e.g., loss of sensation, numbness), or seizure-related (e.g., psychogenic non-epileptic seizures) (Hallett et al., 2022). Previously, FND was termed dissociative (conversion) disorder or hysteria, with the assumption of a solely psychological origin. Although depression, anxiety, and stressful life events are common in FND, they do not predict outcomes or occur more frequently than in other disorders, and many cases lack psychiatric comorbidity entirely (Blanco et al., 2023; Calma et al., 2023; Ludwig et al., 2018; O'Connell et al., 2020). Today, psychological causes such as precipitating stressors are no longer required for an FND diagnosis according to the Diagnostic and Statistical Manual of Mental Disorders, Fifth Edition (DSM-5), though the underlying cause of the disorder remains unknown (Espay et al., 2018; Stone et al., 2014).

FND accounts for ~ 6% of neurology consultations, with high diagnostic reliability (revision rates < 5%) (Carson & Lehn, 2016). Its annual incidence ranges from 10–22/100'000, with prevalence estimates of 80–140/100'000 (Finkelstein et al., 2024). The subtype FP has an annual incidence of 3.9/100'000 (Stone et al., 2010).

In FP, paralysis of specific limbs occurs, clinically resembling SCI but without any detectable structural damage to the brain or spinal cord (Stone & Aybek, 2016). It is one of the most common FND subtypes, occurring in about 20% of cases, similar to functional tremor (Lidstone et al., 2022; O'Connell et al., 2020). FP demonstrates a female predominance, with women affected approximately 2-3 times more frequently than men (typically ~ 70% of cases). The mean age at onset is around 36 years (Lidstone et al., 2022), though FP is also assumed to occur in childhood and adolescence, likely underrepresented in clinical samples (Fang et al., 2021).

The most common onset is sudden (46%), followed by gradual (39%), while symptoms appearing upon waking or after anaesthesia are the least frequent (Stone et al., 2012). The symptoms are often persistent. A 14-year case-control study found that only 20% of the individuals with FP achieved remission, while 31% experienced symptom improvement. However, in the majority of cases (49%), symptoms either remained

unchanged or worsened (Gelauff et al., 2019). Common medical comorbidities in FP include appendectomy, irritable bowel syndrome, and chronic back pain (Stone et al., 2020).

1.3.2 Neural correlates

In FND, the 'software vs. hardware' analogy that is often used to illustrate the condition describes intact brain structure (demonstrated by anatomical MRI scans) while there is a functional disruption ('software bug') (Bègue et al., 2019). This analogy, while useful for patient communication, also mirrors neuroscientific research trends: despite extensive functional magnetic resonance imaging (fMRI, see more in chapter 1.4.1) studies on FND, structural and biochemical research remains underrepresented and often unreplicated.

Some studies report smaller volumes in bilateral basal ganglia and right thalamus in motor FND (Atmaca et al., 2006), while others found increased volumes in supplementary motor area (Kozlowska et al., 2017), premotor cortex (Aybek et al., 2014), and left thalamus (Nicholson et al., 2014), though in these latter studies, none of the volumetric changes correlated with clinical measures. Recent studies found no cortical volumetric differences across FND subtypes (Perez et al., 2017; Sojka et al., 2022; Tomic et al., 2020). White matter microstructural alterations are subtype-specific: while some studies reported microstructural alterations in mixed FND cohorts (Diez et al., 2021), others detected abnormalities exclusively in psychogenic non-epileptic seizures (Hernando et al., 2015; Lee et al., 2015; Sojka et al., 2021).

Glutamatergic dysfunction has been implicated in the motor subtype of FND. A ^{1}H-MRS study by Demartini et al. (2019) reported elevated Glx levels in the anterior cingulate cortex/medial prefrontal cortex. Additionally, the same group later found significantly lower blood levels of glutamate, brain-derived neurotrophic factor, and dopamine in individuals with FND compared to HC (Demartini et al., 2023).

At the initial onset of motor FND, hypometabolism was observed in bilateral frontal regions using ^{18}F-fluorodeoxyglucose positron emission computed tomography, but this normalised by 3 months after onset. Clinical score improvement was associated with hypermetabolism in the prefrontal dorsolateral cortex, right orbitofrontal cortex, and bilateral frontopolar regions. Additionally, onset resting-state metabolism in the right subgenual

anterior cingulate cortex was negatively correlated with motor improvement after 3 months (Conejero et al., 2022).

The meta-analysis on neuroimaging by Boeckle et al. (2016) identified several cortical and subcortical regions as markers for motor FND compared to HC: the primary motor cortex, frontal cortex, anterior and dorsolateral prefrontal cortices, superior temporal lobe, retrosplenial area, red nucleus, amygdala, thalamus, and insula. When comparing affected versus unaffected sides, alterations were observed in the primary somatosensory cortex, frontal cortex, anterior prefrontal cortex, supramarginal gyrus, temporal cortex, dorsal anterior cingulate cortex, and anterior insula. Using classifier approaches on resting-state fMRI results, the most discriminant areas included the sensorimotor cortex, dorsolateral prefrontal cortex, supramarginal and angular gyri, hippocampal regions, cerebellum, as well as cingulate and insular cortex (Waugh et al., 2023; Weber et al., 2022).

In individuals with FP, repetitive transcranial magnetic stimulation applied to the motor cortex increased muscle strength compared to placebo, but no actual motor improvements were observed (Broersma et al., 2015). Using single and paired-pulse transcranial magnetic stimulation, reduced excitability (increased resting motor threshold) and greater inhibition (increased short interval intracortical inhibition) were reported in the affected motor hemisphere compared to the unaffected side, while excitatory circuits (measured as intracortical facilitation) remained normal in both hemispheres, indicating an imbalance of inhibitory circuits (Benussi et al., 2020).

During fMRI of passive hand movement, individuals with FP showed activation in the bilateral inferior frontal gyri, suggesting the involvement of motor inhibition processes, as these regions have been implicated in inhibitory motor control (Hassa et al., 2016). However, in a single-case fMRI study during motor inhibition, aberrant activations during motor preparation of the affected hand were observed (compared to HC) in the left ventromedial prefrontal cortex, left orbitofrontal cortex, and posterior cingulate cortex. Importantly, the inferior frontal gyrus, typically involved in inhibition, was not recruited during motor inhibition, indicating that FP may not be mediated by the typical inhibitory network (Cojan et al., 2009).

1.3.3 Cognitive correlates

Beyond functional brain alterations, emerging evidence suggests possible cognitive deficits in FND, though findings remain inconsistent across studies. In a study analysing a broad range of neurocognitive domains, including information processing speed, attention, and executive functioning (high-level cognitive processes such as planning, inhibition, and cognitive flexibility), individuals with FND showed deficits in all subdomains compared to normative data. However, except for information processing speed and executive functions, their performance was comparable to that of individuals with somatic symptom and related disorders (Vroege et al., 2021). Similarly, children with acute FND showed poorer performance than HC in attention, executive function, and memory domains (Kozlowska et al., 2015).

In FP, attention was thought to be centrally involved in symptom production. In a study of both voluntary (endogenous) and stimulus-driven (exogenous) attention, individuals with FP showed attentional dysfunction not only when using the affected limb but also during verbal responses. This implied that the attentional dysfunction is not purely motoric, suggesting that higher attentional processes interfere with movement preparation (Roelofs et al., 2003). However, attentional processes were also found to improve FP symptoms: individuals with FP had greater difficulty maintaining posture when focused on the task, whereas distraction temporarily normalised balance (Stins et al., 2015). Further, McIntosh et al. (2017) investigated endogenous and exogenous attention across sensory systems (visual and tactile). While participants with FP showed normal attention shifting in the visual task, tactile attention shifting was disrupted only for the affected limb, with the unaffected side remaining intact. This suggests the abnormality may lie not in attention shifting itself but in the consequences of attending to the affected body part.

Comparing individuals with motor FND and 'organic' movement disorders, attention was intact while executive functions showed deficits. This dysfunction was evident as difficulty resolving conflicts between distracting and relevant information (cognitive inhibition tested with a Stroop task) (Huys et al., 2020). Testing executive control, van Wouwe et al. (2020) reported lower performance in individuals with motor FND compared to HC in an action control task and prolonged response times in an action cancellation task, suggesting impaired inhibitory control in FND. Furthermore, studies using go/no-go tasks (with go stimuli leading to behavioural response and no-go stimuli requiring inhibition of that response) to assess motor inhibition suggest a dysfunctional motor inhibitory system that may

contribute to the motor symptoms in FND, as indicated by both lower performance and longer response times in affected individuals, pointing to a broader disruption in cognitive-motor control mechanisms (Hammond-Tooke et al., 2018; Voon et al., 2010).

1.4 Magnetic resonance techniques

Magnetic Resonance (MR) techniques are non-invasive methods that have been used in scientific research for nearly 80 years and in clinical diagnostics for nearly 50 years. These techniques allow in vivo characterisation of tissue anatomy, function, and metabolism in both animals and humans. Data can be acquired in two-dimensional (2D), three-dimensional (3D), or even four-dimensional (4D) formats, where the fourth dimension captures temporal changes such as motion or dynamic processes. The underlying phenomenon is nuclear magnetic resonance (NMR): When biological tissue is placed in a strong static magnetic field (B_0, measured in tesla, T), hydrogen nuclei (or other NMR active nuclei with non-zero spin) align with B_0. By applying a resonant radiofrequency (RF) pulse that generates a B_1 field at the Larmor frequency (which depends on B_0 and the nucleus type) with a certain flip angle (e.g. 90°), the nuclei absorb energy and are tipped away from alignment with B_0 (excitation). After excitation, the nuclei return to equilibrium (relaxation) through two distinct processes: T_1 (longitudinal) and T_2/T_2^* (transverse, where T_2^* includes local tissue dependent B_0 field inhomogeneities) relaxation, each with characteristic time constants (T_1, T_2) determined by the local molecular environment (e.g., tissue type, chemical composition) (Gazzaniga et al., 2014; Yousaf et al., 2018). Higher B_0 increases the signal-to-noise ratio (SNR), which can be leveraged to achieve finer spatial resolution for a given scan duration (see Figure 1) (Boulant et al., 2024).

Most clinical MR scanners detect signals from hydrogen nuclei (^{1}H) in water and fat molecules, as they are abundant in biological tissues. Differences in relaxation times (T_1/T_2) and proton density between tissues generate contrast in MR images, while variations in resonant frequencies (chemical shifts) allow the discrimination of metabolites in MR spectra (see chapter 1.4.2) (Gazzaniga et al., 2014; Yousaf et al., 2018).

Figure 1. Signal-to-noise and resolution scaling with field strength

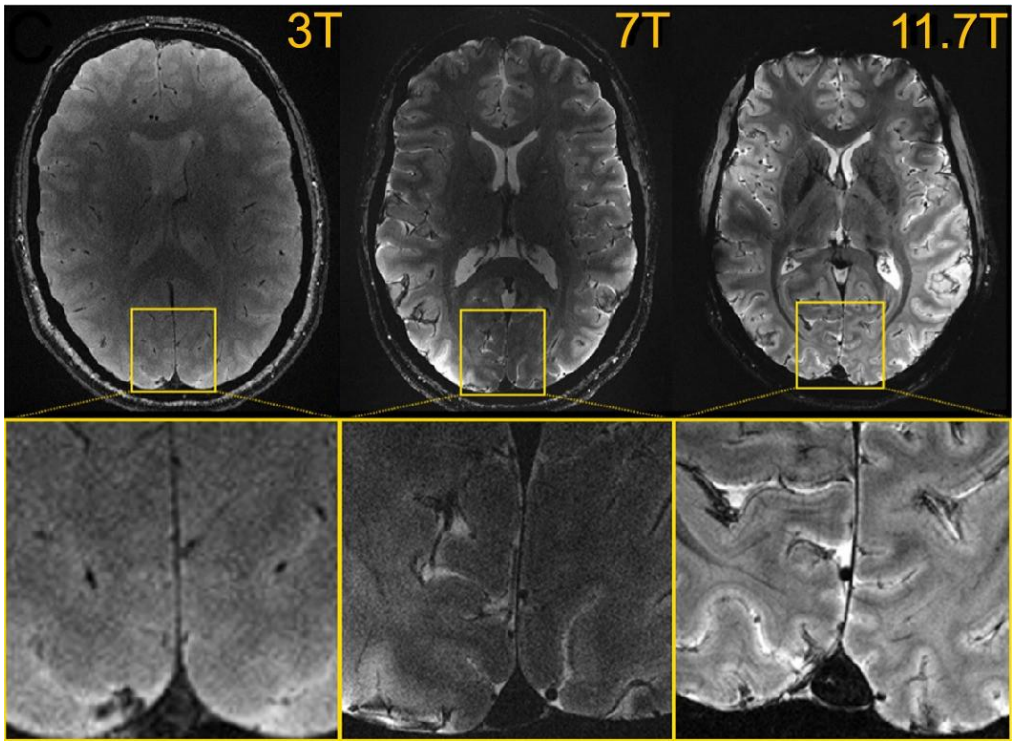

Note: Axial T_2*-weighted images of the human brain acquired with identical scan times (4 min 17 s) at 3 T (left), 7 T (middle), and 11.7 T (right). Contrast-to-noise ratio was maintained across field strengths by adjusting acquisition parameters. Adapted from Boulant et al. (2024).

1.4.1 Functional magnetic resonance imaging (fMRI)

Deoxygenated haemoglobin is paramagnetic due to its unpaired electrons around the exposed iron atom, whereas oxygenated haemoglobin is diamagnetic. This difference in magnetic properties was demonstrated by Ogawa et al. (1990), leading to the definition of blood oxygen level-dependent (BOLD) contrast (see Figure 2). The presence of deoxyhaemoglobin creates local magnetic field inhomogeneities, which reduces the T_2* relaxation time by dephasing spinning protons. Because T_2*-weighted imaging is sensitive to these inhomogeneities, it allows changes in blood oxygenation levels to become visible. Since increased neural activity is typically coupled with elevated blood flow and oxygenation (neurovascular coupling), the BOLD signal serves as an indirect marker for brain activity (Iadecola, 2017). Building upon this principle, fMRI measures BOLD signal fluctuations over time to localize active brain regions. And with this, a revolution in cognitive neuroscience

began, as this technique allows for the non-invasive investigation of the human mind (Gazzaniga et al., 2014; Logothetis & Wandell, 2004).

Figure 2. Contrast depended on the blood oxygen level

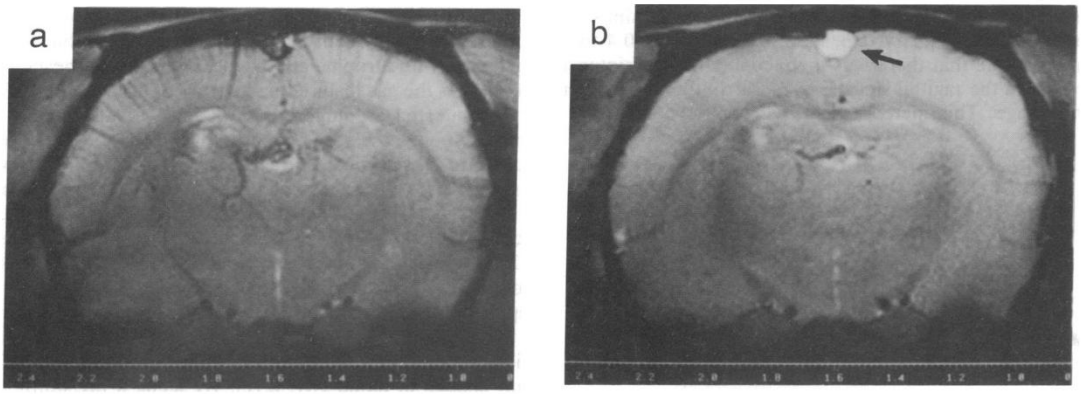

Note: (a) shows the brain of an anaesthetised rat breathing air with 21% oxygen (normal atmospheric composition), and (b) shows the same rat after increasing the inspired oxygen to 90%. When oxygen levels are increased, the venous system becomes less visible. This is because image contrast in T_2*-weighted imaging depends on the amount of deoxygenated haemoglobin in the blood. Adapted from Ogawa et al. (1990).

However, it is important to keep in mind that the BOLD signal reflects metabolic and vascular changes, rather than the firing of neurons (spiking). It correlates more reliably with local field potentials (LFPs), which represent synaptic input and intracortical processing, than with action potentials from individual neurons. As a result, BOLD signals can appear in brain regions where no neuronal spiking occurs, reflecting passive input or inhibitory processes rather than active output (Logothetis, 2012). These metabolic changes arise from the energy demands of neural processing, which involves both excitation and inhibition (Moon et al., 2021). The relationship between BOLD signals and underlying neuronal activity is therefore complex and not yet fully understood.

The hemodynamic response, and consequently the BOLD signal, evolves over seconds (see Figure 3), whereas neuronal activity occurs within milliseconds (Gazzaniga et al., 2014; West et al., 2019). The BOLD signal follows a characteristic hemodynamic response function: after stimulus onset, it rises to a peak at around 5 seconds, then slowly

returns to baseline, often with a post-stimulus undershoot. Experimental paradigms in fMRI are tailored to capture the hemodynamic response effectively. In task-based fMRI, two common experimental designs are used: block design, where conditions are alternated in blocks of several seconds (e.g. task vs. control), and event-related design, typically applied in more complex paradigms (e.g. decision making), where individual trials of task and control conditions are presented in a randomised order. In the latter, the BOLD response is time-locked to specific events, such as stimulus onset or movement initiation (Huettel, 2012). In resting-state fMRI, spontaneous fluctuations of the BOLD signal are recorded over time in the absence of a task (Biswal et al., 1995). Altered connectivity patterns in these networks are observed in many neurological and psychiatric disorders (Fox & Greicius, 2010).

Figure 3. Time course of the BOLD signal

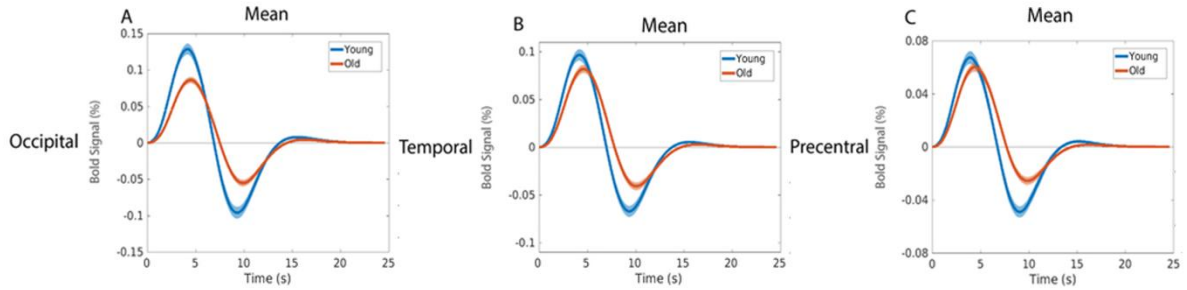

Note: Mean blood oxygen level-dependent (BOLD) signal time courses across three brain regions (A–C) in younger and older individuals. The peak response typically occurs around 5 seconds post-stimulus onset but varies by brain region and age group. Adapted from West et al. (2019). With permission from Elsevier.

The human cortex contains approximately 10 billion neurons and 10 trillion synaptic connections. To study their dynamic interactions, we must move beyond single-cell methods and employ techniques that capture population-level co-activation patterns (Logothetis, 2012). For enable this, functional connectivity (FC) was introduced, which refers to the temporal correlation of the BOLD signal in spatially separated brain areas, where no directionality or structural connection is implicated. FC is particularly useful for identifying large-scale brain networks, comparing group-level differences (e.g., patients vs. controls), and exploring the brain's intrinsic functional architecture in both task-based and resting-state fMRI (Friston, 2011).

1.4.2 Proton magnetic resonance spectroscopy (^{1}H-MRS)

Even though NMR-active nuclei respond principally to the forces of B_0 and B_1, their local molecular environment affects how they resonate: Electrons circulate around the nucleus, and depending on their density, a local electron-induced field is created that opposes B_0, reducing the net magnetic field at the nucleus and making it resonate at a lower frequency (shielding). In the unshielded case, the electron-induced field fails to oppose B_0 (due to low electron density) or reinforces it (due to paramagnetic or anisotropic effects), making the nucleus resonate at a higher frequency. The molecular structure and neighbouring atoms change how the same nucleus (e.g., ^{1}H) resonates, giving each metabolite its characteristic frequency. This phenomenon is called chemical shift, and it is the basis of MRS. Since absolute frequencies in Hz depend on the field strength, they are usually expressed as relative units in parts per million (ppm), with water as the reference point. This convention is most widely used in ^{1}H-MRS, which is the most common MRS modality, due to the high natural abundance and strong NMR signal of ^{1}H compared to other nuclei (e.g., ^{31}P, ^{13}C). The peaks in the spectra are termed resonances, which may split into doublets or multiplets due to interactions with neighbouring nuclei (J-coupling). The concentration of metabolites is calculated from the area under the curve, and ratios with Cr are typically reported for reproducible quantification, as Cr is assumed to remain stable (Arnold et al., 1951; Grover et al., 2015; Hahn & Maxwell, 1952; Proctor & Yu, 1950).

These are the 6 most abundantly present metabolites in the brain spectrum at field strengths of ≤ 3 T (see Figure 4):

N-Acetylaspartate (NAA) is one of the most abundant metabolites in the brain, with a major resonance at ~ 2.01 ppm. NAA is considered a marker of neuronal integrity and function, involved in myelin lipid synthesis, osmoregulation, and mitochondrial metabolism. It is degraded in oligodendrocytes by the enzyme aspartoacylase, yielding acetate and aspartate. Chemically, NAA is an N-acetylated derivative of aspartic acid (Moffett et al., 2007; Shannon et al., 2016; Zheng et al., 2025). Reduced NAA levels are indicative of neuronal loss or dysfunction and are observed in conditions such as multiple sclerosis, brain tumours, and neurodegenerative disorders (De Stefano & Filippi, 2007; Murray et al., 2014; Pedrosa De Barros et al., 2016).

Choline (Cho) resonance in vivo appears around 3.2 ppm and represents a combination of choline-containing compounds: primarily free choline (a precursor for

phospholipid metabolism), phosphocholine (involved in membrane synthesis), and glycerophosphocholine (a breakdown product of phospholipid degradation). Because membrane turnover increases in pathological states involving inflammation or rapid cell proliferation, Cho is considered a marker of cellular membrane dynamics, with elevated levels observed in brain tumours, demyelination (e.g., multiple sclerosis), and gliosis (Horská & Barker, 2010). Conversely, decreased Cho levels may occur in neurodegenerative disorders (Guo et al., 2017).

Creatine components (Cr) peak in vivo appears at 3.0 ppm, with a smaller resonance at 3.9 ppm. These resonances belong to Cr, an essential molecule for biological energy storage and transfer, and phosphocreatine (PCr), a high-energy phosphate reservoir used in adenosine triphosphate (ATP) regeneration. Since total creatine (Cr + PCr) is relatively stable in the brain under normal conditions, it is often used as an internal reference for metabolite quantification in ^{1}H-MRS (Yazigi Solis et al., 2014). However, altered creatine levels can be observed in certain pathological conditions, such as creatine deficiency syndromes, brain tumours, and neurodegenerative diseases (Mercimek-Andrews & Salomons, 2022).

Glutamate (Glu) and glutamine (Gln) have multiple resonances between 2.1–2.5 ppm and 2.1–2.6 ppm. Due to overlapping resonance patterns, Glu and Gln are often reported as a combined peak (Glx), especially at field strengths ≤ 3 T, where spectral resolution is limited. Glu is the primary excitatory neurotransmitter playing a crucial role in synaptic transmission, plasticity, and metabolism. Gln serves as a precursor and regulator of glutamate metabolism within the glutamate-glutamine cycle. Elevated Glx levels are associated with excitotoxicity in conditions like epilepsy, while decreased levels can be seen in some neurodegenerative diseases (Ramadan et al., 2013; Sarlo & Holton, 2021).

Myo-inositol (mI) appears at 3.5–3.6 ppm and serves as a glial and neuroinflammation marker, primarily found in astrocytes. It plays a crucial role in osmoregulation (maintaining cellular fluid balance), phospholipid metabolism, and second messenger systems. Increased mI levels are associated with astrocytosis and gliosis, processes where glial cells (mainly astrocytes) proliferate in response to neural damage. Elevated levels are found in neuroinflammatory conditions such as multiple sclerosis (Haris et al., 2011), while reduced levels are seen in hypo-osmolar states and certain psychiatric disorders (Coupland et al., 2005).

Figure 4. Example ^{1}H magnetic resonance spectra

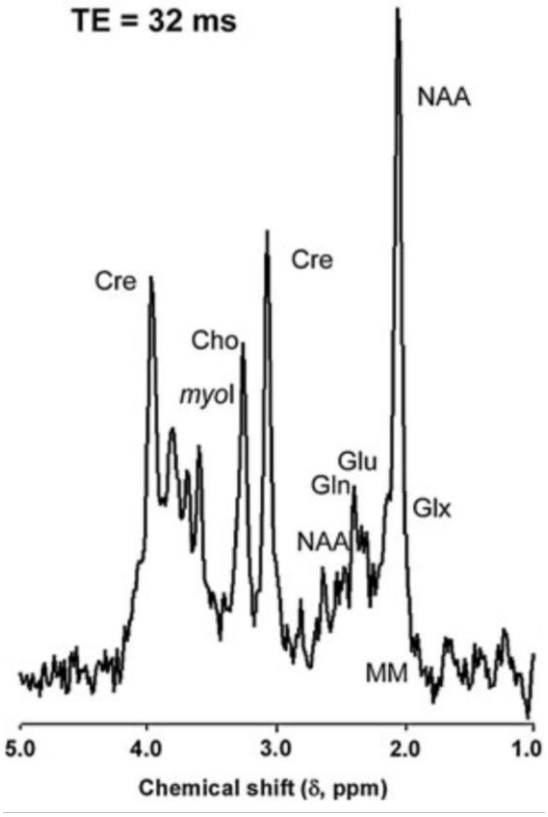

Note: A ^{1}H-MR spectrum from the human brain shown in parts per million (ppm) at echo time (TE) = 32 ms using a point-resolved spectroscopy (PRESS) sequence at a field strength of 3 T. Abbreviations: NAA, N-acetylaspartate; Cre, creatine; Cho, choline; myoI, myo-inositol; Glu, glutamate; Gln, glutamine; Glx, combined glutamate + glutamine; MM, macromolecules. Adapted from Rae (2014). With permission from Springer Nature.

There are several key difficulties in interpreting metabolites in MRS. Resonance frequency overcrowding, where peaks overlap due to low field strength and poor spectral resolution, makes signal separation challenging, but manageable using prior knowledge based fitting strategies (Slotboom et al., 1998). Although metabolites act as markers for biochemical processes, most are involved in multiple pathways, complicating their clinical or functional interpretation. Furthermore, the relationship between metabolite concentrations and specific pathological or physiological states remains poorly understood for many compounds, limiting diagnostic certainty (Rae, 2014).

1.5 Research aims and hypotheses

The overall goal of this thesis is to describe how paralysis alters brain function and metabolism, focusing on two approaches:

1. Mapping brain reorganisation patterns in SCI across subacute and chronic phases.
2. Comparing SCI and FP — two conditions that share paralysis as the main symptom but differ in aetiology — to disentangle brain changes related to the symptom of paralysis itself (i.e., loss of voluntary movement) from those specific to the underlying condition.

Study 1: Brain reorganisation after SCI

The aim of this study is to determine how paralysis alters spontaneous neuronal activity and functional connectivity in subacute vs. chronic SCI. The assumptions are that individuals with subacute SCI exhibit aberrant spontaneous neuronal activity, reflecting early neuroplasticity. Individuals with chronic SCI show consolidated reorganisation with altered brain connectivity patterns, indicating long-term adaptation.

Study 2: The role of motor inhibition in FP

This study aims to test whether FP-specific symptoms are driven by impaired motor inhibitory processes, distinct from SCI-related paralysis. It is assumed that individuals with FP show behavioural deficits in motor inhibition and altered connectivity within inhibitory networks.

Study 3: Metabolic profile in FP

The goal is to identify whether FP is associated with altered metabolic profiles in brain regions involved in symptom generation. The hypothesis of this study is that individuals with FP exhibit distinct metabolite patterns, differentiating them from individuals with SCI and HC.

2. Empirical studies

2.2 Brain reorganisation after spinal cord injury

Functional connectivity and amplitude of low-frequency fluctuations changes in people with complete subacute and chronic spinal cord injury

Vallesi, V., Richter, J. K., Hunkeler, N., Abramovic, M., Hashagen, C., Christiaanse, E., Shetty, G., Verma, R. K., Berger, M., Frotzler, A., Eisenlohr, H., Eriks-Hoogland, I., Scheel-Sailer, A., Michels, L., Wyss, P. O.

Contribution:

I performed data analysis, figure design, data interpretation, manuscript drafting, and revision.

Published in Scientific Reports (2022): https://doi.org/10.1038/s41598-022-25345-5

Functional connectivity and amplitude of low-frequency fluctuations changes in people with complete subacute and chronic spinal cord injury

Authors:

Vanessa Vallesi[1], Johannes K. Richter[1,2], Nadine Hunkeler[1], Mihael Abramovic[1], Claus Hashagen[1], Ernst Christiaanse[1,3], Ganesh Shetty[1], Rajeev K. Verma[1], Markus Berger[1], Angela Frotzler[4,5], Heidrun Eisenlohr[1], Inge Eriks Hoogland[6], Anke Scheel-Sailer[7], Lars Michels[8,9], Patrik O. Wyss[1 *]

[1] Department of Radiology, Swiss Paraplegic Centre, Nottwil, Switzerland

[2] Department of Diagnostic, Interventional, and Pediatric Radiology, University Hospital of Bern, Inselspital, University of Bern, Bern, Switzerland

[3] Division Imaging and Oncology, Image Sciences Institute, University Medical Center Utrecht, Utrecht, the Netherlands

[4] Digital Trial Intervention Platform, ETH Zurich, Zurich, Switzerland

[5] Clinical Trial Unit, Swiss Paraplegic Centre, Nottwil, Switzerland

[6] Outpatient Care Unit, Swiss Paraplegic Centre, Nottwil, Switzerland

[7] Department of Paraplegia, Rehabilitation and Quality Management, Swiss Paraplegic Centre, Nottwil, Switzerland

[8] Department of Neuroradiology, University Hospital Zurich, Zurich, Switzerland

[9] Neuroscience Center Zurich, University of Zurich and Swiss Federal Institute of Technology Zurich, Zurich, Switzerland

Corresponding author:

Patrik O. Wyss, PhD
Swiss Paraplegic Centre,
Department of Radiology
Guido A. Zaech – Strasse 1
CH-6207 Nottwil

Switzerland
E-Mail: wyssp.sci@gmail.com

Abstract

After spinal cord injury (SCI), reorganization processes and changes in brain connectivity occur. Besides the sensorimotor cortex, the subcortical areas are strongly involved in motion and executive control. This exploratory study focusses on the cerebellum and vermis. Resting-state functional magnetic resonance imaging (fMRI) was performed. Between-group differences were computed using analysis of covariance and post-hoc tests for the seed-based connectivity measure with vermis and cerebellum as regions of interest. Twenty participants with complete SCI (five subacute SCI, 15 with chronic SCI) and 14 healthy controls (HC) were included. Functional connectivity (FC) was lower in all subjects with SCI compared with HC in vermis IX, right superior frontal gyrus (p_{FDR} = 0.008) and right lateral occipital cortex (p_{FDR} = 0.036). In addition, functional connectivity was lower in participants with chronic SCI compared with subacute SCI in bilateral cerebellar crus I, left precentral- and middle frontal gyrus (p_{FDR} = 0.001). Furthermore, higher amplitude of low-frequency fluctuations (ALFF) was found in the left thalamus in individuals with subacute SCI (p_{FDR} = 0.002). Reduced FC in SCI indicates adaptation with associated deficit in sensory and motor function. The increased ALFF in subacute SCI might reflect reorganization processes in the subacute phase.

Introduction

In spinal cord injury (SCI), the afferent and efferent pathways in the spinal cord are damaged, resulting in long-lasting impairment of motor and sensory function[1]. Nonetheless, neuronal plasticity takes place in the spinal cord, which is a prerequisite for rehabilitation[2,3]. However, there is less known about the neuronal reorganization occurring in the brain and the extent to which this can be detected using neuroimaging methods.

In a resting-state fMRI study, altered local BOLD-signal correlation (regional homogeneity) in the sensorimotor regions, thalamus and cerebellum in acute SCI of maximal 30 days after onset was found[4]. These restructuring processes are also evident in functional

connectivity (FC), namely the reduced covariance of the BOLD time series between primary and secondary somatosensory cortex in monkeys following SCI[5].

Other connectivity measures such as the analysis of the amplitude of low-frequency fluctuations (ALFF), revealed alterations in complete SCI as reduced ALFF in the right lingual gyrus but increased ALFF in the right frontal gyrus[6]. This is also shown in the relative measurement of ALFF, namely fractional amplitude of low-frequency fluctuations (fALFF), where low fALFF was found in complete and incomplete SCI in superior medial frontal gyrus and higher fALFF in putamen and thalamus, which was negatively correlated with motor and sensory function[7]. The described changes might be different due to lesion characteristic, but also related to patient characteristics and therapeutic interventions[7]. Graph theory-based connectome analyses indicated decreased betweenness centrality in the left precentral gyrus, right caudal middle frontal gyrus and left transverse temporal gyrus in SCI[8].

There are major differences in reorganization between humans with complete and incomplete disruption of the nerve signal from the corticospinal tract. In humans with SCI, lower FC has been reported in resting-state networks (salience, dorsal-attention, sensorimotor and default-mode networks) comparing in complete SCI to incomplete SCI[9]. Brain connectivity was lower in complete SCI than in incomplete SCI, and therefore the focus of this study was to investigate exclusively complete SCI.

In previous FC studies in SCI, the majority of the focus was on sensorimotor cortex[9–11]. Beside this area, however, the anterior and posterior portions of the cerebellum are also involved in motion and body representation[12,13], making it relevant for SCI. Moreover, recent studies emphasize the role of the cerebellum in executive control[14,15]. The cerebellar vermis, located between the two cerebellar hemispheres, has structural connections to motor areas. Using transneuronal tracers, a large number of neurons projecting from the motor cortex to the vermis were identified[16]. In addition to local proximity, strong relationship has been demonstrated between the vermis and cerebellum[16]. SCI induced in rats indicated cellular-level alterations in cerebellar circuits[17].

Accordingly, in the case of deficits in somatosensory and motor activity, a series of reorganization processes is assumed to take place in the subcortical regions after a complete SCI, assuming that a longer duration of the SCI should result in a lower FC. In this study, we examined FC in the vermis and cerebellum in complete SCI. Our working hypothesis presumed that the functional connectivity is lower in complete SCI representing altered

connectivity and is distinct between the subacute and chronic phase. The aim of this study is to clarify, first, brain connectivity and whether it is affected by the disruption of neural information from the lower limbs, and second, whether these impacts differ in the subacute compared to chronic phase after spinal cord injury.

Results

Demographics

A total of 36 subjects were recruited for the study at the outpatient clinics of our institution. All participants completed the MRI measurement and clinical assessments. Due to too high values in the Hospital Anxiety and Depression Scale (HADS) (≥ 7 score) indicating comorbidity of depression, two subjects had to be excluded in order to prevent the possible influence of depressive mood on resting state fMRI data. Thus, the final study sample consisted of 34 participants, 15 persons with chronic SCI (13 males, mean age = 53.5 ± 11.3 years, mean time since injury = 21.9 ± 13.6 years), 5 with subacute SCI (2 males, mean age = 39.4 ± 5.55 years, mean time since injury = 12.2 ± 4.8 weeks) and 14 HC (8 males, mean age = 41.2 ± 14.8 years) (see Table 1 for details of the SCI participants). The original target subsample of 15 participants with subacute SCI was not achieved due to recruitment difficulties. However, the total sample actually achieved is comparable to previous studies on SCI[9,18]. To determine whether there is a significant relationship between groups and sex, Fisher's exact test was used. There was no statistically significant association between the groups and sex (two-sided $p = 0.08$). However, the Kruskal–Wallis test showed that there is a statistically significant difference between the groups and age ($\chi^2_{(2)} = 7.29$, $p = 0.03$). Therefore, age was included as a covariate in all further analyses. The Kruskal–Wallis test examining the influence of motion showed that the three groups did not move on average differently during the fMRI scan. ($\chi^2_{(2)} = 0.177$, $p = 0.92$).

Table 1

Demographics for spinal cord injury participants

Subject	Sub-group	Sex	Age (in years)	Handedness	TSI (in years)	NLI	NP
1	cSCI	m	59	right	34.89	Th4	Yes[1]
2	cSCI	m	57	right	36.87	Th4	No
3	cSCI	m	49	right	15.55	Th6	Yes [1]
4	cSCI	m	31	left	4.91	Th6	No
5	cSCI	m	35	right	12.79	Th6	Yes[2]
6	cSCI	m	65	left	11.89	Th10	No
7	cSCI	m	57	right	8.65	Th9	Yes [1]
8	cSCI	f	62	right	22.91	Th2	No
9	cSCI	m	41	right	11.39	Th10	No
10	cSCI	m	57	right	50.26	Th3	No
11	cSCI	m	66	right	35.16	Th3	No
12	cSCI	f	45	right	37.19	Th5	No
13	cSCI	m	50	right	18.97	Th4	No
14	cSCI	m	62	right	19.28	Th6	No
15	cSCI	m	67	right	8.50	Th11	No
16	sSCI	f	42	right	0.35	Th10	No
17	sSCI	m	46	right	0.24	Th6	No
18	sSCI	m	38	left	0.31	Th11	No
19	sSCI	f	31	right	0.14	Th3	No
20	sSCI	f	40	left	0.16	Th4	Yes [1]

Note. [1]at neurological level, [2]below neurological level

cSCI: chronic SCI; NLI: Neurological Level of Injury; NP: Neuropathic pain; sSCI: subacute SCI; SCI: Spinal Cord Injury; TSI: Time since injury

Connectivity analyses.

The results of the seed-based FC analysis of covariance (ANCOVA) with age as covariate showed that there was a significant difference between HC vs. cSCI vs. sSCI with the seed vermis IX to the right superior frontal gyrus ($F_{(1, 31)} = 28.77$, $p_{FDR} = 0.008$, $\eta 2 = 0.48$, cluster size = 103 voxels) and to the right lateral occipital cortex ($F_{(1, 31)} = 25.07$, $p_{FDR} = 0.036$, $\eta 2 = 0.45$, cluster size = 73 voxels) as shown in Fig. 1. The Bonferroni post-hoc test revealed that cSCI have significant lower resting state FC compared to HC in both clusters (cluster 1: $t_{(1, 31)} = 6.56$, $p_{adj.} < 0.001$, 95% CI [0.18, 0.29]) (cluster 2: $t_{(1, 31)} = 4.03$, $p_{adj.} = 0.001$, 95% CI [0.15, 0.26]). There was also a significant difference between sSCI and HC (cluster 1: $t_{(1, 31)} = 4.81$, $p_{adj.} < 0.001$, 95% CI [0.17, 0.26]) (cluster 2: $t_{(1, 31)} = 4.38$, $p_{adj.} < 0.001$, 95% CI [0.19, 0.37]). The other vermis substructures were not significant regarding the FC in HC vs. cSCI vs. sSCI.

Figure 1

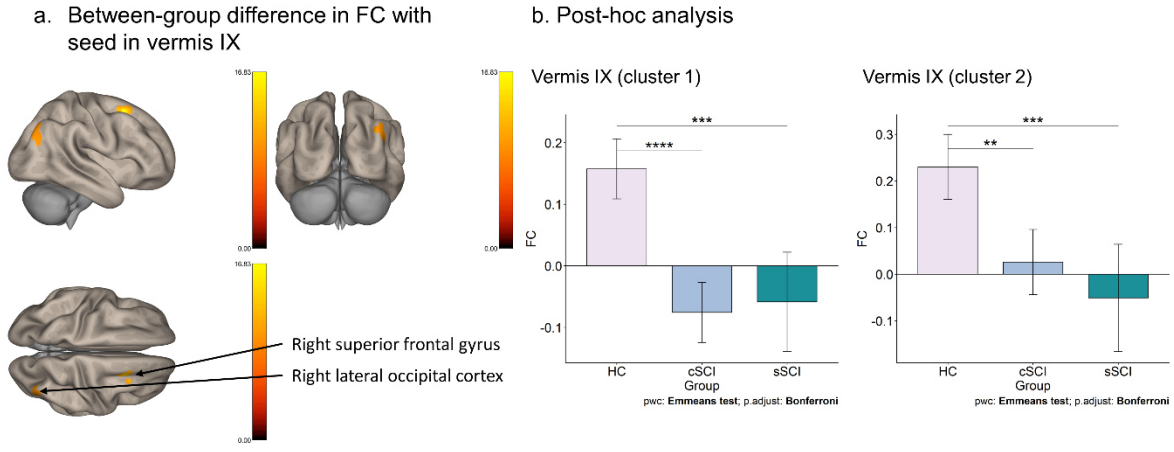

Functional connectivity group differences in the vermis. (**a**) The significant group differences of the functional connectivity (FC) in vermis IX between HC, cSCI and sSCI are shown ($p_{FDR} < 0.05$). (**b**) Estimated marginal mean (Emmean) FC is shown on the y-axis for the different groups on the x-axis for cluster 1 (right superior frontal gyrus) and cluster 2 (right lateral occipital cortex). All comparisons are Bonferroni corrected. Cluster 1: HC (Emmean

= 0.16; Standard Error (SE) = 0.02); cSCI (Emmean = −0.08; SE = 0.02); sSCI (Emmean = −0.06; SE = 0.04). Cluster 2: HC (Emmean = 0.23; SE = 0.03); cSCI (Emmean = 0.03; SE = 0.03); sSCI (Emmean = −0.05, SE = 0.06). ** $p < 0.01$, *** $p < 0.001$, **** $p < 0.0001$.

Furthermore, there was a significant group means difference of FC in the cerebellum crus I left ($F_{(1, 31)} = 10.11$, $p_{FDR} = 0.001$, $\eta^2 = 0.25$, cluster size = 82 voxels and 65 voxels, resp.) and right ($F_{(1, 31)} = 7.08$, $p_{FDR} = 0.001$, $\eta^2 = 0.19$, cluster size = 82 voxels and 65 voxels, resp.) to the left precentral gyrus and the left middle frontal gyrus (see Fig. 2).

Figure 2

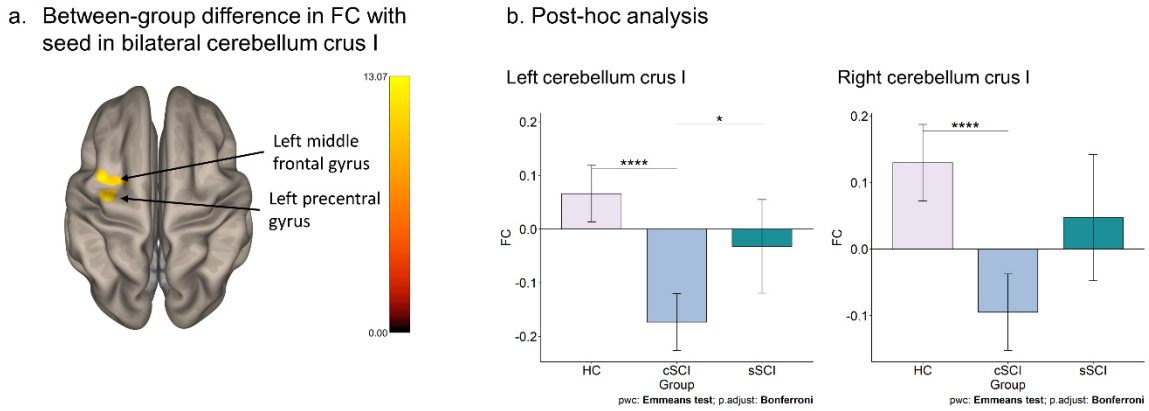

Functional connectivity group differences in the vermis. (**a**) The significant group differences of the functional connectivity (FC) in vermis IX between HC, cSCI and sSCI are shown ($p_{FDR} < 0.05$). (**b**) Estimated marginal mean (Emmean) FC is shown on the y-axis for the different groups on the x-axis for cluster 1 (right superior frontal gyrus) and cluster 2 (right lateral occipital cortex). All comparisons are Bonferroni corrected. Cluster 1: HC (Emmean = 0.16; Standard Error (SE) = 0.02); cSCI (Emmean = −0.08; SE = 0.02); sSCI (Emmean = −0.06; SE = 0.04). Cluster 2: HC (Emmean = 0.23; SE = 0.03); cSCI (Emmean = 0.03; SE = 0.03); sSCI (Emmean = −0.05, SE = 0.06). ** $p < 0.01$, *** $p < 0.001$, **** $p < 0.0001$.

In the left cerebellum crus I, the post-hoc test showed that cSCI differed significantly from HC ($t_{(1, 31)} = 6.23$, $p_{adj.} < 0.001$, 95% CI [0.18, 0.30]) and from sSCI ($t_{(1, 31)} = -2.73$, $p_{adj.} = 0.032$, 95% CI [−0.10, −0.18]). The cSCI group showed lower resting-state FC compared to HC and sSCI. In the right cerebellum crus I, FC in the cSCI was significantly different to HC ($t_{(1, 31)} = 5.38$, $p_{adj.} < 0.001$, 95% CI [0.17, 0.28]), but not to sSCI ($t_{(1, 31)} = 1.56$, $p_{adj.} = 0.386$). There was no significant difference between sSCI and HC ($t_{(1, 31)} = -2.53$, $p_{adj.} = 0.051$). No other cerebellar substructures differed within the three groups regarding FC.

The voxel-based morphological analysis did not reveal any differences in the grey matter volume (GMV) for any of the three ROIs with significant group FC differences (vermis IX: $F_{(2, 31)} = 0.094$, $p = 0.91$; left cerebellum crus I: $F_{(2, 31)} = 0.346$, $p = 0.710$; right cerebellum crus I: $F_{(2, 31)} = 0.295$, $p = 0.747$).

The results of the ANCOVA with the ALFF values revealed significant differences in the left thalamus ($F_{(1, 31)} = 9.04$, $p_{FDR} = 0.002$, $\eta^2 = 0.23$, cluster size = 41 voxels) between sSCI and HC ($t_{(1, 31)} = -4.84$, $p_{adj.} < 0.001$, 95% CI [−0.16, −0.32]) as well as sSCI and cSCI ($t_{(1, 31)} = -5.35$, $p_{adj.} < 0.001$, 95% CI [−0.20, −0.37]) (see Fig. 3).

Figure 3

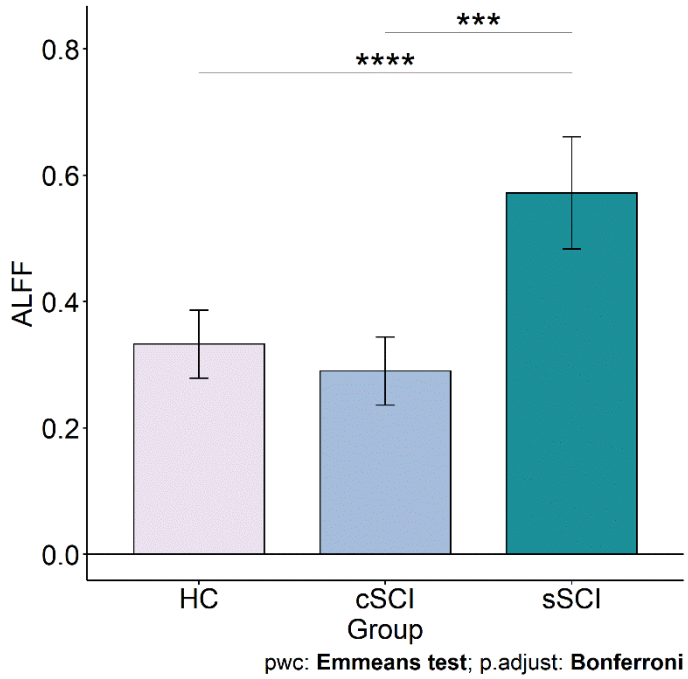

Group differences in the amplitude of low-frequency fluctuations (ALFF). Estimated marginal mean (Emmean) ALFF is shown on the y-axis for the groups on the x-axis. All comparisons are Bonferroni corrected. HC (Emmean = 0.33; Standard Error (SE) = 0.03); cSCI (Emmean = 0.29; SE = 0.03); sSCI (Emmean = 0.57; SE = 0.04). *** $p < 0.001$, **** $p < 0.0001$.

Discussion

In this study, a resting-state fMRI was conducted in participants with complete subacute and chronic SCI and HC at 3 T. Significant differences were found in several brain connectivity analyses between SCI and HC as well as between sSCI and cSCI.

The two SCI groups showed lowered FC compared to HC in vermis IX (uvula of vermis), superior frontal gyrus right and lateral occipital cortex. This specific vermis structure might be relevant for SCI since both SCI subgroups have lower FC than healthy controls. However, in the FC of bilateral cerebellum crus I, the left precentral gyrus and the left middle frontal gyrus, sSCI and HC were found to have a similar level of FC whereas cSCI showed a lower FC. These findings may indicate functional reorganization in SCI in the chronic phase. Differences in FC were found between cSCI and sSCI, which might be due to the state. In previous resting-state fMRI studies, reduced FC was also found in SCI, but so far only with the seed regions in the sensorimotor areas. Decreased FC was found in the primary motor and primary sensory areas in pre- and post-comparison of induced SCI in mice, with the post measurement during the chronic phase[19]. Lower FC in people with complete SCI was found in sensorimotor cortex, but also higher FC in the left postcentral gyrus and bilateral thalamus[11]. Furthermore, reduced FC was found in complete SCI in the right lingual gyrus and vermis III[6]. So far, the vermis IX subregion has been associated with spatial orientation[20]. According to our results, the substructures of the vermis and cerebellum seem to be relevant in relation to SCI, and future studies might analyze the subcortical area as single subdivisions.

Only sSCI showed higher ALFF in the left thalamus compared to cSCI and HC. This finding might reflect ongoing plasticity processes in sSCI, which might also be a factor contributing to the higher BOLD signal fluctuation. It has been shown that after upper limb amputation in humans, ALFF increases over time in thalamus, among others[21]. The ALFF

results of this study are to some extent consistent with the pre-clinical results[22], where non-human primates with induced SCI showed variations of fALFF in the left thalamus, left cerebellum, right lateral geniculate nucleus, right superior parietal lobule and posterior cingulate gyrus. It has been shown that 6 months after induced SCI in rats, i.e. the subacute phase, BOLD activity is increased in the thalamus, which has been linked to plasticity processes[23]. In a study with both complete and incomplete SCI in humans, where ALFF was examined in the early stage of the subacute phase (4 – 14 weeks), reduced BOLD fluctuation was found in the primary sensorimotor cortex and increased ALFF in the cerebellum and orbitofrontal cortex[10]. More in-depth research on ALFF following the time course of SCI is required as it shows effects on BOLD fluctuation especially in the early phase of SCI.

There was no difference between SCI and HC in terms of global and local efficiency in the network analysis, which is in line with previous results[24]. Similar to our findings, no network difference regarding global efficiency was found in subjects with complete SCI and HC, but they did show a significant difference in local efficiency[18]. However, the sample included patients with injury at the cervical level C4 – C7 (tetraplegia), whereas in this study we only included paraplegia (i.e. injury at the thoracic level). It has also been shown that there are differences in reorganization between tetraplegia and paraplegia, as humans with tetraplegia showed lower brain activity in a positron emission tomography study[25]. Probably the lesion height and thus the proximity of the injury might lead to differences in neuronal networks efficiency. Future studies are required to investigate this association between injury level and functional networks.

Whether the lower FC in cSCI compared to sSCI and HC using the bilateral cerebellum crus I is due to the chronic phase remains open. Future studies are required to examine the time course of SCI with several measurement points from the acute to the chronic phase. Another issue is the definition of subacute and chronic phase in SCI as it is a continuous process between subacute and chronic phases. Therefore, in this study a clear cut-off point was chosen for the recruitment to ensure comparison of the two subgroups sSCI and cSCI. Consistent with the guidelines according to which the strongest recovery after SCI occurs in the first 3 months and lasts up to 18 months[26], subjects with subacute SCI up to 7 months and subjects with chronic SCI from 2 years onwards were considered. Thus, the phase in between from the months 8 to 24 after SCI was not covered in order to achieve a more distinct separation. The sex ratio in our sample was unbalanced, with a larger proportion of men. However, this corresponds to the prevalence of SCI, where 68.3 % are

men[27]. Furthermore, the small sample in this study (especially that of the sSCI) is another limitation to generalization. To reduce the risk of alpha error (error type I), only adjusted *p*-values were considered, and the effect sizes were included. In addition, only people with complete paraplegic SCI were included in the sample to minimize strong variations within the group. This is relevant and therefore a strength of this study, as reorganization processes of incomplete SCI varies widely compared to complete SCI[9].

Reduced FC was found in the substructures vermis IX and bilateral cerebellum crus I in complete SCI, especially in the chronic phase, which can be related to the deficit of sensory and motor activity of SCI. Increased ALFF was found only in sSCI, which provides evidence for plasticity processes, as it was not present in cSCI. Thus, this study demonstrates the relevance for future investigations in SCI involving the subcortical area. A detailed understanding of functional reorganization processes in cortical as well as subcortical regions will support therapy recommendations and rehabilitation in SCI.

Methods

Institutional review board approval

This cohort study was approved by the Institutional Review Board (local ethics committee northwest and central Switzerland (EKNZ), approval number: PB 2019-01624), and was conducted in accordance with the Declaration of Helsinki. To increase the quality of reporting of this observational study, STROBE guidelines were followed[28]. All participants signed an informed consent form before participating in the study.

Participants

The recruitment took place from September 2019 to November 2021. The data were acquired on the same day. The inclusion age for all participants ranged from 18 to 80 years. The guidelines for clinical trials with SCI were followed for recruitment regarding the time since injury for SCI to differ between subacute and chronic state[26]. Therefore, the subsequent additional inclusion criteria were pursued for people with SCI: Less than 7 months (for subacute, sSCI) or more than 24 months (for chronic, cSCI) since the SCI, having a complete injury with American Spinal Injury Association Impairment Scale (AIS) A and a lesion level between Th1 to Th12 (paraplegic). The exclusion criteria for the overall sample were MRI

contraindication, traumatic brain injury, and neurological or mental disorders assessed by a survey.

Experimental design

Clinical assessments

All participants with SCI were assessed for severity and level of SCI by certified physicians with the International Standards for Neurological Classification of Spinal Cord Injury (ISNCSCI)[29]. Furthermore, the questionnaire HADS[30] was conducted to control for comorbidity of depressive and/or anxiety symptoms (exclusion if score > 7), as depression has been reported to alter FC[31]. To assess neuropathic pain, which has been shown to increase FC in SCI[32], the International Spinal Cord Injury Pain Classification (ISCIP) was carried out[33].

Imaging acquisition

The neuroimaging data were acquired with a 3 T MRI unit (Philips Achieva, release: 5.4.1; Philips Healthcare, Best, the Netherlands) using a 32-channel head coil (Philips Healthcare). Participants were placed supine in the scanner. MR measurement sequences included a survey acquisition, anatomic acquisitions and resting state fMRI measurements with a total examination duration of 14 min.

The anatomic T1-weighted images were acquired with a repetition time (TR)/echo time (TE) of 8.12 ms/3.71 ms, flip angle of 8°, slice thickness of 1 mm, field of view (FoV) of 256 × 256 × 180 mm^3, voxel size of 1 × 1 × 1 mm^3 and bandwidth of 19 Hz. This resulted in a duration of 2 min 6 s. The functional T2-weighted echo-planar images were collected using a TR/TE of 2700 ms/26.7 ms, flip angle of 80°, voxel size of 3 × 3 × 3 mm^3, bandwidth of 2116 Hz, FoV of 240 × 240 × 160 mm^3 and 220 repetitions. The duration of this sequence took about 9 min 54 s. During the fMRI sequence, the participants were instructed to relax, think of nothing in particular, keep their eyes closed but stay awake. No music was played during this measurement. Immediately afterwards, all participants were asked whether they had adhered to it.

Data preprocessing

CONN toolbox, version 21b[34], based on SPM, was used for analysis of functional MRI data. The following preprocessing steps were conducted: The first 10 images were

excluded to allow the spin-system to reach steady state. The functional images were realigned according to the first image and co-registered to the anatomical images. Normalization was performed as well as segmentation with respect to Montreal Neurological Institute (MNI) space so that gray matter, white matter, and cerebrospinal fluid (CSF) tissue could be separated[35]. All spikes above five standard deviations of the global BOLD signal were removed. To reduce physiological influences, e.g. head movement, slow frequency fluctuations in the range of 0.008 – 0.09 Hz were filtered out in the BOLD signal. The motion correction included the three translational and three rotational regressors, and their derivatives. Finally, a Gaussian-smoothing kernel of 6 mm (isotropic) full-width-at-half-maximum was applied. The whole brain was parcellated into 274 regions according to the Brainnetome Atlas[36].

Functional connectivity and statistical analysis

Statistical analyses were done with CONN toolbox[34] and R software[37] using the package emmeans[38]. Cerebellum and vermis were used separately in their subdivisions as seed regions for seed-based connectivity maps. In the Brainnetome Atlas, these seed structures are segmented into fine-grained subdivisions, resulting in 10 substructures of the cerebellum in the left and right hemisphere respectively and eight vermis substructures. For the cerebellum, the left and right substructures were combined in the model as an average effect. Fisher-transformed bivariate correlations between the individual seeds and every voxel of the brain were calculated and implemented in an ANCOVA for assessing group differences with age as covariate. Only clusters with False Discovery Rate (FDR) correction and a significance threshold of $p_{FDR} < 0.05$ were considered thereby minimizing the alpha error (error type I). Post-hoc group comparisons were then calculated with a Bonferroni correction and a significance level of $p < 0.05$. Confidence intervals (CI) of 95% and effect sizes eta-squared (η^2) were calculated for all significant results. Kruskal–Wallis tests examined the influence of age and average motion.

The graph theory-based measures of centrality (global efficiency) and locality (local efficiency) were used for the analysis of functional network organization[39]. This involves examining the nodes (regions of interest, ROIs) with their edges (functional connections) in the entire brain. Global efficiency is calculated using the average of the inverse distance between a node and all other nodes and local efficiency is computed using the inverse of the shortest path length between a node and each of its adjacent nodes[40]. Both network metrics

were calculated using a cost-function threshold range of 0.1 – 0.5 with 0.01 step size, which means that only the 10 – 50 % highest correlations are kept for comparison between the groups. This was done to minimize the false positive rate[40].

In addition, but complementary to the FC, a comparison was made between the groups in terms of ALFF to investigate whether in the selected frequency range the BOLD signal strengths differed[41].

To determine the influence of voxel composition, we calculated the GMV for the ROIs with significant results. Thereby, we subject-specific overlaid the results of the grey matter segmentation with the atlas.

Data availability

The data that support the findings of this study are available from the corresponding author upon reasonable request.

References

1. Athanasiou, A. et al. A systematic review of investigations into functional brain connectivity following spinal cord injury. Front. Hum. Neurosci. 11, 1–9 (2017).

2. Pearson, K. G. Neural adaptation in the generation of rhythmic behavior. Annu. Rev. Physiol. 62, 723–753 (2000).

3. Dietz, V. Neuronal plasticity after a human spinal cord injury: Positive and negative effects. Experimental Neurology 235, 110–115 (2012).

4. Zhu, L. et al. Altered spontaneous brain activity in patients with acute spinal cord injury revealed by resting-state functional MRI. PLoS ONE 10, 1–11 (2015).

5. Wu, R., Yang, P.-F. & Chen, L. M. Correlated Disruption of Resting-State fMRI, LFP, and Spike Connectivity between Area 3b and S2 following Spinal Cord Injury in Monkeys. J. Neurosci. 37, 11192–11203 (2017).

6. Zheng, W. et al. Functional Reorganizations Outside the Sensorimotor Regions Following Complete Thoracolumbar Spinal Cord Injury. Journal of Magnetic Resonance Imaging 54, 1551–1559 (2021).

7. Kim, A. R. et al. Impact of fractional amplitude of low-frequency fluctuations in motor- and sensory-related brain networks on spinal cord injury severity. NMR in Biomedicine 1–9 (2021) doi:https://doi.org/10.1002/nbm.4612.

8. Alizadeh, M. et al. Graph theoretical structural connectome analysis of the brain in patients with chronic spinal cord injury: preliminary investigation. Spinal Cord Ser Cases 7, 60 (2021).

9. Hawasli, A. H. et al. Spinal cord injury disrupts resting-state networks in the human brain. Journal of Neurotrauma 35, 864–873 (2018).

10. Hou, J. M. et al. Alterations of resting-state regional and network-level neural function after acute spinal cord injury. Neuroscience 277, 446–454 (2014).

11. Oni-Orisan, A. et al. Alterations in cortical sensorimotor connectivity following complete cervical spinal cord injury: A prospective resting-state fMRI study. PLoS ONE 11, 1–13 (2016).

12. Manni, E. & Petrosini, L. A century of cerebellar somatotopy: a debated representation. Nat Rev Neurosci 5, 241–249 (2004).

13. Rijntjes, M., Buechel, C., Kiebel, S. & Weiller, C. Multiple somatotopic representations in the human cerebellum: NeuroReport 10, 3653–3658 (1999).

14. D'Angelo, E. Physiology of the cerebellum. in Handbook of Clinical Neurology vol. 154 85–108 (Elsevier, 2018).

15. Schmahmann, J. D. The cerebellum and cognition. Neuroscience Letters 688, 62–75 (2019).

16. Coffman, K. A., Dum, R. P. & Strick, P. L. Cerebellar vermis is a target of projections from the motor areas in the cerebral cortex. Proc. Natl. Acad. Sci. U.S.A. 108, 16068–16073 (2011).

17. Visavadiya, N. P. & Springer, J. E. Altered cerebellar circuitry following thoracic spinal cord injury in adult rats. Neural Plasticity 2016, 1–5 (2016).

18. Kaushal, M. et al. Evaluation of Whole-Brain Resting-State Functional Connectivity in Spinal Cord Injury: A Large-Scale Network Analysis Using Network-Based Statistic. Journal of Neurotrauma 34, 1278–1282 (2017).

19. Matsubayashi, K. et al. Assessing cortical plasticity after spinal cord injury by using resting-state functional magnetic resonance imaging in awake adult mice. Sci Rep 8, 14406 (2018).

20. Angelaki, D. E., Yakusheva, T. A., Green, A. M., Dickman, J. D. & Blazquez, P. M. Computation of Egomotion in the Macaque Cerebellar Vermis. Cerebellum 9, 174–182 (2010).

21. Bao, B. et al. Changes in Temporal and Spatial Patterns of Intrinsic Brain Activity and Functional Connectivity in Upper-Limb Amputees: An fMRI Study. Neural Plasticity 2021, 1–13 (2021).

22. Rao, J.-S. et al. Fractional amplitude of low-frequency fluctuation changes in monkeys with spinal cord injury: A resting-state fMRI study. Magnetic Resonance Imaging 32, 482–486 (2014).

23. Endo, T., Spenger, C., Tominaga, T., Brene, S. & Olson, L. Cortical sensory map rearrangement after spinal cord injury: fMRI responses linked to Nogo signalling. Brain 130, 2951–2961 (2007).

24. Min, Y.-S. et al. Change of brain functional connectivity in patients with spinal cord injury: Graph theory based approach. Ann Rehabil Med 39, 374 (2015).

25. Bruehlmeier, M. et al. How does the human brain deal with a spinal cord injury? European Journal of Neuroscience 10, 3918–3922 (1998).

26. Fawcett, J. W. et al. Guidelines for the conduct of clinical trials for spinal cord injury as developed by the ICCP panel: spontaneous recovery after spinal cord injury and statistical power needed for therapeutic clinical trials. Spinal Cord 45, 190–205 (2007).

27. Barbiellini Amidei, C., Salmaso, L., Bellio, S. & Saia, M. Epidemiology of traumatic spinal cord injury: a large population-based study. Spinal Cord (2022) doi:10.1038/s41393-022-00795-w.

28. Vandenbroucke, J. P., Poole, C., Schlesselman, J. J. & Egger, M. Strengthening the Reporting of Observational Studies in Epidemiology (STROBE): Explanation and Elaboration. PLoS Medicine 4, 27 (2007).

29. Kirshblum, S. C. et al. Reference for the 2011 revision of the international standards for neurological classification of spinal cord injury. The Journal of Spinal Cord Medicine 34, 547–554 (2011).

30. Snaith, R. P. The hospital anxiety and depression scale. Health and Quality of Life Outcomes 1–4 (2003).

31. Kaiser, R. H., Andrews-Hanna, J. R., Wager, T. D. & Pizzagalli, D. A. Large-Scale Network Dysfunction in Major Depressive Disorder: A Meta-analysis of Resting-State Functional Connectivity. JAMA Psychiatry 72, 603 (2015).

32. Huynh, V. et al. Supraspinal nociceptive networks in neuropathic pain after spinal cord injury. Hum Brain Mapp 42, 3733–3749 (2021).

33. Bryce, T. N. et al. International Spinal Cord Injury Pain (ISCIP) Classification: Part 2. Initial validation using vignettes. Spinal Cord 50, 404–412 (2012).

34. Whitfield-Gabrieli, S. & Nieto-Castanon, A. CONN: A functional connectivity toolbox for correlated and anticorrelated brain networks. Brain Connectivity 2, 125–141 (2012).

35. Ashburner, J. & Friston, K. J. Unified segmentation. NeuroImage 26, 839–851 (2005).

36. Fan, L. et al. The human brainnetome atlas: A new brain atlas based on connectional architecture. Cereb. Cortex 26, 3508–3526 (2016).

37. R Core Team. R: A Language and Environment for Statistical Computing. (R Foundation for Statistical Computing, 2021).

38. Lenth, R. V. emmeans: Estimated Marginal Means, aka Least-Squares Means. (2022).

39. Bullmore, E. & Sporns, O. Complex brain networks: graph theoretical analysis of structural and functional systems. Nat Rev Neurosci 10, 186–198 (2009).

40. Achard, S. & Bullmore, E. Efficiency and cost of economical brain functional networks. PLoS Comput Biol 3, 175–183 (2007).

41. Zang, Y.-F. et al. Altered baseline brain activity in children with ADHD revealed by resting-state functional MRI. Brain Dev 29, 83–91 (2007).

2.3 The role of motor inhibition in functional paralysis

Revisiting Motor Inhibition in individuals with Functional Paralysis and Spinal Cord Injury

Vallesi, V., Galléa, C., Sritharan, J., Hurni, E., Eriks-Hoogland, I., Gegusch, M., Slotboom, J., Worbe, Y., Roze, E., Scheel-Sailer, A., Verma, R., Zito, A. G.

Contribution:

I contributed to all aspects of this study, including conceptualization, participant recruitment, data collection, data analysis, data interpretation, and manuscript drafting.

Accepted for publication in Brain Communications (https://academic.oup.com/braincomms).

Revisiting Motor Inhibition in individuals with Functional Paralysis and Spinal Cord Injury

Authors:

Vallesi Vanessa[1, 2 ,3], Galléa Cécile[4], Sritharan Jothini[2, 3], Hurni Elia[2, 3], Eriks-Hoogland Inge[2, 3, 5], Gegusch Michaela[6], Slotboom Johannes[1], Worbe Yulia[4], Roze Emmanuel [4], Scheel-Sailer Anke[7], Verma Rajeev Kumar[2, 3], Zito Giuseppe Angelo[2]

[1] Support Centre for Advanced Neuroimaging (SCAN), Institute for Diagnostic and Interventional Neuroradiology, Inselspital, Bern University Hospital, University of Bern, Bern, Switzerland

[2] Swiss Paraplegic Research, Nottwil, Switzerland

[3] Swiss Paraplegic Centre, Nottwil, Switzerland

[4] Paris Brain Institute, INSERM, CNRS, Sorbonne Université, Paris, France

[5] University of Lucerne, Lucerne, Switzerland

[6] Clinic for Neurology, Cantonal Hospital St. Gallen, St. Gallen, Switzerland

[7] Centre for Rehabilitation and Sport Medicine, Inselgroup, Bern University Hospital, Bern, Switzerland

Corresponding author:

Dr. Giuseppe Angelo Zito

Guido A. Zäch Strasse 4

6207 Nottwil, Switzerland

E-mail: giuseppe.zito@paraplegie.ch

Abstract

Background

Functional paralysis (FP), a subtype of functional neurological disorder (FND), is characterized by symptoms of paralysis without clinically evident damage to the nervous system. Previous research has reported impaired inhibitory control in FND, such as weaker inhibition and slower response latencies, yet the underlying neural correlates remain unclear. Moreover, it is unknown whether such neural correlates depend on the symptoms, or are a specific trait of the disorder. To address this gap, we compared individuals with chronic FP,

healthy controls (HC) and individuals with spinal cord injury (SCI), who present a similar symptom phenotype but differ in the cause of their condition, hence provided the opportunity to disentangle disorder-specific from symptom-specific patterns of neural activity.

In this observational study, 16 patients with FP (6 males/10 females; mean age = 39.4 ± 13.1 years), 24 patients with SCI (18 males / 6 females; mean age = 42.4 ± 11.6 years), and 29 HC (8 males / 21 females; mean age = 35.5 ± 12.6 years) underwent event-related functional magnetic resonance imaging (fMRI) while performing a go/no-go task. We conducted a task-related validation analysis to isolate functional networks involved in response inhibition, and implemented a generalized psychophysiological interaction (gPPI) focusing on the associative motor network. We then compared behavioral performance and patterns of functional connectivity across groups with a general linear model.

No group differences in task performance emerged, suggesting intact motor inhibition in FP. Validation analysis over the whole sample showed the recruitment of typical regions of the motor inhibition network. Compared to HC, we identified significant differences in functional connectivity ($p < 0.05$, family-wise error corrected) in both paralysis groups (FP and SCI), which exhibited higher functional connectivity between the right precentral gyrus and the left insula during response inhibition. Functional connectivity during response inhibition was similar between patient groups.

These findings suggest a shared neural pattern associated with symptoms of paralysis, rather than a disorder-specific deficit, and may reflect an abnormal limbic drive of the motor network involved in movement initiation.

Keywords: functional neurological disorder, spinal cord injury, functional connectivity, go/no-go, task-based fMRI

Introduction

Functional neurological disorder (FND) presents with neurological symptoms without clinically evident damage to the nervous system, although emerging neuroimaging studies suggest potential group-level microstructural brain alterations[1,2]. The clinical presentation of FND encompasses a wide range of symptoms, including, but not limited to, functional

seizures, persistent perceptual postural dizziness, functional cognitive disorder and functional movement disorders[3].

To date, the underlying pathophysiology of FND is still unknown, and consequently, effective treatments and prognostic indicators are lacking[4]. The etiology of FND is considered to involve a complex interplay of biological, psychological, and social factors, none of which alone is sufficient to causally explain the disorder[5–7]. While psychiatric comorbidities, such as depression and anxiety, are frequently observed in FND, they do not appear to directly influence the disorder's outcome[8]. Moreover, given the heterogeneity among individuals with FND, multiple combinations of predisposing factors may result in similar functional symptoms[9].

Studies focusing on FND as a whole have documented neurocognitive impairments in multiple domains. For instance, information processing speed is more severely affected in FND than in other somatic disorders[10]. Additional deficits include spatial working memory and attention[11] as well as executive functions[12]. It is assumed that the impaired cognitive integrative functions observed in FND are not directly associated with comorbid symptoms of anxiety or depression but may underlie disorder-specific processes[13]. Notably, inhibitory control, a subdomain of executive functions, is impaired, with the functional seizure subtype showing greater deficits than genetic generalized epilepsy[14]. Van Wouwe et al.[15] found that individuals with FND exhibit slower response latencies in both action initiation and action cancellation tasks compared to healthy controls (HC), and make more errors in interference control when responding to conflicting stimuli. Similarly, Hammond-Tooke et al.[16] reported that people with FND demonstrate longer response time and a higher number of errors in motor inhibition tasks using the go/no-go paradigm compared to HC.

One possible explanation for the impaired neurocognitive domain, specifically motor inhibition in FND, is alterations in the serotonergic system. Individuals with FND exhibit changes in their serotonergic pathways, which are associated with clinical outcomes and symptom severity[17]. Moreover, direct serotonin release is known to influence performance in motor inhibition tasks[18].

To date, little is known about the brain activity associated with impaired motor inhibition in FND. In a study on functional paralysis (FP), a subtype of FND characterized by motor deficits such as paralysis, the left inferior frontal gyrus was found active during passive movements of the affected hand, and impaired inhibitory control was suggested to contribute

to symptom production[19]. However, another case report examined brain activity during motor inhibition using a go/no-go task found abnormal activity in the precuneus, ventromedial prefrontal cortex, and left orbitofrontal cortex—regions typically associated with self-related representations rather than inhibitory control. Conversely, the same study reported that a group of HC exhibited activation in the right inferior frontal gyrus and inferior parietal lobule, areas more commonly involved in inhibitory control[20]. Building upon this initial single-case finding, our research aims to generalize these insights to a broader FP cohort. We investigated patterns of functional connectivity associated with proactive motor inhibitory control in FP using event-related functional magnetic resonance imaging (fMRI) during a go/no-go task. Functional connectivity analysis allows for the examination of network-level interactions between brain regions, which is particularly relevant in FP, where large-scale network disruptions are central to the disorder[21].

According to Bayesian Brain Theory and the Predictive Processing framework, the brain continuously predicts sensory inputs and updates these predictions based on prediction errors—discrepancies between expected and actual sensory experiences. This process facilitates efficient energy regulation (allostasis)[22]. In FND, chronic prediction errors may lead to a brain state of 'fatigue' or 'hyperarousal' as the brain attempts to maintain allostasis despite a constant mismatch, resulting in energy mismanagement[23]. In FP, we hypothesize that these chronic mismatches extend beyond sensory processing to motor control, disrupting large-scale networks involved in motor inhibition.

The novelty of our study is that, in order to determine whether motor inhibition and its neural correlates in FP are due to the underlying disorder processes, we included two comparison groups: individuals with spinal cord injury (SCI) exhibiting similar motor symptoms and a second control group of healthy participants. In SCI, paralysis arises from disruptions in afferent and efferent sensorimotor pathways[24], whereas in FP, such disruptions are not identifiable. Despite this difference, both conditions present a similar phenotypic manifestation of motor deficits. Furthermore, individuals with SCI are affected by neurocognitive impairment, with traumatic brain injury, psychiatric disorders, medication side effects and pain being contributing factors[25]. Of note, individuals with SCI show impaired executive functions, such as verbal fluency[26], but not in the specific domain of inhibitory control.

FP and SCI share phenotypically similar motor impairments but differ in their neurobiological mechanisms. Investigating motor-related regions within the inhibitory control network[27] allows us to differentiate symptom-related alterations (neural changes resulting from the presence of paralysis, regardless of aetiology) from condition-specific changes. We focused on motor-associated regions, such as the precentral gyrus and supplementary motor area, as these areas may reflect disorder- or symptom-specific connectivity changes.

If motor inhibition alterations in FP arise from central dysfunction (energy mismanagement), we would expect FP-specific connectivity changes in motor-inhibitory regions, distinct from SCI, where motor impairments stem from peripheral neuronal disruption. Conversely, overlapping alterations in both groups would suggest symptom-related effects.

Material and methods

Design and ethical approval

This study employed a cross-sectional design. The reporting of this study was conducted according to the STROBE guidelines. Ethical approval was obtained from the local Ethics Committee of Northwest and Central Switzerland (EKNZ, approval number: 2021-01775). All participants provided written informed consent in accordance with the Declaration of Helsinki. The study was preregistered on ClinicalTrials.gov (ID: NCT05139732).

Participants

The study was conducted at the Swiss Paraplegic Centre in Nottwil, Switzerland. Participants were primarily recruited through the Swiss Paraplegic Centre via online and in-clinic flyers, as well as physician referrals. Additional participants came from the Clinic for Neurology at the Cantonal Hospital St. Gallen. The sample size of 74 was determined a priori using G*Power[28] (see supplementary material for parameter details). The total initial sample size consisted of 71 participants, with 2 participants excluded due to excessive motion during fMRI scans, resulting in a final sample size of 69. The FP group (n = 16, 6 males / 10

females, mean age = 39.4 ± 13.1 years) was age-matched with HC (n = 29, 8 males / 21 females, mean age = 35.5 ± 12.6 years). The SCI group consisted of 24 participants (18 males / 6 females, mean age = 42.4 ± 11.6 years). Detailed demographic information is provided in Supplementary Table 1 and 2. The inclusion criteria were: (i) having symptoms for at least 6 months (for all patients); (ii) being able to hold a pen (for all patients); and (iii) age between 18 and 60 years. The exclusion criteria were: (i) having contraindications for magnetic resonance imaging; (ii) having a history of neurological disorders (except for FND and SCI for the respective patient groups); (iii) having any acute psychological disorder; and (iv) having red-green color vision deficiency.

Psychometric and functional assessment tools

The Hospital Anxiety and Depression Scale (HADS) was used to assess anxiety and depression levels among the participants. This includes two subscales: one for anxiety (HADS-A) and one for depression (HADS-D)[29]. Pain intensity during the measurement and over the past 7 days was measured using the Numeric Rating Scale (NRS)[30]. To evaluate quality of life, the Satisfaction with Life Scale (SWLS) was administered[31]. Additionally, all patients completed the Spinal Cord Independence Measure (SCIM) to assess their functional independence[32]. The International Standards for Neurological Classification of Spinal Cord Injury (ISNCSCI)[33] was performed by certified physicians to determine the severity of paralysis in both FP and SCI groups (see Supplementary Table 1).

Go/no-go task

All participants completed an event-related go/no-go task during fMRI scanning using their dominant hand. The task, adapted from Cojan et al.[20] and implemented in PsychoPy[34], is detailed in Fig. 1. Participants were instructed to respond as quickly as possible by pressing a button on an MR-safe device when presented with a go signal, and to withhold their response when a no-go signal appeared. Response times and accuracy were recorded for each trial. Response times were analyzed only for correct go and no-go trials, and outliers (defined as response times greater than 2 standard deviations from the mean) were excluded from the analysis[35]. Overall task accuracy was calculated for each participant as the percentage of correct responses (correct trials / total trials × 100), where correct trials included both hits

(correct responses to go trials) and correct rejections (withheld responses on no-go trials). These individual accuracy percentages were then averaged across groups for statistical comparisons. Detailed accuracy analyses for each condition are reported in the supplementary material, including go trial accuracy (hit rate: hits/[hits + misses] × 100) and no-go trial accuracy (correct rejection rate: correct rejections/[correct rejections + false alarms] × 100).

Following eight practice trials inside the scanner, participants completed four blocks of 52 trials each. To maintain consistent motivation, performance feedback, expressed as a percentage of correct responses, was provided after each block. Stimuli were presented in a pseudorandom order, with go stimuli comprising 75% of trials and no-go stimuli 25%, ensuring the unpredictability of the no-go stimuli[20]. This ratio produces the highest error rates[36], maximizing sensitivity for detecting inhibitory control deficits.

Figure 1: Go/no-go task design.

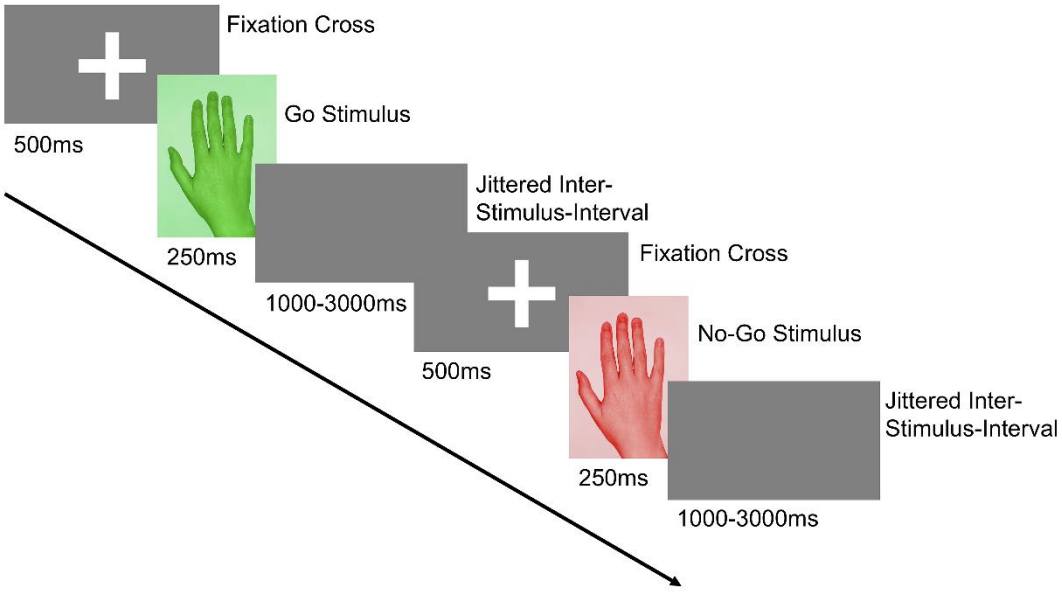

Note: In this inhibitory control task, each trial began with a fixation cross, followed by the pseudo-random presentation of either a go-stimulus (a green hand) or a no-go stimulus (a red hand). After the stimulus, a blank screen with a jittered interstimulus interval of 1000 to 3000 ms was displayed.

Brain imaging acquisition and pre-processing

Neuroimaging data were collected using a 3 T MRI scanner (Philips Achieva, release 5.4.1; Philips Healthcare, Best, the Netherlands) equipped with a 32-channel head coil (Philips Healthcare). Participants were positioned supine within the scanner with an MR-safe response device placed in their dominant hand. The MR imaging protocol included anatomical scans, and task-based fMRI sequences, with the entire procedure lasting approximately 20 minutes (for acquisition parameters see supplementary material). Functional and anatomical data were preprocessed using the CONN Toolbox, version 22a[37] including realignment with correction of susceptibility distortion interactions, outlier detection, direct segmentation and MNI-space normalization, and smoothing. Excessive motion during fMRI was defined as mean motion estimates exceeding the third quartile plus three times the interquartile range (Q3 + 3IQR) or falling below the first quartile minus three times the interquartile range (Q1 - 3IQR)[38]. Participants exceeding these thresholds were excluded from further analysis. The detailed pre-processing steps are listed in the supplementary material.

Functional connectivity and statistical analysis

To ensure that participants remained focused throughout the task-based fMRI session, we performed control measurements on behavioral performance. We examined participants' response time across the entire time series and assessed accuracy within each of the four task blocks. Behavioral data were analyzed using non-parametric methods due to violations of parametric model assumptions (see supplementary material). Mean response time and accuracy in percentages were calculated for each participant, and group differences were tested using the Kruskal-Wallis test.

For the imaging data, the conditions of correct rejection versus hit , were analyzed to isolate inhibition-specific neural activity, controlling for shared visual processing[39]. To ensure the validity of the go/no-go task for the functional connectivity analysis, we assessed activation patterns during motor inhibition (correct rejection vs. hit) and motor execution (hit vs. correct rejection) across the entire sample. This validation was conducted via a voxel-wise analysis using a flexible factorial design in the Statistical Parametric Mapping software (SPM12) running under MATLAB R2021a (The MathWorks, Inc., Natick, MA). The model included two factors: (1) group and (2) condition (hit and correct rejection), as well as their

interaction. This allowed us to identify the networks involved and verify whether the task elicited the expected activation patterns, confirming its successful implementation. Contrasts of interest compared activation between groups and across conditions, thresholded at $p < 0.001$ (voxel-level) with $p < 0.05$ family-wise error (FWE) correction at the cluster level.

To study changes in functional connectivity (FC) across these conditions, a generalized psychophysiological interaction (gPPI) analysis was used [40]. The Automated Anatomical Labelling Atlas 3 (AAL3)[41] was used for all neuroimaging analyses. Based on the meta-analyses of the go/no-go task by Zhang et. al.[27], we selected motor-associated regions of interest (ROIs) that are implicated in motor inhibition. Specifically, we tested three seeds, i.e., the right and left precentral gyrus, which have been linked to the execution and control of voluntary movements[42], and the right supplementary motor area, which is known to play a crucial role in motor planning and timing of inhibitory processes[43]. The seed blood-oxygen-level-dependent (BOLD) signals were considered the physiological term, whereas the time course of the conditions was considered the psychological term. The multiplication of these two factors formed the psychophysiological interaction term, and functional connectivity changes were characterized using Fisher-transformed semipartial correlation coefficients, providing an estimate of connectivity changes across conditions.

A separate General Linear Model (GLM) was calculated for each voxel[44], where the dependent variables were the connectivity measures obtained from the gPPI analysis. For each subject, a connectivity value corresponding to each task condition (hit and correct rejection) was estimated at every voxel. A random-effects analysis was performed at the group level using an analysis of covariance (ANCOVA), with age and handedness as covariates.

Using the Gaussian Random Field theory[45], only cluster-level results with FWE correction and a significance threshold of $p_{FWE} < 0.05$ were considered, thereby minimizing the Type I error (alpha error). Post-hoc group comparisons were then performed with a Bonferroni correction and a significance level of $p < 0.05$. Confidence intervals (CI) of 95% and generalized eta-squared (η^2_G) effect sizes were calculated for all significant results. Additionally, η^2G was reported for non-significant results to provide context for observed effect sizes.

To assess the robustness of our primary findings, all significant FC and behavioral models were re-estimated with additional covariates known to influence both neural and

behavioural measures, namely sex, anxiety/depression scores (HADS-A and HADS-D scores) and medication intake.

In order to verify the association between behavioral performance and neural activity, the Spearman correlation coefficient was calculated between the accuracy on the go/no-go task and patterns of functional connectivity in the clusters showing a significant difference among the three groups. The bootstrap method (10'000 bootstrap samples) was employed to study the robustness of the correlation. To further assess potential confounds, we examined the relationship between time since symptom onset and functional connectivity in both paralysis groups (FP and SCI) separately.

All analyses were conducted using the CONN Toolbox, version 22a[37] and R software[46], with the packages emmeans[47] and tidyverse[48].

Results

Patient characteristics

There were no significant differences in age across the groups, and no statistically significant association was found for handedness distribution. However, a significant association was found between sex and education among the groups. No significant differences were found between the FP and SCI groups in terms of functional independence, as measured by the SCIM. Similarly, symptom severity, assessed using the ISNCSCI, was comparable between the two patient groups, indicating similar severity of the sensorimotor symptoms.

For HADS-A, 56 out of 69 participants scored within the normal range, 6 (n = 2 FP, n = 2 SCI, n = 2 HC) scored in the mild anxiety range, and 7 (n = 6 FP, n = 1 HC) scored in the severe range, and a significant group difference was observed. For HADS-D, 59 out of 69 participants were in the normal range, 5 (n = 2 FP, n = 3 SCI) were in the mild range, and 5 (n = 4 FP, n = 1 SCI) in the severe range, with significant group differences.

On average, participants reported no or mild pain during the experiment. However, the FP group reported moderate pain over the past seven days, which showed a statistically significant difference between the groups. A significant group difference was also found in the SWLS, with the FP group being less satisfied than the SCI and HC groups

(Supplementary Table 1). Supplementary Table 2 shows the post-hoc comparisons of demographic and clinical characteristics between the HC, FP and SCI groups.

Behavioral performance

No significant changes in response time over time were observed, indicating stable sustained attention during the experiment (see Supplementary Fig. 1). In the go/no-go task, accuracy showed no significant group difference (see Fig. 2) ($\chi2 = 4.33$, df = 2, $p = 0.115$, $\eta^2_G = 0.06$) with the following distribution per group: FP group (median = 98.6%, interquartile range = 2.52%); SCI group (median = 99.0%, interquartile range = 1.44%); HCs (median = 99.5%, interquartile range = 0.96%). The variability across groups was further examined using Levene's test, which indicated significant differences in variance across groups (see supplementary material).

The response time for hits did not significantly differ between groups (see Fig. 3A) ($\chi2 = 2.71$, df = 2, $p = 0.258$, $\eta^2_G = 0.04$) with the following response time per group: FP group (median = 0.40s, interquartile range = 0.10s); SCI group (median = 0.41s, interquartile range = 0.07s); HCs (median = 0.40s, interquartile range = 0.07s). The variability in response time between groups was further tested with the coefficient of variation, which showed no difference in variation between groups (see supplementary material). The model analyzing incorrect response time (false alarms) included only a small fraction of the total trials (140 out of 14,352) since accuracy was high, and showed no significant group differences (see Fig. 3B) ($\chi2 = 5.74$, df = 2, $p = 0.057$, $\eta^2_G = 0.12$).

Figure 2: Task accuracy across groups.

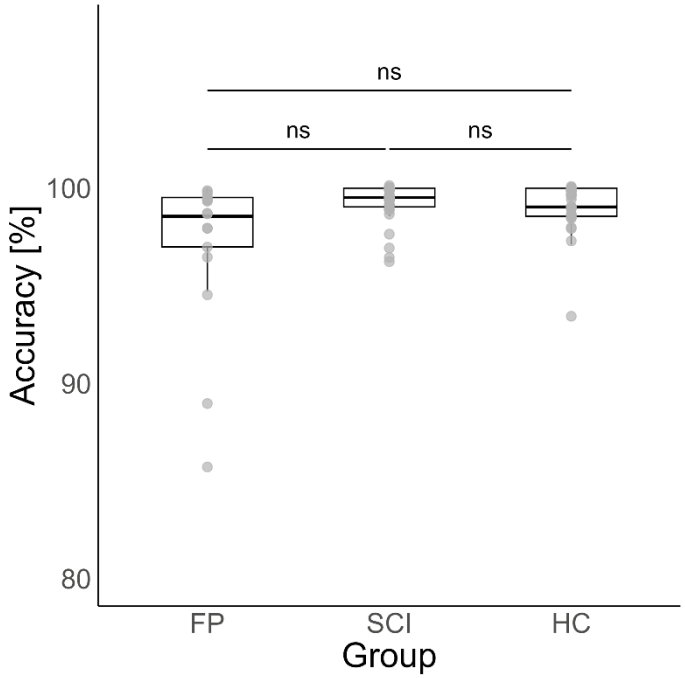

Note: Overall accuracy during the go/no-go task is shown as a percentage (total n = 69). Data were analyzed using Kruskal-Wallis test, revealing no significant group differences between individuals with functional paralysis (FP), with spinal cord injury (SCI), and healthy controls (HC) ($\chi 2 = 4.33$, df = 2, p = 0.115, $\eta^2_G = 0.06$). Note that the y-axis is zoomed in for clarity. Individual data points represent participant-level accuracy.

Abbreviation: ns = not significant.

Figure 3: Response times across groups.

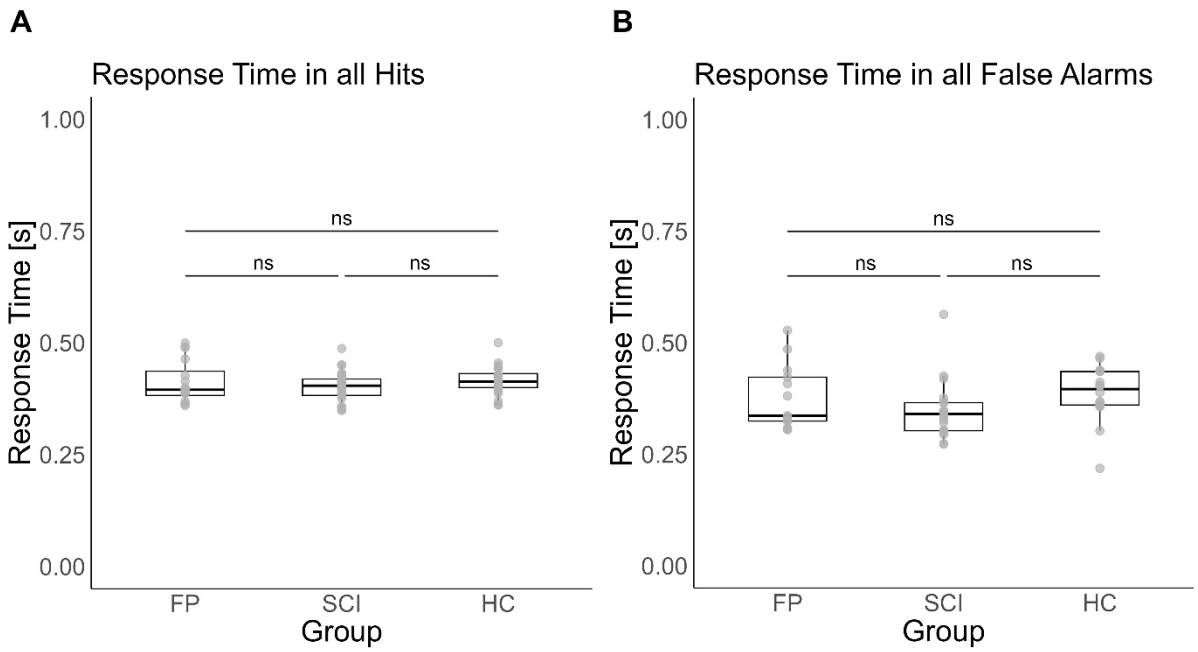

Note: A Kruskal-Wallis test was conducted to examine group differences in response time during the go/no-go task. Individual data points represent participant-level mean response time. (**A**) There were no significant group differences in response time during correct trials (hits) between the functional paralysis (FP), spinal cord injury (SCI) group and healthy controls (HC) ($\chi 2 = 2.71$, df = 2, p = 0.258, $\eta^2_G = 0.04$) (total n = 69). (**B**) There were no significant group differences in incorrect responses (false alarms) between the FP group, SCI group and HC ($\chi 2 = 5.74$, df = 2, p = 0.057, $\eta^2_G = 0.12$) (total n = 48).

Abbreviation: ns = not significant.

Functional networks of motor inhibition

The validation analysis confirmed activation in the motor inhibitory network across the whole sample (i.e., both patients' groups and HC together) (see Supplementary Fig. 2 for motor inhibition and Supplementary Fig. 3 for the separate effects of hit and correct rejection).

Voxel-wise comparisons of BOLD activity during correct rejection versus hit trials revealed significant group differences in task-related activation. The flexible factorial analysis identified greater activation in the FP group compared to HC in the left insula and

left superior temporal gyrus (Supplementary Table 3). The FP group also showed increased activation relative to HC in the left posterior cingulate cortex and bilateral precuneus. For the contrast HC > FP, significant clusters were located in the left postcentral gyrus and left inferior parietal lobule. Comparisons involving the SCI group demonstrated increased activation relative to both FP and HC in the right postcentral gyrus and right precentral gyrus. The SCI > HC contrast additionally revealed significant activation differences in the bilateral precuneus. Complete statistical results are provided in Supplementary Table 3.

Out of the three tested seeds (i.e, right supplementary motor area, right and left precentral gyrus) with the gPPI, one showed significant alterations in functional connectivity among the groups. The FC of the right precentral gyrus (seed) and left insula (cluster 1: $F_{(2, 64)} = 12.92$, $p_{FWE} = 0.02$, $\eta^2_G = 0.35$, cluster size = 92 voxels), as well as the left medial superior frontal gyrus and the bilateral supplementary motor area (cluster 2: $F_{(2, 64)} = 19.84$, $p_{FWE} = 0.03$, $\eta^2_G = 0.32$, cluster size = 85 voxels) differed among the groups (Fig. 4 and Table 1). Bonferroni-corrected post-hoc tests revealed that, in the first cluster, the FP group demonstrated significantly higher functional connectivity compared to HC, as did the SCI group compared to the HC. There was no significant difference between the two patient groups. Detailed statistical results are shown in Table 1. In the second cluster, post-hoc tests showed that the SCI group had significantly lower functional connectivity compared to the HC and to the FP group. The FP group showed no significant difference to HC (see Table 1).

Sensitivity analyses confirmed the robustness of the behavioral and functional connectivity findings when including covariates (Supplementary Table 4).

The correlation analysis revealed that functional connectivity in cluster 1 ($\rho = -0.31$, $p = 0.009$), but not cluster 2 ($\rho = -0.06$, $p = 0.614$), significantly correlated with accuracy on the go/no-go task across the entire sample (see Fig. 5). Bootstrapped Spearman correlation analysis confirmed the robustness of this relationship, with a 95% bias-corrected and accelerated confidence interval of [-0.51, -0.06]. The small bias (0.005) and standard error (0.113) further support the reliability of the correlation estimate. When excluding two low-accuracy outliers, the correlation remained significant with $\rho = -0.285$ and $p = 0.019$. Time since symptom onset was not significantly associated with functional connectivity (cluster 1) in either the FP group ($\rho = -0.24$, $p = 0.380$) or the SCI group ($\rho = 0.03$, $p = 0.905$).

Table 1. Functional connectivity differences using the right precentral gyrus as seed

Cluster 1

Brain Region(s)	Peak MNI	k (voxels)	F-value$_{(2,64)}$	P-value$_{FWE}$	FP vs HC	FP vs SCI	SCI vs HC
Left insula	-32 20 14	92	12.92	0.02	5.10^{***} [0.04, 0.11]	0.48^{ns} [-0.03, 0.04]	4.93^{***} [0.03, 0.10]
Cluster 2							
Left medial superior frontal gyrus, bilateral supplementary motor area	-04 30 44	85	19.84	0.03	-0.04^{ns} [-0.03, 0.03]	-4.49^{***} [-0.09, -0.03]	-5.01^{***} [-0.09, -0.03]

Abbreviations: FP, functional paralysis group; HC, healthy controls; SCI, spinal cord injury group; ***, $p < 0.001$; ns, not significant; FWE, family-wise error; MNI, Montreal Neurological Institute.

Note: All p-values are family-wise error corrected for 0.05, with a 95% confidence interval and post-hoc tests are adjusted using Bonferroni.

Figure 4: Group differences in motor inhibition-related functional connectivity.

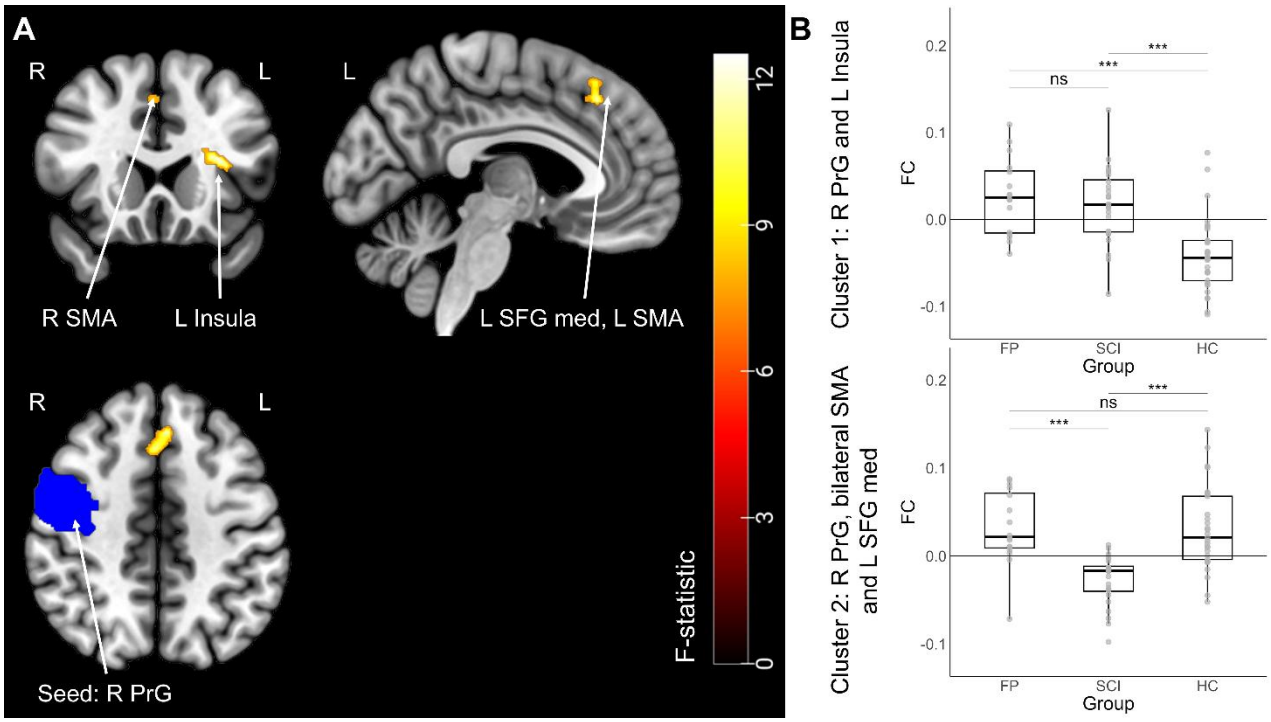

Note: (A) Functional connectivity differences between groups during motor inhibition (using generalized psychophysiological interaction analysis) were observed (total n = 69). (B) The right precentral gyrus (R PrG) seed showed significant group differences in functional connectivity (FC) with two clusters. The first cluster included the left insula ($F(2, 64) = 12.92$, family-wise error-corrected (FWE) $p = 0.02$, $\eta 2G = 0.35$, cluster size = 92 voxels), and the second cluster included the left medial superior frontal gyrus (L SFG med) and the bilateral supplementary motor area (SMA) ($F(2, 64) = 19.84$, $pFWE = 0.03$, $\eta 2G = 0.32$, cluster size = 85 voxels). In cluster 1, the functional paralysis (FP) group and the spinal cord injury (SCI) group had significantly higher FC than the healthy controls (HC). In cluster 2, only the SCI group had significantly lower FC compared to both the FP group and HC.

Abbreviations: R, right; L, left; SMA, supplementary motor area; SFG med, medial superior frontal gyrus; PrG, precentral gyrus; FC, functional connectivity; FP, functional paralysis group; SCI, spinal cord injury group; HC, healthy controls; ns, not significant; *** $p < 0.001$.

Figure 5: Precentral gyrus-insula connectivity negatively correlates with inhibitory accuracy.

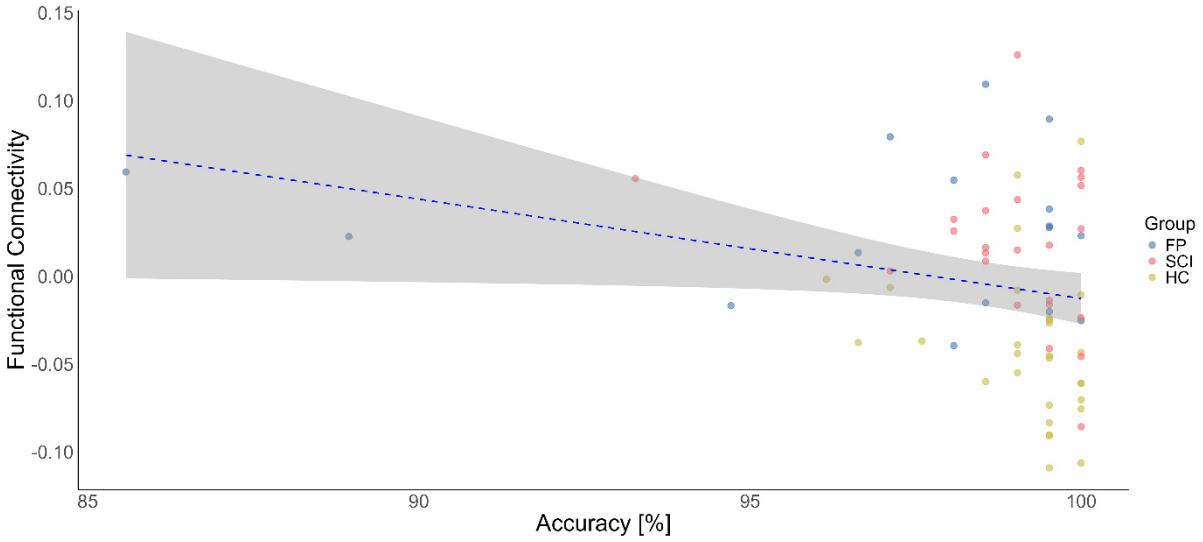

Note: Spearman correlation between the functional connectivity of the right precentral gyrus and the left insula (cluster 1) with overall accuracy in the whole sample ($n = 69$, $\rho = -0.31$, $p = 0.009$). Sensitivity analysis excluding two low-accuracy outliers yielded an attenuated but persistent effect ($n = 67$, $\rho = -0.285$, $p = 0.019$).

Abbreviations: FP, functional paralysis group; SCI, spinal cord injury group; HC, healthy controls.

Discussion

In this task-based fMRI study on motor inhibition, no group differences were observed in accuracy on the go/no-go task, nor in response time during hits and false alarms, contrary to our hypothesis. In contrast, functional connectivity during motor inhibition revealed significant group differences. Both the FP and SCI groups exhibited similar connectivity patterns between the right precentral gyrus and the left insula, with both patient groups showing higher connectivity in these regions compared to HC. Notably, connectivity values in this network significantly correlated with accuracy across the whole sample, including FP, SCI and HC groups, indicating that performance during motor inhibition is associated with communication within this functional network. In addition, the SCI group demonstrated lower functional connectivity between the right precentral gyrus, the left medial

superior frontal gyrus, and the bilateral supplementary motor area, in contrast to the FP group and the HC. This finding was contrary to our hypothesis. These connectivity values were not correlated with accuracy.

While some gPPI findings co-localized with activation differences (notably in FP's left insula and SCI's precentral seed, see Supplementary Table 3), most connectivity effects occurred independently of local BOLD changes. This suggests both region-specific coupling between activation and connectivity, and network-level reorganization distinct from local processing.

Contrary to our findings, prior behavioural studies investigating the go/no-go task in FND have reported reduced accuracy[49,50]. Hammond-Tooke et al.[16] observed longer response time, with around 15% higher false alarms compared to HC. One possible explanation for the discrepancy in behavioural findings is that previous studies on motor inhibition in FND often focused on positive motor symptoms, such as functional tremor and dystonia[49], or mixed subtypes of FND, including functional weakness and co-existing functional seizures[15,16,50]. In contrast, this is the first study to focus on a homogeneous subtype of FND characterised solely by symptoms of paralysis, in comparison to a population exhibiting similar motor symptoms, such as SCI. Furthermore, in our study, the hand used for the task was unaffected for all participants, excluding the possibility of reduced performance due to a mere motor impairment. It is then possible that previous findings on impaired motor inhibition may have been influenced by the inclusion of participants with positive motor symptoms. These symptoms could have introduced additional complexity, potentially affecting the interpretation of motor inhibition deficits in FND. Because FND encompasses a broad spectrum of behavioral differences, it is essential to consider these variations in behavioral assessments—particularly those relying on response times, such as in our study. Indeed, a recent meta-analysis reported inconsistent results regarding the impairment of neurocognitive functions in FND across various studies and phenotypes[51]. Acknowledging distinct FND subtypes in both behavioral and neuroimaging research is therefore crucial for deepening the understanding of the mechanisms underpinning FND as a whole, as well as the unique features of each subtype.

Using a version of the go/no-go task similar to that employed by Cojan et al. [20], our FP group demonstrated overall accuracy (~ 97% correct responses) comparable to the HC in that study. Their response time (~ 0.4 s) was also in line with typical measurements, thereby

indicating normal task performance across the FP, SCI, and HC groups. In fact, response times of around 0.4–0.6 s are generally considered standard in these types of behavioral assessments[52,53].

Both FP and SCI groups in our study displayed altered functional connectivity between the right precentral gyrus and the left insula during motor inhibition (FC cluster 1). This network is associated with inhibitory control. According to Hoffstaedter[54], the premotor cortex is part of the "what-network," which governs movement selection, whereas the insular cortex is part of the "when-network," which governs movement timing. The anterior insula is described as a gatekeeper in executive control because it integrates both internal and external multisensory stimuli[55]. These regions have frequently been discussed in the broader context of FND. For instance, reduced left anterior insular volume has been reported in individuals with FND who experience severe physical health impairments, compared to HC[56]. In addition, both sensorimotor and insular cortices have been identified as neural correlates of FND in a meta-analysis[21], and they have emerged as classifiers for FND in large-scale cross-validation studies involving mixed FND samples[57,58]. Although we found no significant association between these FC alterations and time since symptom onset, the shared network changes in both paralysis groups could reflect a common neural adaptation—potentially arising in the chronic stage of paralysis. Interestingly, the connectivity between the precentral gyrus and the supplementary motor area (FC cluster 2) showed significant decreases in SCI, compared to FP and HC, consistent with known motor-network alterations in SCI[59] and potentially reflecting specific disruptions in afferent and efferent spinal–motor pathways unique to SCI.

Within a predictive-processing framework, the insula's interoceptive and salience functions imply that heightened precentral–insula coupling may reflect increased precision-weighting of motor predictions[22,23]. In SCI, this could arise from persistent mismatches between intended movement and disrupted sensory feedback (deafferentation), driving compensatory network reorganization. In FP, chronic prediction errors likely stem from maladaptive priors or aberrant attentional focus on bodily signals—though the precise origin of these mismatches remains unknown. Crucially, our data do not allow us to distinguish whether the same connectivity change reflects adaptive plasticity in SCI versus maladaptive processes in FP.

Limitations and Future Directions

One limitation of this study is the high accuracy across all groups on the go/no-go task, indicating a possible ceiling effect. While a more demanding inhibition paradigm may be required to reveal subtler deficits, simple go/no-go designs reliably detect gross motor-inhibition impairments in other patient populations (e.g. Parkinson's disease [60]). The absence of any group differences here thus suggests that large-scale inhibition deficits are unlikely in our FP sample, though finer-grained paradigms may uncover more nuanced alterations. Interpretation of the false-alarm response time model should be approached with caution, as only a small fraction of trials were included due to the high overall accuracy.

Future studies might also consider different phases of the disorder—for example, by comparing subacute and chronic phases—to capture how these conditions evolve over time.

Another limitation of this study is that the FP group exhibited higher mean scores of depression and anxiety compared to both the SCI and HC groups. However, these scores remained in the subclinical range and did not translate into measurable performance deficits: behavioural accuracy and response times were equivalent across all three groups. Moreover, we conducted sensitivity analyses controlling for both depression and anxiety (Supplementary Table 4), which confirmed that neither behavioural nor functional-connectivity results were altered by these comorbidities. Thus, neural-connectivity differences in the FP group appear robust to variation in affective symptoms.

The desired sample size for the FP group was not achieved due to challenges in recruitment. However, the target sample sizes for the SCI and HC groups were successfully met. To ensure the robustness of our findings and facilitate generalization, effect sizes were included in all analyses.

It remains challenging to disentangle the neural activity stemming from the underlying disorder processes from that generated by the symptom itself. Hence, it is important for future studies to include control groups with comparable symptom presentations. This approach would help clarify whether observed brain activity patterns are truly tied to the pathophysiology of FND or instead reflect broader, symptom-related effects.

Funding

This work was supported in part by the UniBE Doc.Mobility Grant from the University of Bern, which funded a portion of the author's time dedicated to this research.

Data availability

The data underpinning the results of this study are accessible from the corresponding author upon reasonable request. The analysis code used in this study is provided in the supplementary material.

Acknowledgements

We thank Andrea Federspiel and Patrik Oliver Wyss for the MR-technical inputs as well as Nadia Sauder and Corinne Kehl for their support in participant recruitment and data collection. We also gratefully acknowledge the MR technicians at the Radiology Department of the Swiss Paraplegic Centre for their assistance with the scans.

Competing interests

The authors report no competing interests.

References

1. Diez I, Williams B, Kubicki MR, Makris N, Perez DL. Reduced limbic microstructural integrity in functional neurological disorder. *Psychol Med*. 2021;51(3):485-493. doi:10.1017/S0033291719003386

2. Perez DL, Nicholson TR, Asadi-Pooya AA, et al. Neuroimaging in Functional Neurological Disorder: State of the Field and Research Agenda. *NeuroImage: Clinical*. 2021;30:102623. doi:10.1016/j.nicl.2021.102623

3. Hallett M, Aybek S, Dworetzky BA, McWhirter L, Staab JP, Stone J. Functional neurological disorder: new subtypes and shared mechanisms. *The Lancet Neurology*. 2022;21(6):537-550. doi:10.1016/S1474-4422(21)00422-1

4. Edwards MJ, Fotopoulou A, Pareés I. Neurobiology of functional (psychogenic) movement disorders: *Current Opinion in Neurology*. 2013;26(4):442-447. doi:10.1097/WCO.0b013e3283633953

5. Mavroudis I, Kazis D, Kamal FZ, et al. Understanding Functional Neurological Disorder: Recent Insights and Diagnostic Challenges. *IJMS*. 2024;25(8):4470. doi:10.3390/ijms25084470

6. Weber S, Bühler J, Vanini G, Loukas S, Bruckmaier R, Aybek S. Identification of biopsychological trait markers in functional neurological disorders. *Brain*. 2023;146(6):2627-2641. doi:10.1093/brain/awac442

7. Keynejad RC, Frodl T, Kanaan R, Pariante C, Reuber M, Nicholson TR. Stress and functional neurological disorders: mechanistic insights. *J Neurol Neurosurg Psychiatry*. 2019;90(7):813-821. doi:10.1136/jnnp-2018-318297

8. Calma AD, Heffernan J, Farrell N, et al. The Impact of Depression, Anxiety and Personality Disorders on the Outcome of Patients with Functional Limb Weakness – Individual Patient Data Meta-Analysis. *Journal of Psychosomatic Research*. 2023;175:111513. doi:10.1016/j.jpsychores.2023.111513

9. Fobian AD, Elliott L. A review of functional neurological symptom disorder etiology and the integrated etiological summary model. *jpn*. 2019;44(1):8-18. doi:10.1503/jpn.170190

10. Vroege L, Koppenol I, Kop WJ, Riem MME, Feltz-Cornelis CM. Neurocognitive functioning in patients with conversion disorder/functional neurological disorder. *J Neuropsychol*. 2021;15(1):69-87. doi:10.1111/jnp.12206

11. O'Brien FM, Fortune GM, Dicker P, et al. Psychiatric and neuropsychological profiles of people with psychogenic nonepileptic seizures. *Epilepsy & Behavior*. 2015;43:39-45. doi:10.1016/j.yebeh.2014.11.012

12. Hamouda K, Senf-Beckenbach PA, Gerhardt C, Irorutola F, Rose M, Hinkelmann K. Executive Functions and Attention in Patients With Psychogenic Nonepileptic Seizures Compared With Healthy Controls: A Cross-Sectional Study. *Psychosomatic Medicine*. 2021;83(8):880-886.

13. Bakvis P, Spinhoven P, Putman P, Zitman FG, Roelofs K. The effect of stress induction on working memory in patients with psychogenic nonepileptic seizures. *Epilepsy & Behavior*. 2010;19(3):448-454. doi:10.1016/j.yebeh.2010.08.026

14. Simani L, Raminfard S, Asadollahi M, Roozbeh M, Ryan F, Rostami M. Neurochemicals of limbic system and thalamofrontal cortical network: Are they different between patients with idiopathic generalized epilepsy and psychogenic nonepileptic seizure? *Epilepsy & Behavior*. 2020;112:107480. doi:10.1016/j.yebeh.2020.107480

15. van Wouwe NC, Mohanty D, Lingaiah A, Wylie SA, LaFaver K. Impaired Action Control in Patients With Functional Movement Disorders. *JNP*. 2020;32(1):73-78. doi:10.1176/appi.neuropsych.19030076

16. Hammond-Tooke GD, Grajeda FT, Macrorie H, Franz EA. Response inhibition in patients with functional neurological symptom disorder. *Journal of Clinical Neuroscience*. 2018;56:38-43. doi:10.1016/j.jocn.2018.08.005

17. Weber S, Rey Álvarez LT, Ansede-Bermejo J, et al. The impact of genetic variations in the serotonergic system on symptom severity and clinical outcome in functional neurological disorders. *Journal of Psychosomatic Research*. 2024;186:111909. doi:10.1016/j.jpsychores.2024.111909

18. Colwell MJ, Tagomori H, Shang F, et al. Direct serotonin release in humans shapes aversive learning and inhibition. *Nat Commun*. 2024;15(1):6617. doi:10.1038/s41467-024-50394-x

19. Hassa T, de Jel E, Tuescher O, Schmidt R, Schoenfeld MA. Functional networks of motor inhibition in conversion disorder patients and feigning subjects. *NeuroImage: Clinical*. 2016;11:719-727. doi:10.1016/j.nicl.2016.05.009

20. Cojan Y, Waber L, Carruzzo A, Vuilleumier P. Motor inhibition in hysterical conversion paralysis. *NeuroImage*. 2009;47(3):1026-1037. doi:10.1016/j.neuroimage.2009.05.023

21. Boeckle M, Liegl G, Jank R, Pieh C. Neural correlates of conversion disorder: overview and meta-analysis of neuroimaging studies on motor conversion disorder. *BMC Psychiatry*. 2016;16(1):195. doi:10.1186/s12888-016-0890-x

22. Bottemanne H. Bayesian brain theory: Computational neuroscience of belief. *Neuroscience*. 2025;566:198-204. doi:10.1016/j.neuroscience.2024.12.003

23. Jungilligens J, Paredes-Echeverri S, Popkirov S, Barrett LF, Perez DL. A new science of emotion: implications for functional neurological disorder. *Brain*. 2022;145(8):2648-2663. doi:10.1093/brain/awac204

24. Athanasiou A, Klados MA, Pandria N, et al. A systematic review of investigations into functional brain connectivity following spinal cord injury. *Front Hum Neurosci*. 2017;11:1-9. doi:10.3389/fnhum.2017.00517

25. Papageorgiou NA, Papageorgiou P, Kotroni A, Vasiliadis E. A Comprehensive Review of the Importance of the Main Comorbidities in Developing Cognitive Disorders in Patients With Spinal Cord Injuries. *Cureus*. Published online September 24, 2024. doi:10.7759/cureus.70071

26. Chiaravalloti ND, Weber E, Wylie G, Dyson-Hudson T, Wecht JM. The impact of level of injury on patterns of cognitive dysfunction in individuals with spinal cord injury. *The Journal of Spinal Cord Medicine*. 2020;43(5):633-641. doi:10.1080/10790268.2019.1696076

27. Zhang R, Geng X, Lee TMC. Large-scale functional neural network correlates of response inhibition: an fMRI meta-analysis. *Brain Struct Funct*. 2017;222(9):3973-3990. doi:10.1007/s00429-017-1443-x

28. Faul F, Erdfelder E, Lang AG, Buchner A. G*Power 3: A flexible statistical power analysis program for the social, behavioral, and biomedical sciences. *Behavior Research Methods*. 2007;39(2):175-191. doi:10.3758/BF03193146

29. Snaith RP. The hospital anxiety and depression scale. *Health and Quality of Life Outcomes*. Published online 2003:1-4.

30. Correll DJ. Chapter 22 - The Measurement of Pain: Objectifying the Subjective. In: *Pain Management*. Second Edition. ; 2011:191-201.

31. Diener E, Emmons RA, Larsen RJ, Griffin S. The satisfaction with life scale. *Journal of Personality Assessment*. 1985;49(1):71-75.

32. Itzkovich M, Gelernter I, Biering-Sorensen F, et al. The Spinal Cord Independence Measure (SCIM) version III: Reliability and validity in a multi-center. *Disability and Rehabilitation*. 2007;29(24):1926-1933. doi:https://doi.org/10.1080/09638280601046302

33. Kirshblum SC, Waring W, Biering-Sorensen F, et al. Reference for the 2011 revision of the international standards for neurological classification of spinal cord injury. *The Journal of Spinal Cord Medicine*. 2011;34(6):547-554. doi:10.1179/107902611X13186000420242

34. Peirce J, Gray JR, Simpson S, et al. PsychoPy2: Experiments in behavior made easy. *Behav Res*. 2019;51(1):195-203. doi:10.3758/s13428-018-01193-y

35. Berger A, Kiefer M. Comparison of Different Response Time Outlier Exclusion Methods: A Simulation Study. *Front Psychol*. 2021;12. doi:10.3389/fpsyg.2021.675558

36. Zhang N, An W, Yu Y, Wu J, Yang J. Go/No-Go Ratios Modulate Inhibition-Related Brain Activity: An Event-Related Potential Study. *Brain Sciences*. 2024;14(5):414. doi:10.3390/brainsci14050414

37. Whitfield-Gabrieli S, Nieto-Castanon A. CONN: A functional connectivity toolbox for correlated and anticorrelated brain networks. *Brain Connectivity*. 2012;2(3):125-141. doi:10.1089/brain.2012.0073

38. Morfini F, Whitfield-Gabrieli S, Nieto-Castañón A. Functional connectivity MRI quality control procedures in CONN. *Front Neurosci*. 2023;17:1092125. doi:10.3389/fnins.2023.1092125

39. Konishi S, Nakajima K, Uchida I, Kikyo H, Kameyama M, Miyashita Y. Common inhibitory mechanism in human inferior prefrontal cortex revealed by event-related functional MRI. *Brain*. 1999;122(5):981-991. doi:10.1093/brain/122.5.981

40. McLaren DG, Ries ML, Xu G, Johnson SC. A generalized form of context-dependent psychophysiological interactions (gPPI): A comparison to standard approaches. *NeuroImage*. 2012;61(4):1277-1286. doi:10.1016/j.neuroimage.2012.03.068

41. Rolls ET, Huang CC, Lin CP, Feng J, Joliot M. Automated anatomical labelling atlas 3. *NeuroImage*. 2020;206:116189. doi:10.1016/j.neuroimage.2019.116189

42. Cooke DF, Graziano MSA. Sensorimotor Integration in the Precentral Gyrus: Polysensory Neurons and Defensive Movements. *Journal of Neurophysiology*. 2004;91(4):1648-1660. doi:10.1152/jn.00955.2003

43. Hoshi E, Tanji J. Differential Roles of Neuronal Activity in the Supplementary and Presupplementary Motor Areas: From Information Retrieval to Motor Planning and Execution. *Journal of Neurophysiology*. 2004;92(6):3482-3499. doi:10.1152/jn.00547.2004

44. Nieto-Castanon A. General Linear Model. In: *Handbook of Functional Connectivity Magnetic Resonance Imaging Methods in CONN*. Hilbert Press; 2020:63-82.

45. Worsley KJ, Marrett S, Neelin P, Vandal AC, Friston KJ, Evans AC. A unified statistical approach for determining significant signals in images of cerebral activation. *Hum Brain Mapp*. 1996;4(1):58-73. doi:10.1002/(SICI)1097-0193(1996)4:1<58::AID-HBM4>3.0.CO;2-O

46. R Core Team. R: A Language and Environment for Statistical Computing. Published online 2021. https://www.R-project.org/

47. Lenth RV. emmeans: Estimated Marginal Means, aka Least-Squares Means. Published online 2022. https://CRAN.R-project.org/package=emmeans

48. Wickham H, Averick M, Bryan J, et al. Welcome to the Tidyverse. *JOSS*. 2019;4(43):1686. doi:10.21105/joss.01686

49. Voon V, Ekanayake V, Wiggs E, et al. Response inhibition in motor conversion disorder: Response Inhibition in Conversion Disorder. *Mov Disord*. 2013;28(5):612-618. doi:10.1002/mds.25435

50. Kozlowska K, Palmer DM, Brown KJ, et al. Conversion disorder in children and adolescents: A disorder of cognitive control. *J Neuropsychol*. 2015;9(1):87-108. doi:10.1111/jnp.12037

51. Millman LSM, Williams IA, Jungilligens J, Pick S. Neurocognitive performance in functional neurological disorder: A systematic review and meta-analysis. *Euro J of Neurology*. 2025;32(1):e16386. doi:10.1111/ene.16386

52. Gomez P, Ratcliff R, Perea M. A model of the go/no-go task. *Journal of Experimental Psychology: General*. 2007;136(3):389-413. doi:10.1037/0096-3445.136.3.389

53. Danek RH, Mordkoff JT. Unequal motor durations under simple-, go/no-go, and choice-RT tasks: Extension of Miller and Low (2001). *Journal of Experimental Psychology: Human Perception and Performance*. 2011;37(4):1323-1329. doi:10.1037/a0023092

54. Hoffstaedter F, Grefkes C, Zilles K, Eickhoff SB. The "What" and "When" of Self-Initiated Movements. *Cerebral Cortex*. 2013;23(3):520-530. doi:10.1093/cercor/bhr391

55. Molnar-Szakacs I, Uddin LQ. Anterior insula as a gatekeeper of executive control. *Neuroscience & Biobehavioral Reviews*. 2022;139:104736. doi:10.1016/j.neubiorev.2022.104736

56. Perez DL, Williams B, Matin N, et al. Corticolimbic structural alterations linked to health status and trait anxiety in functional neurological disorder. *J Neurol Neurosurg Psychiatry*. 2017;88(12):1052-1059. doi:10.1136/jnnp-2017-316359

57. Weber S, Heim S, Richiardi J, et al. Multi-centre classification of functional neurological disorders based on resting-state functional connectivity. *NeuroImage: Clinical*. 2022;35:103090. doi:10.1016/j.nicl.2022.103090

58. Waugh RE, Parker JA, Hallett M, Horovitz SG. Classification of Functional Movement Disorders with Resting-State Functional Magnetic Resonance Imaging. *Brain Connectivity*. 2023;13(1):4-14. doi:10.1089/brain.2022.0001

59. Wang W, Xie W, Zhang Q, et al. Reorganization of the brain in spinal cord injury: a meta-analysis of functional MRI studies. *Neuroradiology*. 2019;61(11):1309-1318. doi:10.1007/s00234-019-02272-3

60. Yang XQ, Lauzon B, Seergobin KN, MacDonald PA. Dopaminergic Therapy Increases Go Timeouts in the Go/No-Go Task in Patients with Parkinson's Disease. *Front Hum Neurosci*. 2018;11. doi:10.3389/fnhum.2017.00642

Supplementary material

Sample

The following parameters were used to calculate the sample size: Based on previous magnetic resonance (MR) studies conducted by our team, a power of 0.8 was estimated with an expected effect size of 0.37, and the significance level (alpha) was set at 0.05. For an analysis of covariance (ANCOVA) comparing three independent groups, a total sample size of 74 participants was calculated, which results in approximately 25 participants per group. Due to recruitment difficulties, the target sample size was not quite reached for the functional paralysis (FP) group but was reached for the spinal cord injury (SCI) group and the healthy controls (HC).

Acquisition parameters

The anatomic T1-weighted images were acquired using a magnetization-prepared rapid gradient-echo (MPRAGE) sequence with the following parameters: repetition time (TR) / echo time (TE) of 8.3 ms / 3.9 ms, inversion time (TI) = 950 ms, turbo field echo (TFE) factor = 128, flip angle of 8°, slice thickness of 1 mm, field of view (FoV) of 256 × 256 × 180 mm^3, voxel size of 1 × 1 × 1 mm^3, and bandwidth of 191 Hz. For the functional T2-weighted echo-planar images, the following parameters were used: TR / TE of 2700 ms / 27 ms, flip angle of 80°, voxel size of 3 × 3 × 3 mm^3, bandwidth of 2119 Hz, FoV of 240 × 240 × 159 mm^3, and 356 repetitions.

Normality test

Normality of the data was assessed using the Shapiro–Wilk test for both response times ($W = 0.95$, $p = 0.013$) and accuracy ($W = 0.56$, $p < 0.001$), indicating that these data deviate significantly from a normal distribution.

Pre-processing and denoising

The realignment of the functional data was conducted with the SPM realign and unwarp procedure[1]. All scans were realigned to the first scan of the session using a least

squares approach and a 6-parameter (rigid body) transformation[2]. To correct for motion and magnetic susceptibility interactions, the scans were resampled using b-spline interpolation. Potential outlier scans were identified using artifact detection tools[3]. The mean functional image was co-registered to each subject's T1-weighted anatomical scan during normalization. The functional and anatomical images were normalized into standard MNI space and segmented into gray matter, white matter, and cerebrospinal fluid (CSF). Subsequently, the images were resampled into 2 mm isotropic voxels[4,5] following a direct normalization procedure[6]. Finally, the functional images were smoothed using spatial convolution with a Gaussian kernel of 6 mm full width at half maximum.

The following confounders were denoised from the functional data[7,8]: white matter and CSF timeseries, motion parameters and their first-order derivatives (12 factors) to account for subject movement during the scan, outlier scans, session and task effects and their first-order derivatives (4 factors) to control for variability due to different scanning sessions, and cubic trends (4 factors) to account for low-frequency drifts within each functional run. Simultaneous high-pass frequency filtering of the BOLD timeseries above 0.01 Hz was applied.

Characteristics

Supplementary Table 1. Demographics and clinical characteristics

	Median (IQR)			**Test statistics**	**P-value**
Variable	**FP-group (n= 16)**	**SCI-group (n = 24)**	**Healthy controls (n=29)**		
Age [in years]	37.5 (18.8)	41 (16.2)	33 (18)	$\chi 2 = 4.28$	0.118
Sex [n of men]	6	18	8	n.a.	0.002
Education [n]				n.a.	0.024
Compulsory education	2	2	2		
Upper secondary education	2	0	4		
Vocational	7	5	4		

training/apprenticeship					
Post-secondary non-tertiary education	4	6	4		
University/college	1	11	15		
Handedness [n of right-handed]	14	19	29	n.a.	0.022
Anagesics [n]	5	4	1	n.a.	0.036
Psychotropics [n]	6	3	3	n.a.	0.081
Hospital Anxiety and Depression Scale (range: 0 - 21)					
Total score depression	4 (7)	2.5 (4)	2 (3)	$\chi2 = 10.42$	0.005
Total score anxiety	7 (7)	3.5 (4.25)	4 (3)	$\chi2 = 10.39$	0.006
Satisfaction with Life Scale (range: 5 - 35)	23 (13.8)	28.5 (6.25)	30 (3)	$\chi2 = 10.81$	0.004
Numeric Rating Scale (range: 0 - 10)					
Pain experienced now	3 (6.25)	0 (3)	0 (1)	$\chi2 = 13.09$	0.001
Pain experienced in the past 7 days	5 (4.5)	1 (3.25)	0 (1)	$\chi2 = 18.30$	< 0.001
Time since symptom onset [years]	2.5 (3.5)	11 (18.5)	n.a.	$\chi2 = 9.48$	0.002
Spinal Cord Independence Measure (range: 0 - 100)	88.5 (24.8)	75 (27)	n.a.	$\chi2 = 2.49$	0.114
ISNCSCI					
Total score motor (range: 0 - 100)	85 (31)	69 (46)	n.a.	$\chi2 = 1.57$	0.21
Total score light touch (range: 0 - 112)	18.5 (20.8)	13.5 (13.8)	n.a.	$\chi2 = 0.71$	0.399
Total score pinprick (range: 0 - 112)	9 (16.2)	15.5 (13.8)	n.a.	$\chi2 = 1.26$	0.262

Abbreviations: FP, functional paralysis; SCI, spinal cord injury; n.a., not applicable; ISNCSCI, International Standards for Neurological Classification of Spinal Cord Injury

Note: Test statistics from the Kruskal-Wallis rank sum test are reported. For Fisher's exact test, test statistics are not applicable. A p-value of less than 0.05 was considered significant.

Supplementary Table 2. Post hoc comparisons of demographic and clinical characteristics

Variables	HC vs FP	FP vs SCI	HC vs SCI
Sex	$p_{FWE} = 1.000$	$p_{FWE} = 0.074$	$p_{FWE} = 0.003$
Education	$p_{FWE} = 0.037$	$p_{FWE} = 0.082$	$p_{FWE} = 1.000$
Handedness	$p_{FWE} = 0.364$	$p_{FWE} = 1.000$	$p_{FWE} = 0.044$
Analgesics	$p_{FWE} = 0.049$	$p_{FWE} = 1.000$	$p_{FWE} = 0.491$
	W = 106.5	W = 252.5	W = 242.5
HADS-D	$p_{FWE} = 0.008$	$p_{FWE} = 0.280$	$p_{FWE} = 0.170$
	W = 115	W = 298.5	W = 371
HADS-A	$p_{FWE} = 0.0161$	$p_{FWE} = 0.010$	$p_{FWE} = 1.000$
	W = 367.5	W = 119.5	W = 429
SWLS	$p_{FWE} = 0.004$	$p_{FWE} = 0.139$	$p_{FWE} = 0.445$

Abbreviations: HC, healthy controls; FP, functional paralysis group; SCI, spinal cord injury group; FWE, family-wise error rate; HADS-D, Hospital Anxiety and Depression Scale - Depression; HADS-A, Hospital Anxiety and Depression Scale - Anxiety; SWLS, Satisfaction with Life Scale.

Note: Group sizes were HC = 29, FP = 16, SCI = 24. Post-hoc pairwise comparisons were carried out with Fisher's exact test for categorical variables (sex, education, handedness) and Wilcoxon rank-sum test for ordinal/score variables (HADS-D, HADS-A, SWLS). All p-values are two-tailed and Bonferroni-adjusted for family-wise error. "W" denotes the Wilcoxon rank-sum statistic.

Behavioral Results

Further accuracy analyses were conducted to examine performance differences between trial types and groups. Levene's test for homogeneity of variance revealed a significant difference in variances in overall accuracy across groups ($F_{(2, 66)} = 4.62$, $p = 0.013$). For detailed condition-level analysis, we computed two additional accuracy measures: (1) go trial accuracy (hit rate), calculated as hits/(hits + misses) × 100, and (2) no-go trial accuracy (correct rejection rate), calculated as correct rejections/(correct rejections + false

alarms) × 100. Kruskal-Wallis tests comparing these measures across groups showed no significant differences for either go trials ($\chi^2(2) = 2.09$, $p = 0.352$) or no-go trials ($\chi^2(2) = 3.75$, $p = 0.154$).

To test variability in response times across groups, we calculated each participant's coefficient of variation (CV) and compared them using a Kruskal–Wallis test. The result indicated no significant difference between groups ($\chi2 = 4.07$, $p = 0.131$).

Figure 1.

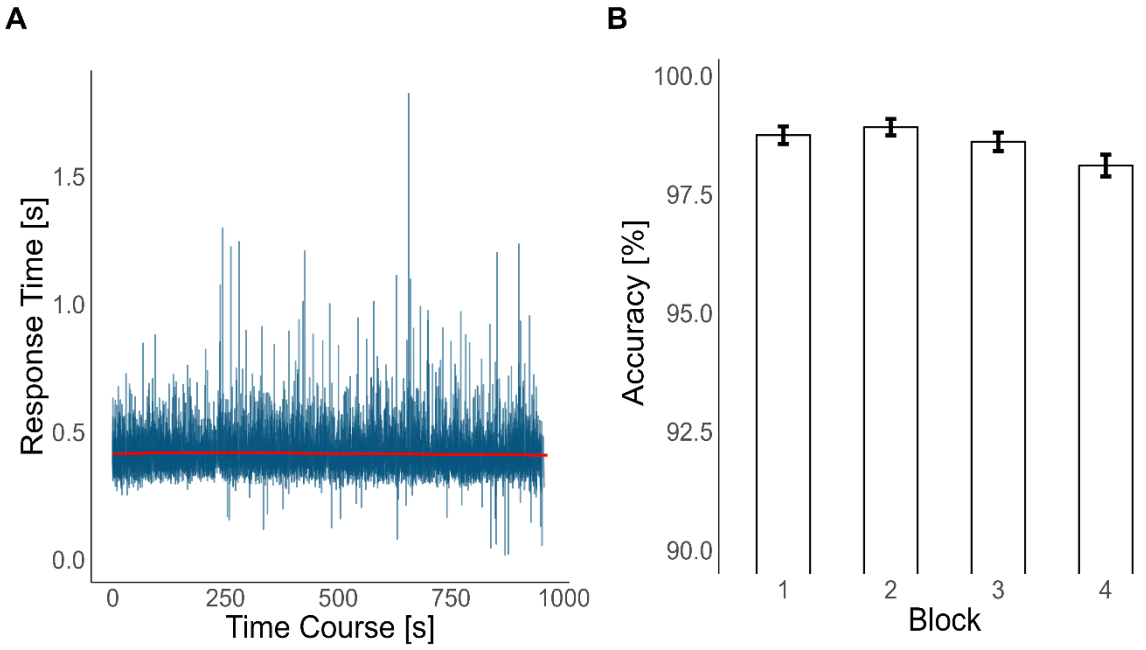

Note: The stability of behavioral performance was assessed throughout the go/no-go task. (A) The blue lines represent individual response times for each trial before filtering extreme outliers, while the red line is the fitted Loess regression using locally weighted smoothing for time series. (B) The y-axis has been zoomed in for visibility. The overall accuracy remained stable across task blocks, with a maximum change of 0.8% for the entire sample.

Voxel-wise Validation of Motor Inhibition BOLD Activity

The validation analysis showed activation of the motor inhibitory network, including regions such as the bilateral precentral gyrus, bilateral supplementary motor area (SMA), left

superior parietal lobule, bilateral supramarginal gyrus, mid-cingulate cortex, right inferior frontal gyrus (triangular and opercular parts), right middle frontal gyrus, right angular gyrus, and left inferior occipital gyrus[9]. Sensorimotor areas, including cerebellar lobules 4, 5, 6, 8, and vermis 6 and 8, were also active[10], alongside cortical regions such as the bilateral posterior cingulate gyrus, paracentral lobule, and inferior parietal lobule. Subcortical activation included the thalamic nuclei and left caudate. Further regions, including the bilateral precuneus, left rolandic operculum, left insula, bilateral superior frontal gyrus, bilateral inferior parietal lobule, and occipital and temporal areas, demonstrated significant activation ($t = 4.88$, $p_{FWE} < 0.05$, $k > 20$ voxels; see Supplementary Fig. 2 for motor inhibition and Fig. 3 for the separate effects of hit and correct rejection).

Figure 2.

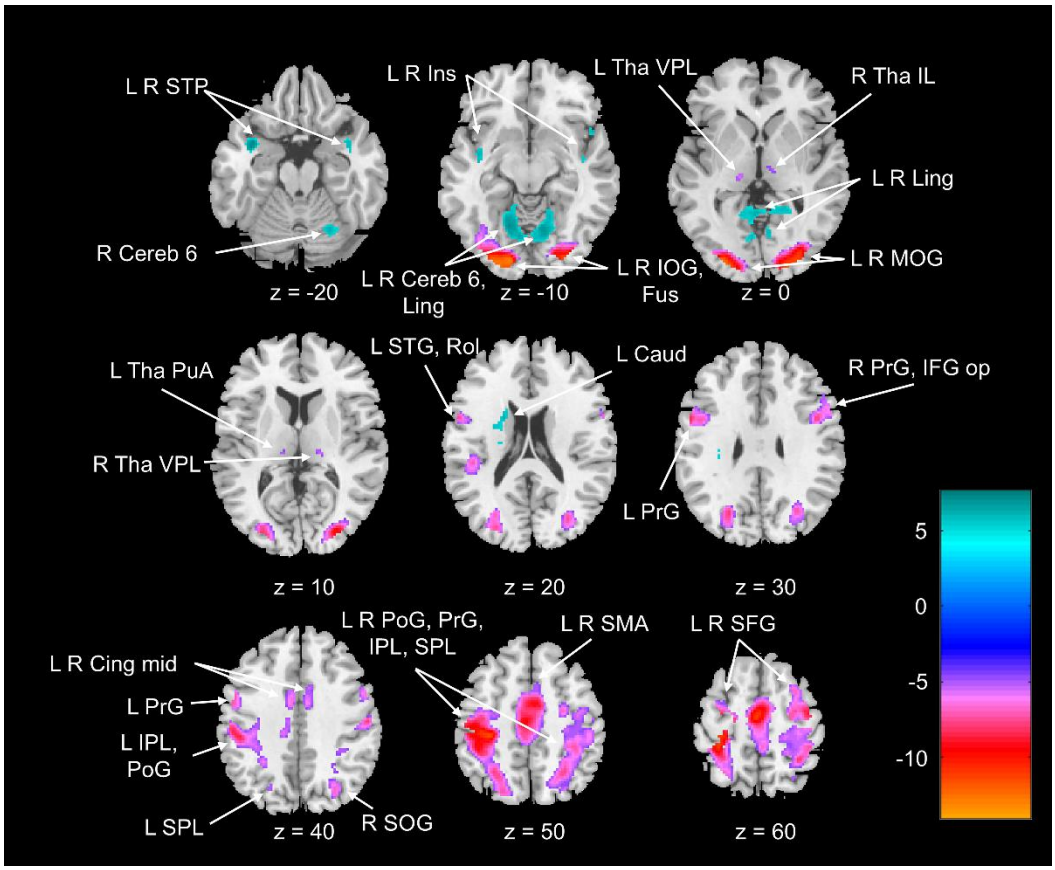

Note: Group-level activation maps for motor inhibition (positive t-values) and execution (negative t-values) during the go/no-go task (n = 69). The color bar represents t-statistic

magnitudes. Maps are thresholded at cluster-level family-wise error-corrected $p < 0.05$ (extent threshold: $k = 20$ voxels; height threshold: $t = 4.88$).

Abbreviations: STP, superior temporal pole; Cereb, cerebellum; Ins, insula; Ling, lingual gyrus; IOG, inferior occipital gyrus; Fus, fusiform gyrus; Tha VPL, thalamus ventral posterolateral nucleus; Tha IL, thalamus intralaminar nuclei; MOG, middle occipital gyrus; Tha PuA, thalamus anterior pulvinar nucleus; STG, superior temporal gyrus; Rol, rolandic operculum; Caud, caudate; PrG, precentral gyrus; IFG op, inferior frontal gyrus opercular part; Cing mid, mid-cingulate cortex; IPL, inferior parietal lobule; PoG, postcentral gyrus; SPL, superior parietal lobule; SOG, superior occipital gyrus; SMA, supplementary motor area; SFG, superior frontal gyrus.

Figure 3.

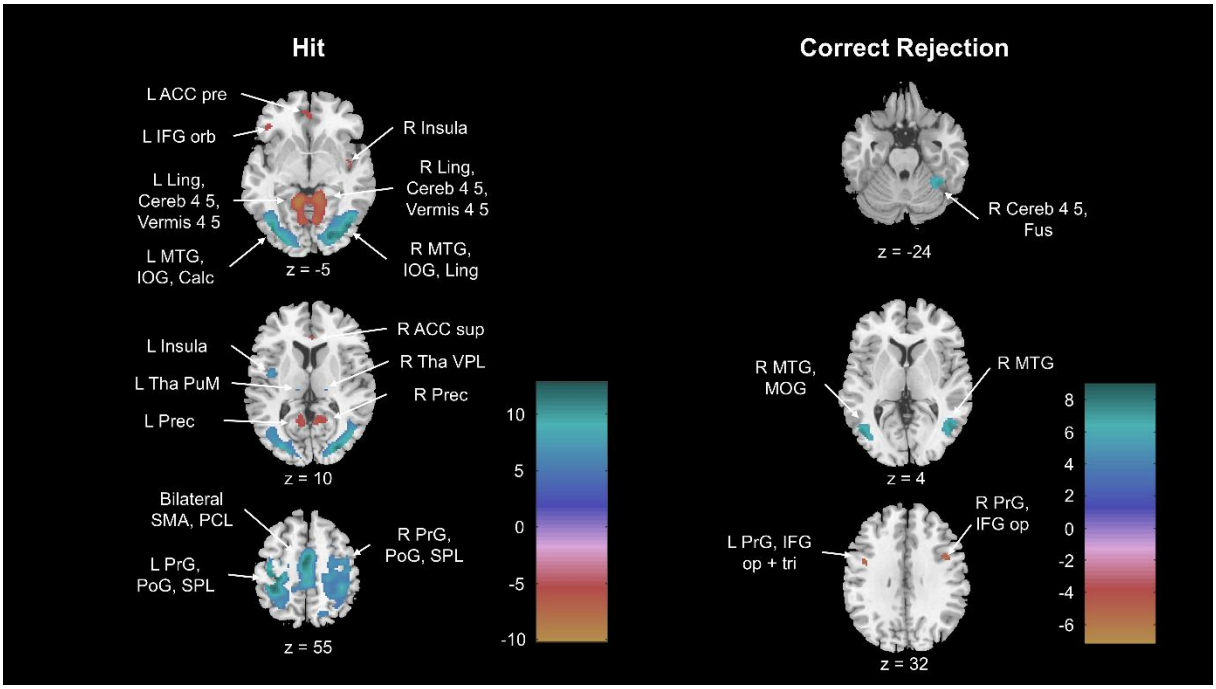

Results ($n = 69$) of the control analysis for only hit (left) and only correct rejection (right). The color bars represent t-statistic magnitudes. Activation maps are thresholded at a cluster-level family-wise error corrected $p < 0.05$, with an extent threshold of $k = 20$ voxels. The height threshold for significance is set at $t = 4.88$.

Abbreviations: ACC pre, pregenual anterior cingulate cortex; IFG orb, inferior frontal gyrus orbital part; Ling, lingual gyrus; Cereb, cerebellum; MTG, middle temporal gyrus; IOG, inferior occipital gyrus; Calc, calcarine cortex; Tha PuM, thalamus medial pulvinar nucleus; Prec, precuneus; ACC sup, supracallosal anterior cingulate cortex; Tha VPL, thalamus ventral posterolateral nucleus; SMA, supplementary motor area; PCL, paracentral lobule; PrG, precentral gyrus; PoG, postcentral gyrus; SPL, superior parietal lobule; Fus, fusiform gyrus; MOG, middle occipital gyrus; IFG op, inferior frontal gyrus opercular part; IFG tri, inferior frontal gyrus triangular part.

Supplementary Table 3. Significant Group Differences in BOLD Activity During Correct Rejection vs. Hit

Contrast	Region	MNI	k (voxels)	p-FWE	statistic
FP > HC	Left insula, left superior temporal gyrus	-44 0 -4	146	0.02	5.02
FP > HC	Left posterior cingulate cortex, bilateral precuneus	-6 -46 16	165	0.011	4.34
HC > FP	Left postcentral gyrus, left inferior parietal lobule	-30 -26 48	176	0.008	4.23
SCI > FP	Right postcentral gyrus, right precentral gyrus	46 -18 38	154	0.016	5.15
SCI > HC	Right postcentral gyrus, right precentral gyrus	42 -20 38	346	< 0.001	5.19
SCI > HC	Bilateral precuneus	0 -70 42	119	0.045	4.3

Note: All contrasts were thresholded at $p < 0.001$ (uncorrected) at the voxel level, with only clusters surviving $p < 0.05$ FWE-corrected at the cluster level reported. Only significant comparisons are shown. BOLD activity reflects differences during correct rejection trials vs. hit trials.

Abbreviations: FP, functional paralysis group; HC, healthy controls; SCI, spinal cord injury group; MNI, Montreal Neurological Institute standard space coordinates; k, cluster size; FWE, Family-wise error-corrected.

Sensitivity Analyses

Supplementary Table 4. Sensitivity Analyses: Behavioral and ROI-Level Functional Connectivity Results

Model	Partial η^2 (group)	statistic (df)	p-value
Response Time (Hits)			
RT ~ group	0.04	$\chi2 = 2.71_{(2)}$	0.258
RT ~ group + age + handedness + sex + HADS-D + HADS-A + analgesics + psychotropics	0.001	$\chi2 = 0.07_{(2)}$	0.968
Response Time (False Alarms)			
RT ~ group	0.12	$\chi2 = 5.74_{(2)}$	0.057
RT ~ group + age + handedness + sex + HADS-D + HADS-A + analgesics + psychotropics	0.01	$\chi2 = 0.46_{(2)}$	0.793
Accuracy			
ACC ~ group	0.06	$\chi2 = 4.33_{(2)}$	0.115
ACC ~ group + age + handedness + sex + HADS-D + HADS-A + analgesics + psychotropics	0.02	$\chi2 = 1.52_{(2)}$	0.467
Cluster 1			
FC ~ group + age + handedness	0.34; CI 95% [0.18, 1.00]	$F = 17.59_{(2, 64)}$	< 0.001
FC ~ group + age + handedness + sex + HADS-D + HADS-A + analgesics + psychotropics	0.36; CI 95% [0.19, 1.00]	$F = 10.22_{(2, 59)}$	< 0.001
Cluster 2			
FC ~ group + age + handedness	0.34; CI 95% [0.18, 1.00]	$F = 15.31_{(2, 64)}$	< 0.001

FC ~ group + age + handedness + sex + HADS-D + HADS-A + analgesics + psychotropics	0.34; CI 95% [0.18, 1.00]	$F = 14.13_{(2, 59)}$	< 0.001

Note: Behavioral models: Group effects were first assessed using Kruskal-Wallis tests (χ^2). Covariate-adjusted models were then fitted by regressing out effects of age, handedness, sex, HADS scores, and medication (analgesics/psychotropics) from residuals before testing group effects. Functional connectivity models: For each cluster (cluster 1: right precentral gyrus [seed] and left insula; cluster 2: right precentral gyrus [seed], left medial superior frontal gyrus, and bilateral supplementary motor area), two models were fitted: (1) a baseline model adjusted for age and handedness, and (2) a sensitivity model further adjusted for sex, HADS-Anxiety, and HADS-Depression to evaluate robustness. The group effect was assessed via partial η^2 and Type III ANOVA p-values; models were compared using likelihood ratio tests, and coefficients were reported with 95% CIs.

Abbreviations: RT, response time; ACC, accuracy; FC, functional connectivity; HADS-A, Hospital Anxiety and Depression Scale – Anxiety; HADS-D, Hospital Anxiety and Depression Scale – Depression; η^2, partial eta squared; CI, confidence interval; df, degrees of freedom.

Analysis Code

```
# go_no_go_analysis.R
# Task-based fMRI analysis for Go/No-Go data
# ------------------------------------------------

# 1. Load packages
library(tidyverse)
library(lme4)
library(car)
library(ggplot2)
library(ggpubr)

# 2. Set working directory to script location (requires RStudio)
setwd(dirname(rstudioapi::getSourceEditorContext()$path))

# 3. Read & preprocess data
go_nogo <- read_csv('go_nogo.csv') %>%
    mutate(condition = factor(condition),
           group     = factor(group))

# Split into hits and false alarms
hit <- filter(go_nogo, condition == 'hit')
FA  <- filter(go_nogo, condition == 'false_al')

# 4. Exclude extreme RTs (±2 SD) and non-positive values
```

```r
summarize_rt <- function(df) {
  m <- mean(df$key_resp.rt, na.rm = TRUE)
  s <- sd(df$key_resp.rt, na.rm = TRUE)
  df %>%
    filter(between(key_resp.rt, m - 2*s, m + 2*s),
           key_resp.rt > 0)
}

hit_filt <- summarize_rt(hit)
FA_filt  <- summarize_rt(FA)

# 5. Test RT differences across groups
# 5a. Descriptives by group
hit_filt %>% group_by(group) %>% summarize(mean_rt = mean(key_resp.rt),
                                           sd_rt   = sd(key_resp.rt))
# 5b. Levene's test for homogeneity
leveneTest(key_resp.rt ~ group, data = hit_filt)

# 5c. Participant-level means and nonparametric test
participant_rt <- hit_filt %>%
  group_by(participant, group, age) %>%
  summarize(mean_rt = mean(key_resp.rt), .groups = 'drop')

kruskal.test(mean_rt ~ group, data = participant_rt)

# 5d. Effect size (generalized η²) for Kruskal–Wallis
compute_eta2G <- function(ranks, groups) {
  grp_sizes  <- table(groups)
  grp_ranks  <- tapply(ranks, groups, sum)
  total_r    <- sum(ranks)
  mean_r     <- total_r / length(ranks)
  ss_eff     <- sum((grp_ranks^2)/grp_sizes) - total_r^2/length(ranks)
  ss_tot     <- sum((ranks - mean_r)^2)
  ss_err     <- ss_tot - ss_eff
  ss_eff/(ss_eff + ss_err)
}
eta2G_rt <- compute_eta2G(rank(participant_rt$mean_rt), participant_rt$group)
cat("RT η²G =", round(eta2G_rt, 3), "\n")

# 6. Sensitivity analysis with covariates
demog <- read_csv2('task_fMRI_FND_demog.csv') %>%
  slice(-c(6, 31)) %>%
  mutate(group = factor(group))
hand  <- read_csv('hand.csv')  %>% slice(-c(6, 31))
hadsa <- read_csv('HADS-A.csv') %>% slice(-c(6, 31))
hadsd <- read_csv('HADS-D.csv') %>% slice(-c(6, 31))
meds  <- read_csv('meds.csv')  %>% slice(-c(6, 31))
```

```r
RT_cov <- participant_rt %>%
  left_join(demog, by = c("participant")) %>%
  bind_cols(hand, hadsa, hadsd, meds, demog)

# Remove covariate effects and rerun KW
RT_cov$rt_resid <- resid(lm(mean_rt ~ age + sex_female + hand +
                              hadsa + hadsd + analgesics + psychotropic,
                            data = RT_cov))
kw_resid <- kruskal.test(rt_resid ~ group, data = RT_cov)
cat("Residual RT KW p-value =", kw_resid$p.value, "\n")

# 7. Response-time plots
# Boxplot of hit RT by group
ggplot(participant_rt, aes(group, mean_rt)) +
  geom_boxplot(outlier.shape = NA, width = 0.6) +
  geom_jitter(width = .1, alpha = .7) +
  labs(x = NULL, y = "Mean RT (s)") +
  theme_minimal()

# RT time series (all trials)
ggplot(go_nogo, aes(trial_start, key_resp.rt)) +
  geom_line(alpha = .6) +
  geom_smooth(method = "loess") +
  labs(x = "Time (s)", y = "RT (s)") +
  theme_minimal()

# 8. Accuracy analyses
accuracy <- go_nogo %>%
  group_by(participant, group, age) %>%
  summarize(
    overall_acc = mean(key_resp.corr, na.rm = TRUE) * 100,
    hit_acc     = mean(condition == "hit",    na.rm = TRUE) * 100,
    rej_acc     = mean(condition == "corr_rej", na.rm = TRUE) * 100,
    .groups = 'drop'
  )

# Nonparametric tests
kruskal.test(overall_acc ~ group, data = accuracy)
# Effect size
eta2G_acc <- compute_eta2G(rank(accuracy$overall_acc), accuracy$group)
cat("Accuracy η²G =", round(eta2G_acc, 3), "\n")

#sensitivity analysis
ACC <- cbind(accuracy, demog, hand, hadsa, hadsd, meds)
ACC$acc_resid <-
resid(lm(overall_acc~age+sex_female+hand+hadsa+hadsd+analgesics+psychotropic,
data=ACC))
kw_acc <- kruskal.test(acc_resid~group, data=ACC)
```

```r
print(kw_acc)
rks <- rank(ACC$acc_resid); gs <- table(ACC$group); gr <- tapply(rks,
ACC$group, sum)
tot <- sum(rks); m_r <- tot/nrow(ACC)
ss_e <- sum((gr^2)/gs) - tot^2/nrow(ACC)
ss_t <- sum((ACC$acc_resid - m_r)^2); ss_err <- ss_t-ss_e
eta2G_acc <- ss_e/(ss_e+ss_err)
cat("Acc cov-adjusted η²G=", round(eta2G_acc,3),"\n")

# Accuracy boxplot
ggplot(accuracy, aes(group, overall_acc)) +
  geom_boxplot(outlier.shape = NA, width = 0.6) +
  geom_jitter(width = .1, alpha = .7) +
  labs(x = NULL, y = "Accuracy (%)") +
  theme_minimal()

# 9. Accuracy over blocks
block_summary <- go_nogo %>%
  group_by(block_loop.thisN) %>%
  summarize(
    mean_acc = mean(key_resp.corr, na.rm = TRUE) * 100,
    se_acc   = sd(key_resp.corr, na.rm = TRUE) / sqrt(n()) * 100
  )

ggplot(block_summary, aes(factor(block_loop.thisN), mean_acc)) +
  geom_col(fill = NA, color = "black") +
  geom_errorbar(aes(ymin = mean_acc - se_acc, ymax = mean_acc + se_acc),
                width = 0.2) +
  labs(x = "Block", y = "Accuracy (%)") +
  theme_minimal()

# task_fMRI_conn_analysis.R
# Streamlined analysis of significant FC clusters from CONN
# ----------------------------------------------------------

# 1. Load packages
library(tidyverse)    # Data wrangling & ggplot2
library(rstatix)      # Statistical tests
library(ggpubr)       # ggplot enhancements
library(broom)        # Tidy model output
library(emmeans)      # Estimated marginal means
library(car)          # Anova type III
library(effectsize)   # Effect size calculations
library(boot)         # Bootstrap

# 2. Set working directory
setwd(dirname(rstudioapi::getSourceEditorContext()$path))
```

```r
# 3. Read & merge data
demog   <- read_csv2('task_fMRI_FND_demog.csv') %>%
  mutate(ID = row_number(), group = factor(group))
clus    <- read_csv('aal_2_clus.csv')
hand    <- read_csv('hand.csv')
hadsa   <- read_csv('HADS-A.csv')
hadsd   <- read_csv('HADS-D.csv')
meds    <- read_csv('meds.csv')
tsi     <- read_csv('tsi.csv')

data <- clus %>%
  bind_cols(demog, hand, hadsa, hadsd, meds, tsi) %>%
  drop_na()

# 4. Medications: Fisher tests by group
# Specify which meds you want to test
meds <- c("psychotropic", "analgesics")

res <- tibble(med = meds) %>%
  rowwise() %>%
  mutate(
    # build the contingency table: rows = 0/1, cols = group
    tbl = list(table(factor(data[[med]], levels = c(0,1)), data$group)),
    # run Fisher's exact test on the 2×3 table
    p_value = fisher.test(tbl)$p.value
  ) %>%
  ungroup() %>%
  # Bonferroni-correct the two p-values
  mutate(p_adj = p.adjust(p_value, method = "bonferroni"))

print(res)

# 5. Recode factors & define contrasts
data <- data %>%
  mutate(
    group       = factor(group, levels=c('FND','SCI','HC')),
    hand        = factor(hand),
    psychotropic= factor(psychotropic),
    analgesics  = factor(analgesics),
    SMA_ch = SMA_PrG_corr_rej - SMA_PrG_hit,
    Ins_ch = Ins_PrG_corr_rej - Ins_PrG_hit
  )

# 6. ANCOVA helper function
run_ancova <- function(df, response) {
  formula <- as.formula(paste(response, '~ age + hand + group'))
  lm_fit  <- lm(formula, data=df)
  aov_res <- Anova(lm_fit, type='III')
```

```
  eta     <- eta_squared(lm_fit, partial=TRUE)
  emm     <- emmeans(lm_fit, pairwise~group, adjust='bonferroni')
  list(
    lm      = lm_fit,
    ancova  = aov_res,
    eta     = eta,
    emmeans = emm
  )
}

# 7. Analyze SMA contrast
sma_res <- run_ancova(data, 'SMA_ch')
print(sma_res$ancova)
print(sma_res$eta)
print(sma_res$emmeans)

# 8. Plot SMA results
p_sma <- ggplot(data, aes(group, SMA_ch)) +
  geom_boxplot() +
  geom_jitter(width=0.1, alpha=0.7) +
  stat_pvalue_manual(
    broom::tidy(sma_res$emmeans$contrasts) %>%
      mutate(
        y.position = max(data$SMA_ch) + seq(0.02, by=0.02, length.out=n()),
        label = case_when(
          p.value<.001 ~ '***', p.value<.01 ~ '**', p.value<.05 ~ '*',
TRUE~'ns'
        )
      ),
    label='label', tip.length=0, size=5
  ) +
  labs(x=NULL, y='Δ FC (SMA)') + theme_minimal()

# 9. Analyze Insula contrast
ins_res <- run_ancova(data, 'Ins_ch')
print(ins_res$ancova)
print(ins_res$eta)
print(ins_res$emmeans)

# 10. Plot Insula results
p_ins <- ggplot(data, aes(group, Ins_ch)) +
  geom_boxplot() +
  geom_jitter(width=0.1, alpha=0.7) +
  stat_pvalue_manual(
    broom::tidy(ins_res$emmeans$contrasts) %>%
      mutate(
        y.position = max(data$Ins_ch) + seq(0.02, by=0.02, length.out=n()),
        label = case_when(
```

```
          p.value<.001 ~ '***', p.value<.01 ~ '**', p.value<.05 ~ '*',
TRUE~'ns'
        )
      ),
    label='label', tip.length=0, size=5
  ) +
  labs(x=NULL, y='Δ FC (Insula)') + theme_minimal()

# Display plots
print(p_sma)
print(p_ins)

# 11. Sensitivity analysis: add covariates
model_full <- lm(SMA_ch ~ group + age + hand + sex_female + `HADS-A` + `HADS-
D` + analgesics + psychotropic,
                 data=data)
eta_orig <- eta_squared(sma_res$lm, partial=TRUE) %>%
filter(Parameter=='group')
eta_full <- eta_squared(model_full, partial=TRUE) %>%
filter(Parameter=='group')
ANOVA_comparison <- anova(sma_res$lm, model_full)
list(eta_orig=eta_orig, eta_full=eta_full, model_comp=ANOVA_comparison)


# 12 Spearman correlations with clinical scores
scores <- data %>% filter(group!='HC')
# TSI vs SMA, Ins
scores %>%
  group_by(group) %>%
  summarise(
    rho_sma = cor(tsi, SMA_ch, method='spearman'),
    p_sma   = cor.test(tsi,SMA_ch,method='spearman')$p.value,
    rho_ins = cor(tsi, Ins_ch, method='spearman'),
    p_ins   = cor.test(tsi,Ins_ch,method='spearman')$p.value
  )

# 13. Correlation vs accuracy
go_nogo <- read_csv('go_nogo.csv') %>%
  group_by(participant, group) %>%
  summarise(
    acc = mean(key_resp.corr)*100,
    rt  = mean(key_resp.rt)
  )
merged  <- inner_join(data, go_nogo, by=c('ID'='participant','group'))

cor.test(merged$Ins_ch, merged$acc, method='spearman')

#Bootstrap Spearman correlation (Ins_ch vs. accuracy)
library(boot)
```

```r
# 1) Define a function that returns Spearman's ρ for a resampled dataset
cor_fun <- function(dat, indices) {
  d <- dat[indices, ]
  cor(d$Ins_ch, d$acc, method = "spearman")
}

# 2) Run the bootstrap (10 000 replications)
set.seed(2025)  # for reproducibility
boot_res <- boot(data = merged, statistic = cor_fun, R = 10000)

# 3) Print the raw bootstrap results
print(boot_res)

# 4) Compute bias-corrected & accelerated confidence intervals
boot_ci <- boot.ci(boot_res, type = "bca")
print(boot_ci)


# 14. Final combined plot: Ins_ch vs accuracy
ggplot(merged, aes(acc, Ins_ch, color=group)) +
  geom_point() + geom_smooth(method='lm', se=TRUE) +
  labs(x='Accuracy [%]', y='FC (Insula)') +
  theme_minimal(base_size=14)
```

References

1. Andersson JLR, Hutton C, Ashburner J, Turner R, Friston K. Modeling Geometric Deformations in EPI Time Series. *NeuroImage*. 2001;13(5):903-919. doi:10.1006/nimg.2001.0746

2. Friston KJ, Ashburner J, Frith CD, Poline JB, Heather JD, Frackowiak RSJ. Spatial registration and normalization of images. *Human Brain Mapping*. 1995;3(3):165-189. doi:10.1002/hbm.460030303

3. Whitfield-Gabrieli S, Nieto-Castanon A, Ghosh S. Artifact detection tools (ART). Published online 2011.

4. Ashburner J, Friston KJ. Unified segmentation. *NeuroImage*. 2005;26(3):839-851. doi:10.1016/j.neuroimage.2005.02.018

5. Ashburner J. A fast diffeomorphic image registration algorithm. *NeuroImage*. 2007;38(1):95-113. doi:10.1016/j.neuroimage.2007.07.007

6. Calhoun VD, Wager TD, Krishnan A, et al. The impact of T1 versus EPI spatial normalization templates for fMRI data analyses. *Human Brain Mapping*. 2017;38(11):5331-5342. doi:10.1002/hbm.23737

7. Friston KJ, Williams S, Howard R, Frackowiak RSJ, Turner R. Movement-related effects in fMRI time-series. *Magnetic resonance in medicine*. 1996;35(3):346-355.

8. Behzadi Y, Restom K, Liau J, Liu TT. A component based noise correction method (CompCor) for BOLD and perfusion based fMRI. *NeuroImage*. 2007;37(1):90-101. doi:10.1016/j.neuroimage.2007.04.042

9. Zhang R, Geng X, Lee TMC. Large-scale functional neural network correlates of response inhibition: an fMRI meta-analysis. *Brain Struct Funct*. 2017;222(9):3973-3990. doi:10.1007/s00429-017-1443-x

10. Schmahmann JD. The cerebellum and cognition. *Neuroscience Letters*. 2019;688:62-75. doi:10.1016/j.neulet.2018.07.005

2.4 Metabolic profile in functional paralysis

Lower Anterior Cingulate N-Acetylaspartate/Creatine Associated with Motor Impairment in Spinal Cord Injury but Not in Functional Paralysis

Vallesi, V., Galléa, C., Branzoli, F., Eriks-Hoogland, I., Gegusch, M., Zito, A. G., Wyss, P. O., Scheel-Sailer, A., Verma, R., Slotboom, J.

Contribution:

I contributed to all aspects of this study, including conceptualization, participant recruitment, data collection, data analysis, data interpretation, and manuscript drafting.

Under review in Translational Psychiatry (https://www.nature.com/tp/).

Lower Anterior Cingulate N-Acetylaspartate/Creatine Associated with Motor Impairment in Spinal Cord Injury but Not in Functional Paralysis

Authors:

Vanessa Vallesi [1, 2, 3], Cécile Galléa [4], Francesca Branzoli [4], Inge Eriks-Hoogland [2, 3, 5], Michaela Gegusch [6], Giuseppe A. Zito [2, 5], Patrik O. Wyss [3], Anke Scheel-Sailer [7], Rajeev K. Verma [2, 3, 5], Johannes Slotboom [1]

[1] Support Centre for Advanced Neuroimaging (SCAN), Institute for Diagnostic and Interventional Neuroradiology, Inselspital, Bern University Hospital, University of Bern, Bern, Switzerland

[2] Swiss Paraplegic Research, Nottwil, Switzerland

[3] Swiss Paraplegic Centre, Nottwil, Switzerland

[4] Paris Brain Institute, INSERM, CNRS, Sorbonne Université, Paris, France

[5] Faculty of Health Sciences and Medicine, University of Lucerne, Lucerne, Switzerland

[6] Clinic for Neurology, Cantonal Hospital St. Gallen, St. Gallen, Switzerland

[7] Centre for Rehabilitation and Sport Medicine, Inselgroup, Bern University Hospital, Bern, Switzerland

Corresponding author:

Vanessa Vallesi
Swiss Paraplegic Research
Guido A. Zäch Strasse 4
6207 Nottwil, Switzerland
E-Mail: vanessa.vallesi@hotmail.com

Abstract

Functional paralysis (FP), a subtype of functional neurological disorders, involves motor strength loss in certain limbs, resembling symptoms in spinal cord injury (SCI). Unlike SCI, caused by structural spinal cord damage, FP shows functional alterations in regions including the anterior cingulate (ACC) and insular cortices. This work aims to investigate metabolic alterations in FP, and compare them to SCI, to see whether these alterations are specific to the condition or represent a common consequence of paralysis, irrespective of its cause. Using Magnetic Resonance Spectroscopic Imaging, we compared metabolites in the ACC and insula of individuals with FP (n = 16, median age = 36 years, interquartile range [IQR] = 25.75, 5 males), individuals with SCI (n = 21, median age = 40 years, IQR = 15, 15 males), and healthy controls (HC) (n = 25, median age = 35 years, IQR = 17, 8 males). In the ACC, individuals with FP showed lower total N-acetyl-aspartate to total creatine ratio (tNAA/tCr) compared to HC (HL = -0.10, p_{adj} = 0.042), and the same was observed for those with SCI (HL = -0.11, p_{adj} = 0.042). Moreover, tNAA/tCr correlated significantly with motor strength in participants with SCI (ρ = 0.56, p = 0.014) but not in those with FP (ρ = 0.05, p = 0.869), indicating that lower tNAA/tCr was associated with greater loss of motor strength only in SCI. In FP, motor-strength severity appears independent of tNAA/tCr reduction, which may reflect the presence of paralysis rather than its magnitude.

Keywords: functional neurological disorder; brain metabolism; anterior cingulate cortex; paralysis; N-acetyl-aspartate

Introduction

Functional neurological disorder (FND) is characterized by a wide spectrum of neurological symptoms, ranging from negative motor symptoms (e.g., paralysis) to positive motor symptoms (e.g., tremor, dystonia) and non-motor manifestations such as functional seizures 0. A hallmark feature of functional paralysis (FP) is a lack of motor strength and/or sensation in certain limbs, a phenotypic presentation that can be quite similar to the paralysis observed in spinal cord injury (SCI). Both conditions result in limited mobility and often require assistive devices, such as wheelchairs, depending on the severity and level of symptoms. While SCI-related paralysis arises from structural damage to the spinal cord [1],

FND is often described as dysregulation of functional brain networks [2]. This distinction is supported by numerous fMRI studies in FND showing differences in brain activity and connectivity [3], though structural injury or damage has not been observed in this disorder [4].

Neuroimaging studies have systematically identified key marker regions of FND, such as the anterior cingulate and the insular cortices. A meta-analysis by Boeckle et al. [5] found that patients with the motor type of FND differ from healthy controls (HC) in regions including the insula, anterior cingulate cortex, the amygdala, thalamus, and prefrontal and motor cortex. When comparing affected versus unaffected sides, differences were particularly notable in the insula, anterior cingulate cortex, as well as in the temporal cortex, prefrontal cortex, and sensorimotor regions. Similarly, Weber et al. [6] used a multivariate machine learning approach to distinguish FND individuals from HC based on whole-brain resting-state functional connectivity, identifying key discriminant features in the insula, cingulate cortex, sensorimotor cortex, and hippocampal regions. In another classifier study, Waugh et al. [7] highlighted the sensorimotor cortex, dorsolateral prefrontal cortex, and insula as markers for FND.

The biological mechanisms underlying these functional differences are not fully understood, but some hypotheses emerge. Neuroinflammation may play a role in FND. Mueller et al. [8] reported higher brain temperature in the anterior cingulate cortex in participants with functional seizures. Brain temperature was shown to be an indicator for low-level neuroinflammation [9]. Additionally, systemic factors such as gut microbiome dysbiosis and chronic inflammation have been proposed as potential contributors to FND symptoms [10]. These findings raise the possibility that functional disruptions in FND may be accompanied by biochemical changes in cellular metabolism and signal transduction pathways, which regulate processes such as inflammation, synaptic transmission, and energy homeostasis.

Magnetic Resonance Spectroscopy (MRS) is a non-invasive method used to characterize the integrity of cellular metabolism in vivo in humans or preclinical models, by quantifying levels of specific metabolites underlying neuroinflammation or neuronal dysfunction. For instance, total N-acetyl-aspartate (tNAA, reflecting the combined pool of N-acetyl-aspartate and N-acetyl-aspartyl-glutamate), a marker of neuronal integrity and function, is involved in myelin lipid synthesis, osmoregulation, and mitochondrial metabolism [11,12]. Total choline-containing compounds (tCho), which plays a role in membrane synthesis, are often altered in neurodegenerative disorders [13,14]. Glutamate (Glu),

the primary excitatory neurotransmitter, is crucial for synaptic transmission, plasticity, and metabolism, while glutamine (Gln) regulates glutamate metabolism within the glutamate–glutamine cycle. Elevated levels of the sum of Glu and Gln (Glx) are associated with excitotoxicity in conditions like epilepsy [15]. Total creatine (tCr, representing the combined signal of creatine and phosphocreatine), essential for energy storage and transfer, is relatively stable in the brain under normal conditions [16], though altered levels are observed in disorders such as creatine deficiency syndromes [17]. A biomarker for neuroinflammation and glial proliferation in brain pathology is myo-inositol (mI), where higher levels are associated with astrocytosis and gliosis and lower levels with hypo-osmolar states [18].

Cellular metabolism measured with MRS is altered in SCI pathology. In the first 14 days after traumatically induced SCI in rats, significantly lower levels of tNAA and tCr were observed in the rostral, epicenter, and caudal segments of the spinal cord, remaining reduced up to 56 days post-injury [19]. In the subacute phase after SCI (2–9 months) in humans, tNAA and Glx increased in the pons, whereas tCr decreased [20], however, lower tNAA levels in the same region were found in the chronic phase [21].

Despite the differing etiologies of FP and SCI, both conditions share overlapping clinical features. This raises the question of whether potential biochemical changes in these regions are driven by the symptom of paralysis itself or by the underlying causality of paralysis. To address this question, we compared the metabolic profiles of FP participants with those of SCI participants and HC. We hypothesized that both paralysis groups would show distinct metabolic alterations compared to HC, and that these alterations would differ between FP and SCI, reflecting their divergent pathophysiologies. Finally, we examined whether aberrant metabolites correlated with motor strength to determine if shared symptoms arise from similar or distinct metabolic disturbances.

In this study, we employed 2D ^{1}H MR Spectroscopic Imaging (MRSI) using Point-Resolved Spectroscopy Sequence (PRESS) localization to investigate the regions of interest (ROIs) of the bilateral anterior cingulate cortex and bilateral insula, which were selected due to their relevance in FND [5–7] and their anatomical location, which allows for high spectral quality by being distant from bone, fat, and air-filled spaces.

Materials and methods

Study design and sample

This cross-sectional study was conducted between November 2022 and February 2024 at the Swiss Paraplegic Centre in Nottwil, Switzerland, and was approved by the local Ethics Committee of Northwest and Central Switzerland (EKNZ, reference number: 2021-01775). All participants provided written informed consent. The study adheres to the STROBE (Strengthening the Reporting of Observational Studies in Epidemiology) guidelines, and the ethical principles of the Declaration of Helsinki were followed. A preregistration is available on ClinicalTrials.gov (identifier: NCT05139732).

The recruitment of participants was conducted through the Swiss Paraplegic Centre and the Clinic for Neurology at the Cantonal Hospital St. Gallen via advertisements, as well as physician referrals. Inclusion was possible for individuals aged 18–60 years and for those in the two paralysis groups who had experienced symptoms for at least 6 months. Exclusion criteria included any MRI contra-indications, a history of neurological disorders (e.g. epilepsy or tumor) other than FP and SCI, as well as any severe psychiatric conditions (e.g. schizophrenia).

A power calculation using G*Power [22] determined a priori a sample size of 74, based on a power of 0.8 (as determined by prior studies from our team), an expected effect size of 0.37, and a significance level (α) of 5%. This resulted in 25 participants per group.

Participants with insufficient spectral quality in a given ROI were excluded (see Table 1). Exclusions resulted from spectral artifacts, or ROIs missed due to spatial planning errors.

Clinical measurements

For the entire sample, the following psychological questionnaires were administered: the Satisfaction with Life Scale (SWLS) [23], pain intensity during the examination and in the past 7 days using the Numeric Rating Scale (NRS) [24], and anxiety and depression using the Hospital Anxiety and Depression Scale (HADS-A and HADS-D) [25]. Symptom severity for the two paralysis groups was measured with the International Standards for Neurological Classification of Spinal Cord Injury (ISNCSCI) [26], which was conducted by certified physicians. With this, scores for motor strength, light touch, and pin prick were obtained. The time since symptom onset (TSS) in years was collected, and additionally, the Spinal Cord Independence Measure (SCIM) [27] for the assessment of functionality was administered.

MRI/MRSI acquisition

Structural MRI and ^{1}H MRSI were conducted using a clinical 3 T MRI unit (Philips Achieva, Release 5.1.7; Philips Healthcare, Best, the Netherlands) with a 32-channel head coil (Philips Healthcare). The MR scan protocol included a three-dimensional anatomical T1-weighted image and a 2D PRESS sequence for spectroscopic imaging. The structural image was acquired with the following parameters: Repetition time (TR) = 8.5 ms; echo time (TE) = 4.1 ms, flip angle = 8°, field of view (FOV) = 256 × 256× 25 mm³, 25 slices and a voxel volume of 1 × 1 × 1 mm³. For the MRSI, the following parameters were used: TR = 1500 ms, TE = 30 ms, spectral bandwidth = 2000 Hz, readout duration = 512 ms, 1024 samples (1.95 Hz/point resolution), with nominal voxel size of 10 × 10 × 15 mm³ (reconstructed to 5 × 5 × 15 mm³, 16 × 16 matrix), totalling 6:20 min scan time. The FOV was 160 × 160 mm², and the excited volume of interest (VOI) was 80 × 80 × 15 mm³. The scan was performed in transverse orientation with the participant in a head-first, supine position. The VOI was consistently positioned based on anatomical landmarks for all participants, ensuring standardised placement across the 2D MRSI plane. Second-order static magnetic field (B_0) shimming was performed automatically using the scanner's volume-based pencil-beam method (PB-volume). Water suppression was achieved using an excitation-based scheme with a suppression window of 140 Hz and a second pulse angle of 300°. Outer volume suppression was implemented using circular saturation slabs (10 slabs, thickness = 30 mm) to minimize signal from metabolic and subcutaneous lipids in tissues surrounding the brain.

^{1}H spectroscopy analysis

MRSI data were analyzed using a model-based fitting approach implemented in SpectrIm version 2.0.12 (available at https://spectrim.diskstation.me/spectrImWeb/) [28]. The raw spectra were preprocessed to improve spectral quality, including water removal using the HLSVDPro algorithm (4 – 9 ppm, 8 components), truncation of the frequency domain (10.943 – 12.509 ppm), frequency shift correction, automatic phasing algorithm (1.5 – 4.4 ppm), and exponential apodization. The preprocessed spectra were fitted using TDFDfit [29], a time/frequency-domain fitting algorithm, with a predefined model incorporating prior knowledge of metabolite spectra. The basis set for spectral fitting was simulated using NMRScope of the jMRUI package [30], and included the metabolite signal profiles of tNAA,

tCho (glycerophosphocholine + phosphocholine), mI + glycine, Glx, lactate, and tCr. The fitting process optimized model parameters to minimize the residual between the observed and modeled spectra, enabling accurate quantification of metabolite peak areas. The quality of the fit of all spectra was individually checked by two of the authors, and any spectra with poor fit quality were excluded from the analysis. The sum of glutamate and glutamine was calculated and reported as Glx, reflecting the combined contribution of these metabolites to the glutamatergic system. Metabolite areas were quantified as ratios relative to tCr. Specifically, the area under the curve for each metabolite was divided by the area under the curve for tCr (e.g., tNAA/tCr, tCho/tCr, mI/tCr, Glx/tCr). This approach was chosen because tCr is considered a stable reference metabolite, and its use is consistent with previous research on FND. Representative spectra and voxel placements for each group are shown in Supplementary Figures S1–S3. Gray matter, white matter, and cerebrospinal fluid volumes were compared between groups; signal-to-noise ratio and spectral linewidth were also assessed (see Supplementary Table 1 and 2 for details).

Statistical analysis

Statistical analyses were performed using R (version 4.4.3). Categorical demographic variables were compared between groups using Fisher's exact test. Continuous clinical measures and metabolite ratios were assessed for normality (Shapiro–Wilk test) and homogeneity of variance (Levene's test); due to violations of these assumptions and unequal sample sizes, non-parametric tests and permutation-based methods were employed. As the omnibus test, group comparisons of metabolite ratios were conducted by permutation-based analysis of covariance (ANCOVA; Freedman–Lane method, 10,000 permutations)[31,32] with sex as a covariate. We then performed sex-stratified post-hoc pairwise comparisons (10,000 permutations), calculating Hodges–Lehmann median differences and their 95 % bootstrapped confidence intervals (10,000 iterations)[33]. To control Type I error, p-values were adjusted within each model using the false discovery rate (FDR) at $\alpha = 0.05$. Effect sizes were reported as partial eta squared, with $\eta_p^2 \geq 0.01$ considered small, $\eta_p^2 \geq 0.06$ medium, and $\eta_p^2 \geq 0.14$ large [34]. Relationships between variables were assessed using partial Spearman's rank correlation (coefficient ρ), with correlations interpreted as weak ($|\rho| < 0.3$), moderate ($0.3 \leq |\rho| < 0.5$), or strong ($|\rho| \geq 0.5$) [35].

Results

Demographics

After ROI-specific spectral quality exclusions, final sample sizes ranged from 56 to 61 participants per region (see Table 1 for details). Exclusions affected 9–14 participants per region from the initial sample (N = 70). All demographic information is reported in Table 2. Age did not differ significantly between the groups. Sex distribution differed significantly between groups (see Table 2), consequently, it was included as a covariate in primary analyses. There was a significant group difference in the SWLS, pain during the examination and in the last 7 days, and anxiety and depression scores. FP and SCI showed no difference in SCIM, motor strength, or light touch, but they differed significantly in terms of TSS and pin prick scores.

Table 1: Sample sizes for each region of interest

ROI	FP	SCI	HC	Total
Anterior cingulate cortex	16	20	25	61
Left insula	15	21	21	57
Right insula	15	21	20	56

Abbreviations: ROI, region of interest; FP, functional paralysis; SCI, spinal cord injury; HC, healthy controls.

Table 2: Demographic characteristics of participants.

	FP (n = 16)	SCI (n = 21)	HC (n = 25)	Test statistic	*p*-Value
Age in years	36 (25.75)	40 (15)	35 (17)	$\chi 2 = 1.15$	0.563
Sex (n males)	5	15	8	n. a.	0.023

SWLS	22.5 (12.25)	28(6)	29 (3)	$\chi2 = 12.41$	0.005
NRS (current moment)	4 (4.5)	0 (3)	0 (0)	$\chi2 = 18.71$	< 0.001
NRS (past 7 days)	4 (4)	1 (4)	0 (1)	$\chi2 = 22.37$	< 0.001
HADS-A	5.5 (5.75)	4 (5)	4 (3)	$\chi2 = 6.59$	0.043
HADS-D	2.5 (6)	2 (4)	2 (2)	$\chi2 = 7.36$	0.035
TSS in years	3 (4.28)	12 (19)	n. a.	W = 93.5	0.023
SCIM	79 (35.25)	75 (30)	n. a.	W = 180	0.724
Motor strength	78.5 (41)	68 (46)	n. a.	W = 193	0.45
Light touch	94 (40.5)	75 (30)	n. a.	W = 214	0.072
Pin prick	98 (38)	70 (35)	n. a.	W = 228	0.024

Abbreviations: ROI, region of interest; FP, functional paralysis; SCI, spinal cord injury; HC, healthy controls; swls, satisfaction with life scale; NRS, numeric rating scale; HADS-A, hospital anxiety and depression scale - anxiety; HADS-D, hospital anxiety and depression scale - depression; TSS, time since symptoms; SCIM, spinal cord independence measure; n.a., not applicable.

Note: In all rows except for sex the median and interquartile range are reported. Test statistics from the Kruskal-Wallis rank sum test or Wilcoxon rank-sum test are reported. For Fisher's exact test, test statistics are not applicable. A false-discovery rate adjusted p-value of less than 0.05 was considered significant.

Metabolic parameters

The metabolite ratios in the anterior cingulate cortex for all three groups are shown in Figure 1. Only tNAA/tCr showed a significant group difference ($F_{(2, 57)} = 4.74$, $p = 0.011$, $\eta_p^2 = 0.14$, large effect) with the FP group differing from HC (HL = -0.10, $p_{adj} = 0.042$, 95 % CI [-0.20, -0.004]) but no difference from the SCI group (HL = -0.01, $p_{adj} = 0.876$, 95 % CI [-0.09, 0.08]). There was a significant difference between the SCI group and HC (HL = -0.11, $p_{adj} = 0.042$, 95% CI [-0.16, -0.03]). There were no group differences in tCho/tCr, mI/tCr or

Glx/tCr (see Table 3). In this ROI, tNAA/tCr correlated significantly with the motor strength score in the SCI group (ρ = 0.55, p = 0.014, large effect), but no correlation was observed in the FP group (ρ = 0.05, p = 0.869) (see Figure 2). This association remained significant in sensitivity analyses adjusting for age, TSS, current pain intensity NRS, and depressive/anxiety symptoms (all $p < 0.05$, Supplementary Table 3). No significant group differences were found in the left insula for tNAA/tCr, tCho/tCr, mI/tCr or Glx/tCr (see Figure 3 and Table 3). In the right insula, only tCho/tCr showed a significant group effect ($F_{(2, 52)}$ = 3.65, p = 0.034, η_p^2 = 0.12, medium effect) with the SCI group differing from HC (HL = -0.04, p_{adj} = 0.018, 95 % CI [-0.11, 0.02]) but no difference from the FP group (HL = -0.06, p_{adj} = 0.063, 95% CI [-0.02, 0.12]). The FP group showed no difference to HC (HL = 0.01, p_{adj} = 0.928, 95% CI [0.002, 0.01]). The tCho/tCr ratio showed no statistically significant correlation with the motor strength score in individuals with SCI (ρ = -0.12, p = 0.606).

Figure 1.

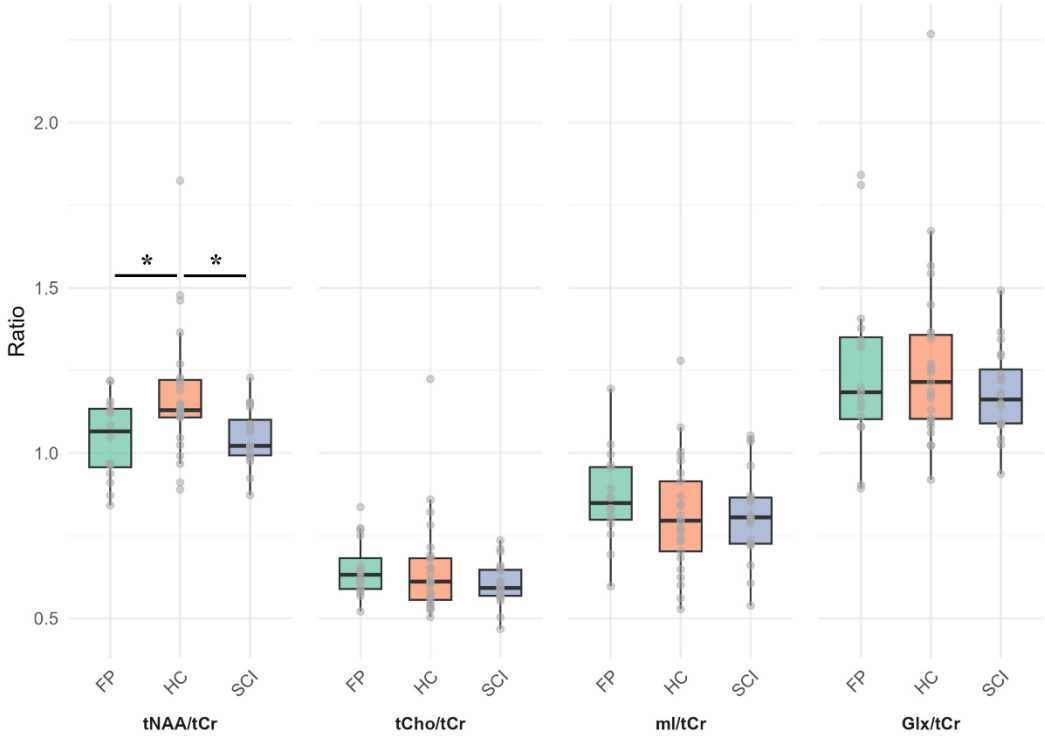

Note: Metabolite ratios in the anterior cingulate cortex among individuals with functional paralysis (FP), spinal cord injury (SCI), and healthy controls (HC). There was a significant group difference in total N-acetyl-aspartate/total creatine (tNAA/tCr) ($F_{(2, 57)}$ = 4.74, p =

0.011, η_p^2 = 0.14), with the FP and the SCI group showing lower ratios compared to HC. However, there were no significant differences in total choline/total creatine (tCho/tCr), myo-inositol/total creatine (mI/tCr) or (glutamate + glutamine)/total creatine (Glx/tCr).

Figure 2.

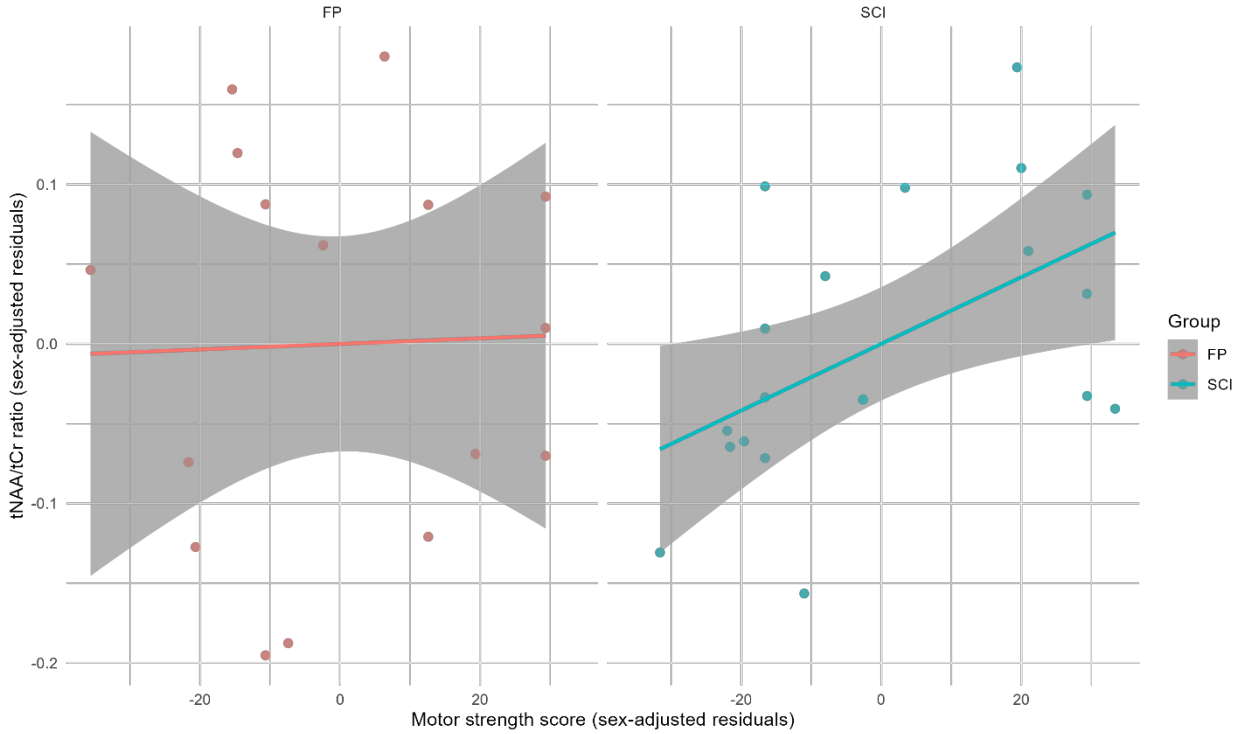

Note: Partial spearman correlation (adjusted for sex residuals) between total N-acetyl-aspartate/total creatine (tNAA/tCr) in the anterior cingulate cortex and the score for motor strength. There was no significant correlation in the functional paralysis (FP) group ($\rho = 0.05$, $p = 0.869$); however, there was a significant positive correlation in the spinal cord injury (SCI) group ($\rho = 0.56$, $p = 0.014$).

Figure 3.

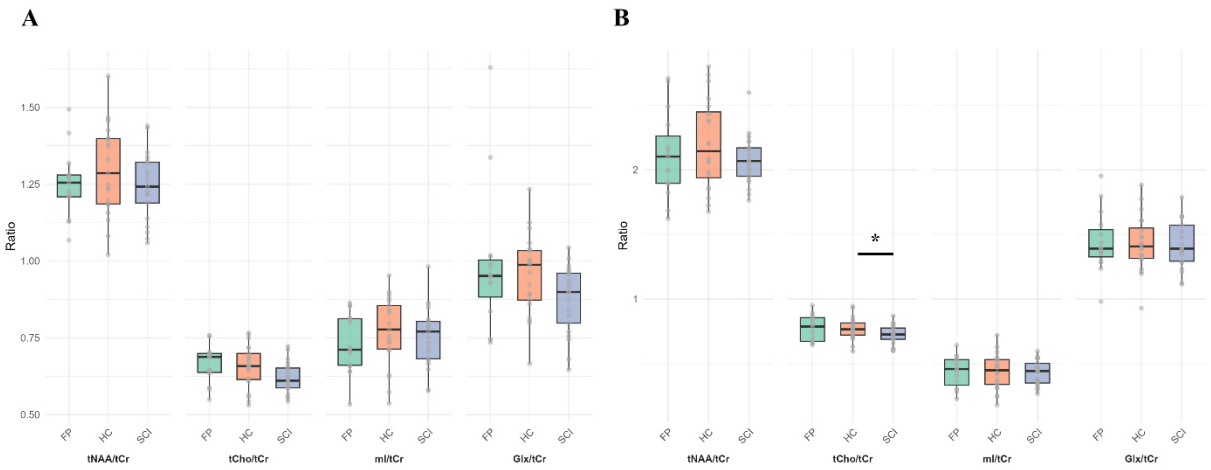

Note In A: Metabolite ratios in the left insula among individuals with functional paralysis (FP), spinal cord injury (SCI), and healthy controls (HC). There were no significant group differences in total N-acetyl-aspartate/total creatine (tNAA/tCr), total choline/total creatine (tCho/tCr), myo-inositol/total creatine (mI/tCr) or (glutamate + glutamine)/total creatine (Glx/tCr).

In B: Metabolite ratios in the right insula between the groups FP, HC, and SCI. Only tCho/tCr differed significantly between groups ($F_{(2, 52)} = 3.65$, $p = 0.034$, $\eta_p^2 = 0.12$), driven by a lower ratio in SCI versus HC. There were no significant differences in tNAA/tCr, mI/tCr or Glx/tCr.

Table 3: Summary of MRSI Metabolite Ratio Comparisons Between Healthy Controls, Functional Paralysis, and Spinal Cord Injury Groups

	Test statistic	P-Value	Effect size	FP vs HC	FP vs SCI	SCI vs HC
Anterior cingulate cortex						
tNAA/tCr	$F_{(2, 57)} = 4.74$	0.011	0.143	HL = -0.10 $p_{adj} = 0.044$ CI [-0.20, -0.004]	HL = -0.01 $p_{adj} = 0.876$ CI [-0.09, 0.08]	HL = -0.11 $p_{adj} = 0.044$ CI [-0.16, -0.03]

tCho/tCr	$F_{(2, 57)} = 0.14$	0.884	0.005			
mI/tCr	$F_{(2, 57)} = 0.70$	0.508	0.024			
Glx/tCr	$F_{(2, 57)} = 0.12$	0.894	0.004			
Left insula						
tNAA/tCr	$F_{(2, 53)} = 0.30$	0.740	0.011			
tCho/tCr	$F_{(2, 53)} = 3.07$	0.055	0.104			
mI/tCr	$F_{(2, 53)} = 0.57$	0.578	0.021			
Glx/tCr	$F_{(2, 53)} = 1.84$	0.169	0.065			
Right insula						
tNAA/tCr	$F_{(2, 52)} = 0.76$	0.473	0.028			
tCho/tCr	$F_{(2, 52)} = 3.65$	0.034	0.123	HL = 0.01 p_{adj} = 0.928 CI [-0.07, 0.08]	HL = 0.06 p_{adj} = 0.066 CI [-0.03, 0.12]	HL = -0.04 p_{adj} = 0.024 CI [-0.10, 0.01]
mI/tCr	$F_{(2, 52)} = 0.05$	0.950	0.002			
Glx/tCr	$F_{(2, 52)} = 0.22$	0.807	0.008			

Abbreviations: FP, functional paralysis; SCI, spinal cord injury; HC, healthy controls; tNAA, total N-acetyl-aspartate; tCho, total choline; tCr, total creatine; mI, myo-inositol; Glx, Glutamate + Glutamine; HL, Hodges-Lehmann; CI, confidence interval.

Note: All omnibus tests were conducted using permutation-based ANCOVA (Freedman–Lane method, 10,000 resamples) with sex as a covariate; the permutation p-values and

partial eta squared effect sizes are reported. Post-hoc pairwise comparisons were performed only when the omnibus group effect was significant, using stratified permutation tests (10'000 resamples) with p-values adjusted by false discovery rate. Hodges–Lehmann median differences and their 95 % bootstrap confidence intervals (10'000 samples) are presented.

Discussion

We aimed to investigate metabolic alterations in FP in comparison to SCI, to decipher their relationship with symptoms, which could be either specific to the condition or represent a common consequence of paralysis, irrespective of its cause. We observed significantly lower tNAA/tCr ratios (a marker of neuronal viability) in the bilateral anterior cingulate cortex of both FP and SCI participants compared to HC. Within the SCI group, lower tNAA/tCr correlated with weaker motor strength, indicating that anterior cingulate neuronal integrity scales with motor function. In contrast, FP participants showed reduced tNAA/tCr regardless of motor strength, suggesting a threshold-like dysfunction rather than a graded effect. This dissociation implies that anterior cingulate tNAA/tCr reductions in SCI reflect spinally mediated neuronal loss or deafferentation, whereas in FP we suggest that they likely arise from dysfunctional higher-order networks. Finally, FP participants did not differ from HC in tCho/tCr (a marker of inflammation), mI/tCr (a marker for neuroinflammation or glial proliferation), or Glx/tCr (a marker of excitatory neurotransmission) [36,37] in either the bilateral anterior cingulate cortex or bilateral insula.

In the context of FND, metabolic alterations appear to vary across symptom subtypes. For instance, Demartini et al. [38] reported higher Glx/tCr in the anterior cingulate cortex, which correlated with symptom severity in individuals with positive FND symptoms (e.g., tremor, gait disorder, or myoclonus), whereas we were unable to detect these glutamatergic changes in the ACC within our FND cohort characterized by negative symptoms. This suggests that elevated glutamatergic levels in the anterior cingulate cortex may be specific to the positive symptom subtype of FND. Conversely, our observed lower tNAA/tCr levels would reflect the presence of negative symptoms — a pattern we also found in individuals with SCI. Consistently, individuals with the positive motor phenotype of functional seizures were characterized by normal tNAA/tCr levels but showed higher mI/tCr in the anterior cingulate cortex [8], indicating neuroinflammation in this region. In children with mixed FND

subtypes, lower tNAA/tCr levels were observed in the posterior cingulate cortex [39], suggesting that metabolic alterations in FND may be region-specific within the cingulate cortex. Future studies should investigate different cingulate subregions to refine the anatomical understanding of FND, with a focus on clinical subtypes to clarify their roles in this disorder [4].

Atrophic and microstructural changes in the sensorimotor cortex emerge within the first few months following SCI [40]. Our 2D-MRSI slab selection excited a volume covering the anterior cingulate and insular cortices but did not include the sensorimotor cortex. It is likely that the changes we observed in the anterior cingulate cortex for the SCI group may be associated with the alterations in the sensorimotor cortex, as motor strength is, in general, tightly associated with properties of the sensorimotor cortex [40]. The association between lower tNAA/tCr levels and motor strength loss in SCI is consistent with the broader literature. Wyss et al. [41] reported lower tNAA concentrations in the cervical spinal cord of SCI participants compared to HC, which were associated with worse motor strength. Furthermore, Liu et al. [42] found a similar relationship in SCI between tNAA levels and motor strength using the same scoring system, reporting a comparably high correlation but focusing on the precentral gyrus. Widerström-Noga et al [43] also reported lower tNAA levels in the anterior cingulate cortex of individuals with SCI and neuropathic pain, linking these changes to pain-related psychosocial impact.

The bilateral insula in our FP group showed levels of tNAA, tCho, mI, and Glx comparable to those in HC, indicating preserved membrane and glial/neurotransmitter metabolism in FP. This observation is particularly notable given that this region is frequently highlighted as a key marker of altered functional activity in FND [5–7]. We hypothesize that functional changes in the insular cortex may reflect differences in information processing (e.g., interoceptive integration) rather than underlying biochemical disturbances. In contrast, our SCI group exhibited significantly lower tCho/tCr levels in the right insula compared to HC. However, the bootstrapped 95% CI included 0, suggesting that while this difference is statistically significant, there is a possibility that there is no effect (i.e., the true difference could be 0). This indicates that, although the observed difference is unlikely to be due to chance, the clinical relevance of the finding may be limited. This conclusion was further supported by the absence of a correlation between tCho/tCr levels and motor strength scores in this cohort.

Several limitations should be considered when interpreting these findings. Although the targeted sample size was achieved for the HC group and nearly achieved for the SCI group, the FP group notably differed from the targeted sample size due to recruitment difficulties. To ensure the robustness and generalizability of our findings, effect sizes were included in all analyses. The study groups showed expected demographic differences: sex distribution varied between paralysis groups, reflecting known epidemiological patterns (FND being female-predominant and SCI male-predominant) [44,45]. Importantly, age was equally distributed across all three groups (FP, SCI, and HC). To maximize statistical power, we controlled only for necessary covariates, specifically including sex in all analyses of metabolite ratios. This approach ensured robust detection of disorder-specific effects while appropriately accounting for the primary demographic confounder. The FP group showed slightly higher HADS-A and HADS-D scores, but these scores remained within the range of mild symptoms, making them negligible. While TSS differed between the FP and SCI groups, our analyses showed that TSS was not significantly associated with metabolite ratios in the ROIs. Importantly, the association between lower tNAA/tCr in the ACC and reduced motor strength in the SCI group remained significant after adjusting for TSS (Supplementary Table 3), suggesting this relationship is independent of chronicity of injury. To directly compare the symptoms between FP and SCI groups, we examined participants with FP using the same standardized neurological examination as the ISNCSCI, even though this examination has not been formally validated for FND. This approach was necessary because the ISNCSCI provides an objective measure of functional impairment (motor and sensory scores) that could be equally applied to both populations. While the sensory score for pinprick showed a significant difference between groups, the sensory score for light touch did not differ significantly. Importantly, motor strength scores also showed no significant differences between groups, and this measure was used for the correlation analysis. Consequently, symptom severity was comparable between the two paralysis groups.

Another limitation relates to the spectroscopy measurements. All spectroscopy data were acquired using the PRESS localization technique. While some may suggest that this technique has limitations [18,46], particularly at 3T and above, due to potential chemical shift displacement artifacts (CSDA) and reduced sensitivity caused by RF-pulse imperfections and B1+ inhomogeneity, it remains a viable option when compared to more advanced techniques such as LASER and semiLASER [47,48]. PRESS was used because the semiLASER-MRSI sequence for the scanner hardware/software version at the time of data acquisition was

unavailable. Strictly speaking, CSDA-related biases may limit the comparability of measurements across different anatomical locations. However, MRSI planning was consistently performed following a fixed protocol, limiting the variability of the field of view covering the ROIs and arbitrary-shaped anatomical regions could be sub-selected from the 2D-MRSI grid during SpectrIm processing. We are confident that inter-subject differences in CSDA are likely negligible. A further limitation concerns the presence of small, highly alternating water residuals in the frequency domain after HLSVDpro-based water suppression. These residuals did not significantly affect the frequency-selective fitting performed by TDFDFit [29], and represent a minor technical limitation given the data processing pipeline.

In conclusion, our findings suggest that while the clinical presentation of paralysis and associated motor impairments was highly similar between FP and SCI groups, with both showing reduced tNAA/tCr levels in the anterior cingulate cortex, a critical difference emerged in their relationship to motor strength. In SCI, lower motor strength scaled with reduced tNAA/tCr, whereas this pattern was absent in FP. This dissociation likely reflects distinct pathophysiological mechanisms underlying these conditions despite their shared symptoms. What mediates the tNAA/tCr reductions in FP remains unclear. To fully unravel the complex pathology of FND, future studies should employ whole-brain MRS across FND subtypes to map metabolic profiles and identify consistent patterns. Such an approach could bridge cellular-level changes with clinical manifestations, advancing our understanding of FND's neurobiology.

Acknowledgements

We thank Elia Hurni, Nadia Sauder, and Corinne Kehl for assistance with recruitment and data collection, and the MR technicians of the Swiss Paraplegic Centre for scan acquisition. V.V. (first author) gratefully acknowledges the Paris Brain Institute for their hospitality during her research stay.

Funding

This work was partially supported by the UniBE Doc.Mobility Grant of the University of Bern.

Data availability

The data underpinning the results of this study are accessible from the corresponding author upon reasonable request.

Conflict of Interest Statement

The authors declare no conflicts of interest related to this work.

References

1. Anjum A, Yazid MD, Daud MF, et al. Spinal Cord Injury: Pathophysiology, Multimolecular Interactions, and Underlying Recovery Mechanisms. *Int J Mol Sci*. Published online 2020:35.

2. Bègue I, Adams C, Stone J, Perez DL. Structural alterations in functional neurological disorder and related conditions: a software and hardware problem? *NeuroImage: Clinical*. 2019;22:101798. doi:10.1016/j.nicl.2019.101798

3. Thomsen BLC, Teodoro T, Edwards MJ. Biomarkers in functional movement disorders: a systematic review. *J Neurol Neurosurg Psychiatry*. 2020;91(12):1261-1269. doi:10.1136/jnnp-2020-323141

4. Hallett M, Aybek S, Dworetzky BA, McWhirter L, Staab JP, Stone J. Functional neurological disorder: new subtypes and shared mechanisms. *The Lancet Neurology*. 2022;21(6):537-550. doi:10.1016/S1474-4422(21)00422-1

5. Boeckle M, Liegl G, Jank R, Pieh C. Neural correlates of conversion disorder: overview and meta-analysis of neuroimaging studies on motor conversion disorder. *BMC Psychiatry*. 2016;16(1):195. doi:10.1186/s12888-016-0890-x

6. Weber S, Heim S, Richiardi J, et al. Multi-centre classification of functional neurological disorders based on resting-state functional connectivity. *NeuroImage: Clinical*. 2022;35:103090. doi:10.1016/j.nicl.2022.103090

7. Waugh RE, Parker JA, Hallett M, Horovitz SG. Classification of Functional Movement Disorders with Resting-State Functional Magnetic Resonance Imaging. *Brain Connectivity*. 2023;13(1):4-14. doi:10.1089/brain.2022.0001

8. Mueller C, Sharma A, Szaflarski JP. Peripheral and Central Nervous System Biomarkers of Inflammation in Functional Seizures: Assessment with Magnetic Resonance Spectroscopy. *NDT*. 2023;Volume 19:2729-2743. doi:10.2147/NDT.S437063

9. Plank JR, Morgan C, Sundram F, et al. Brain temperature as an indicator of neuroinflammation induced by typhoid vaccine: Assessment using whole-brain magnetic resonance spectroscopy in a randomised crossover study. *NeuroImage: Clinical*. 2022;35:103053. doi:10.1016/j.nicl.2022.103053

10. Borrego-Ruiz A, Borrego JJ. Functional neurological disorder and gut microbiome: Casual or causal relationship? *JCBP*. 2024;2(4):4160. doi:10.36922/jcbp.4160

11. Shannon RJ, Van Der Heide S, Carter EL, et al. Extracellular *N* -Acetylaspartate in Human Traumatic Brain Injury. *Journal of Neurotrauma*. 2016;33(4):319-329. doi:10.1089/neu.2015.3950

12. Zheng J, Zhang Y, Zhao B, Wang N, Gao T, Zhang L. Metabolic changes of thalamus assessed by 1H-MRS spectroscopy in patients of cervical spondylotic myelopathy following decompression surgery. *Front Neurol*. 2025;15:1513896. doi:10.3389/fneur.2024.1513896

13. Guo L, Tian J, Du H. Mitochondrial Dysfunction and Synaptic Transmission Failure in Alzheimer's Disease. *JAD*. 2017;57(4):1071-1086. doi:10.3233/JAD-160702

14. Öz G, Alger JR, Barker PB, et al. Clinical Proton MR Spectroscopy in Central Nervous System Disorders. *Radiology*. 2014;270(3):658-679. doi:10.1148/radiol.13130531

15. Sarlo GL, Holton KF. Brain concentrations of glutamate and GABA in human epilepsy: A review. *Seizure*. 2021;91:213-227. doi:10.1016/j.seizure.2021.06.028

16. Yazigi Solis M, De Salles Painelli V, Giannini Artioli G, Roschel H, Concepción Otaduy M, Gualano B. Brain creatine depletion in vegetarians? A cross-sectional^{1} H-magnetic resonance spectroscopy (^{1} H-MRS) study. *Br J Nutr*. 2014;111(7):1272-1274. doi:10.1017/S0007114513003802

17. Mercimek-Andrews S, Salomons GS. Creatine Deficiency Disorders. In: *GeneReviews*. University of Washington; 2022.

18. Wilson M, Andronesi O, Barker PB, et al. Methodological consensus on clinical proton MRS of the brain: Review and recommendations. *Magnetic Resonance in Med*. 2019;82(2):527-550. doi:10.1002/mrm.27742

19. Qian J, Herrera JJ, Narayana PA. Neuronal and Axonal Degeneration in Experimental Spinal Cord Injury: *In Vivo* Proton Magnetic Resonance Spectroscopy and Histology. *Journal of Neurotrauma*. 2010;27(3):599-610. doi:10.1089/neu.2009.1145

20. Wyss PO, Richter JK, Zweers P, et al. Glutathione in the Pons Is Associated With Clinical Status Improvements in Subacute Spinal Cord Injury. *Invest Radiol*. 2023;58(2):131-138. doi:10.1097/RLI.0000000000000905

21. Richter JK, Vallesi V, Zölch N, et al. Metabolic profile of complete spinal cord injury in pons and cerebellum: A 3T 1H MRS study. *Sci Rep*. 2023;13(1):7245. doi:10.1038/s41598-023-34326-1

22. Faul F, Erdfelder E, Lang AG, Buchner A. G*Power 3: A flexible statistical power analysis program for the social, behavioral, and biomedical sciences. *Behavior Research Methods*. 2007;39(2):175-191. doi:10.3758/BF03193146

23. Diener E, Emmons RA, Larsen RJ, Griffin S. The satisfaction with life scale. *Journal of Personality Assessment*. 1985;49(1):71-75.

24. Correll DJ. Chapter 22 - The Measurement of Pain: Objectifying the Subjective. In: *Pain Management*. Second Edition. ; 2011:191-201.

25. Snaith RP. The hospital anxiety and depression scale. *Health and Quality of Life Outcomes*. Published online 2003:1-4.

26. Kirshblum SC, Waring W, Biering-Sorensen F, et al. Reference for the 2011 revision of the international standards for neurological classification of spinal cord injury. *The Journal of Spinal Cord Medicine*. 2011;34(6):547-554. doi:10.1179/107902611X13186000420242

27. Itzkovich M, Gelernter I, Biering-Sorensen F, et al. The Spinal Cord Independence Measure (SCIM) version III: Reliability and validity in a multi-center. *Disability and Rehabilitation*. 2007;29(24):1926-1933. doi:https://doi.org/10.1080/09638280601046302

28. Pedrosa De Barros N, McKinley R, Knecht U, Wiest R, Slotboom J. Automatic quality control in clinical 1H MRSI of brain cancer. *NMR in Biomedicine*. 2016;29(5):563-575. doi:10.1002/nbm.3470

29. Slotboom J, Boesch C, Kreis R. Versatile frequency domain fitting using time domain models and prior knowledge. *Magnetic Resonance in Med*. 1998;39(6):899-911. doi:10.1002/mrm.1910390607

30. Stefan D, Cesare FD, Andrasescu A, et al. Quantitation of magnetic resonance spectroscopy signals: the jMRUI software package. *Meas Sci Technol*. 2009;20(10):104035. doi:10.1088/0957-0233/20/10/104035

31. Frossard J, Renaud O. Permutation Tests for Regression, ANOVA, and Comparison of Signals: The **permuco** Package. *J Stat Soft*. 2021;99(15):1-32. doi:10.18637/jss.v099.i15

32. Winkler AM, Ridgway GR, Webster MA, Smith SM, Nichols TE. Permutation inference for the general linear model. *NeuroImage*. 2014;92:381-397. doi:10.1016/j.neuroimage.2014.01.060

33. Hodges JL, Lehmann EL. Estimates of Location Based on Rank Tests. *The Annals of Mathematical Statistics*. 1963;34(2):598-611. doi:10.1214/aoms/1177704172

34. Lakens D. Calculating and reporting effect sizes to facilitate cumulative science: a practical primer for t-tests and ANOVAs. *Front Psychol*. 2013;4:1-12. doi:10.3389/fpsyg.2013.00863

35. Schober P, Boer C, Schwarte LA. Correlation Coefficients: Appropriate Use and Interpretation. *Anesthesia & Analgesia*. 2018;126(5):1763-1768. doi:10.1213/ANE.0000000000002864

36. Moffett J, Ross B, Arun P, Madhavarao C, Namboodiri A. N-Acetylaspartate in the CNS: From neurodiagnostics to neurobiology. *Progress in Neurobiology*. 2007;81(2):89-131. doi:10.1016/j.pneurobio.2006.12.003

37. Rae CD. A Guide to the Metabolic Pathways and Function of Metabolites Observed in Human Brain 1H Magnetic Resonance Spectra. *Neurochem Res*. 2014;39(1):1-36. doi:10.1007/s11064-013-1199-5

38. Demartini B, Gambini O, Uggetti C, et al. Limbic neurochemical changes in patients with functional motor symptoms. *Neurology*. 2019;93(1):e52-e58. doi:10.1212/WNL.0000000000007717

39. Charney M, Foster S, Shukla V, et al. Neurometabolic alterations in children and adolescents with functional neurological disorder. *NeuroImage: Clinical*. 2024;41:103557. doi:10.1016/j.nicl.2023.103557

40. Freund P, Curt A, Friston K, Thompson A. Tracking Changes following Spinal Cord Injury: Insights from Neuroimaging. *Neuroscientist*. 2013;19(2):116-128. doi:10.1177/1073858412449192

41. Wyss PO, Huber E, Curt A, Kollias S, Freund P, Henning A. MR Spectroscopy of the Cervical Spinal Cord in Chronic Spinal Cord Injury. *Radiology*. 2019;291(1):131-138. doi:10.1148/radiol.2018181037

42. Liu JY, Li YJ, Cong XY, et al. Association between brain N-acetylaspartate levels and sensory and motor dysfunction in patients who have spinal cord injury with spasticity: an observational case-control study. *Neural Regen Res*. 2023;18(3):582. doi:10.4103/1673-5374.350216

43. Widerström-Noga E, Pattany PM, Cruz-Almeida Y, et al. Metabolite concentrations in the anterior cingulate cortex predict high neuropathic pain impact after spinal cord injury. *Pain*. 2013;154(2):204-212. doi:10.1016/j.pain.2012.07.022

44. Barbiellini Amidei C, Salmaso L, Bellio S, Saia M. Epidemiology of traumatic spinal cord injury: a large population-based study. *Spinal Cord*. 2022;60(9):812-819. doi:10.1038/s41393-022-00795-w

45. Finkelstein SA, Diamond C, Carson A, Stone J. Incidence and prevalence of functional neurological disorder: a systematic review. *J Neurol Neurosurg Psychiatry*. Published online December 11, 2024:jnnp-2024-334767. doi:10.1136/jnnp-2024-334767

46. Öz G, Deelchand DK, Wijnen JP, et al. Advanced single voxel^{1} H magnetic resonance spectroscopy techniques in humans: Experts' consensus recommendations. *NMR in Biomedicine*. 2021;34(5):e4236. doi:10.1002/nbm.4236

47. Garwood M, DelaBarre L. The Return of the Frequency Sweep: Designing Adiabatic Pulses for Contemporary NMR. *Journal of Magnetic Resonance*. 2001;153(2):155-177. doi:10.1006/jmre.2001.2340

48. Slotboom J, Mehlkopf AF, Bovée WMMJ. The Effects of Frequency-Selective RF Pulses on J-Coupled Spin-1/2 Systems. *Journal of Magnetic Resonance*. Published online 1994:38-50.

Supplementary material

Quality control and tissue composition checks

Supplementary figure 1. Anterior cingulate cortex and representative spectra.

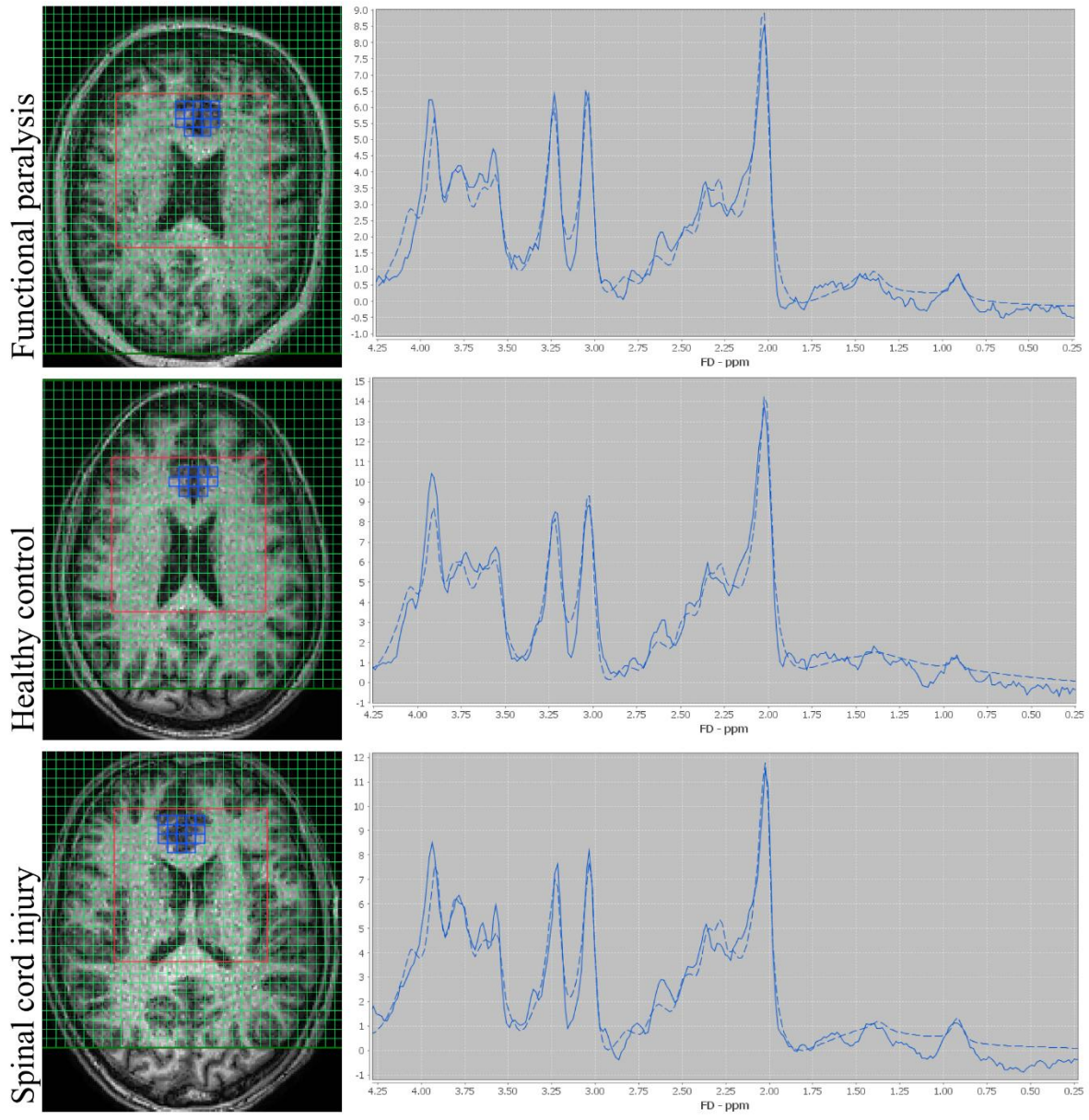

Note: On the left: MRSI planning for a representative participant of each group. The red square denotes the excited volume of interest, and blue squares highlight the analyzed voxels. Spectra correspond to the marked voxels.

On the right: Frequency-domain (FD) spectra from the selected region of interest (ROI), showing key metabolite peaks (total N-acetyl-aspartate [tNAA]: 2.01 parts per million [ppm],

total creatine [tCr]: 3.03 ppm and 3.94 ppm, total choline [tCho]: 3.21 ppm, myo-inositol [mI]: 3.56 ppm, glutamate + glumatine [Glx]: 2.1–2.5 ppm). The dashed line represents the fitted model.

Supplementary figure 2. Left insula and representative spectra.

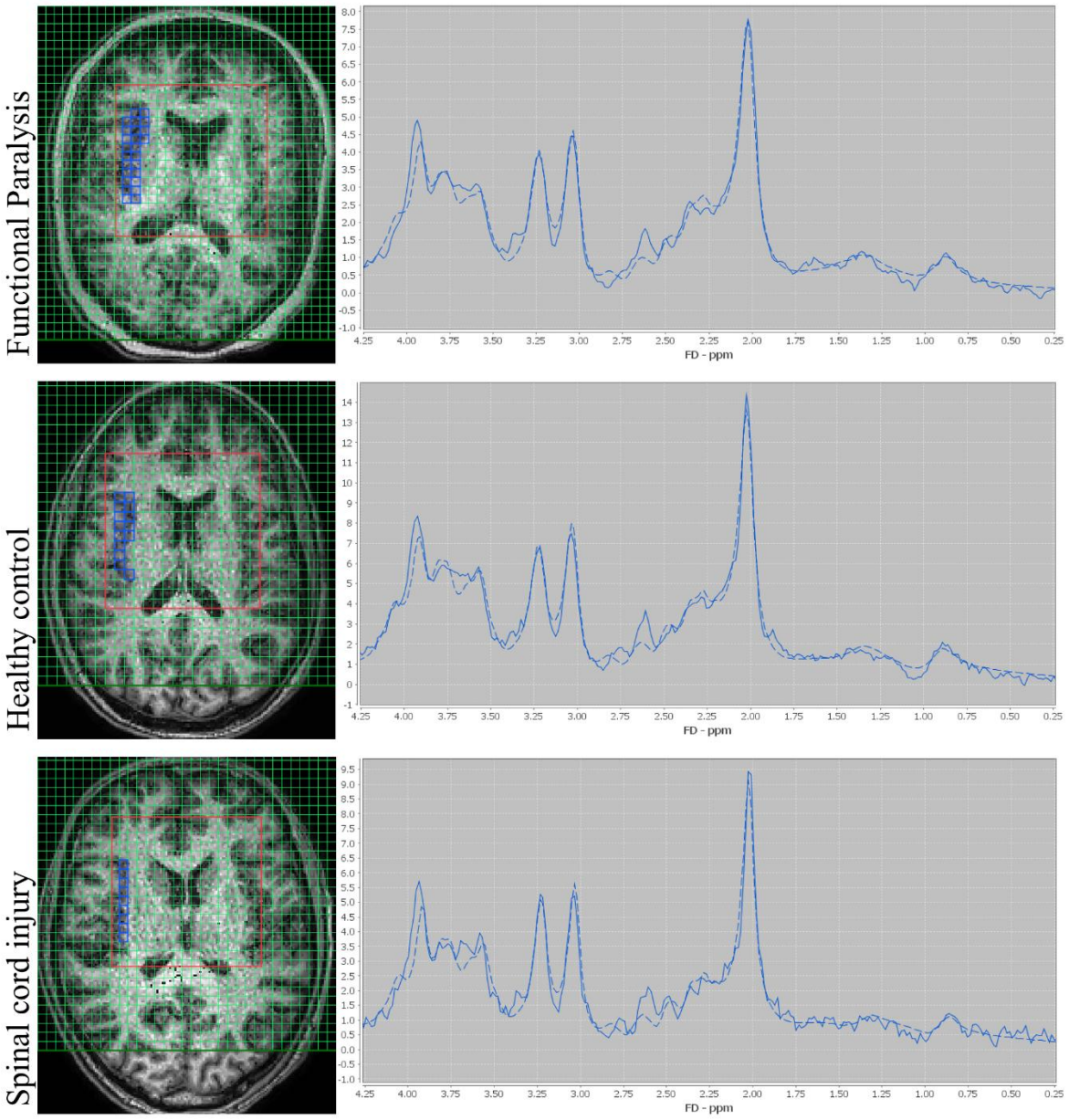

Note: On the left: MRSI planning for a representative participant of each group. The red square denotes the excited volume of interest, and blue squares highlight the analyzed voxels. Spectra correspond to the marked voxels.

On the right: Frequency-domain (FD) spectra from the selected region of interest (ROI), showing key metabolite peaks (total N-acetyl-aspartate [tNAA]: 2.01 parts per million [ppm], total creatine [tCr]: 3.03 ppm and 3.94 ppm, total choline [tCho]: 3.21 ppm, myo-inositol [mI]: 3.56 ppm, glutamate + glumatine [Glx]: 2.1–2.5 ppm). The dashed line represents the fitted model.

Supplementary figure 3. Right insula and representative spectra.

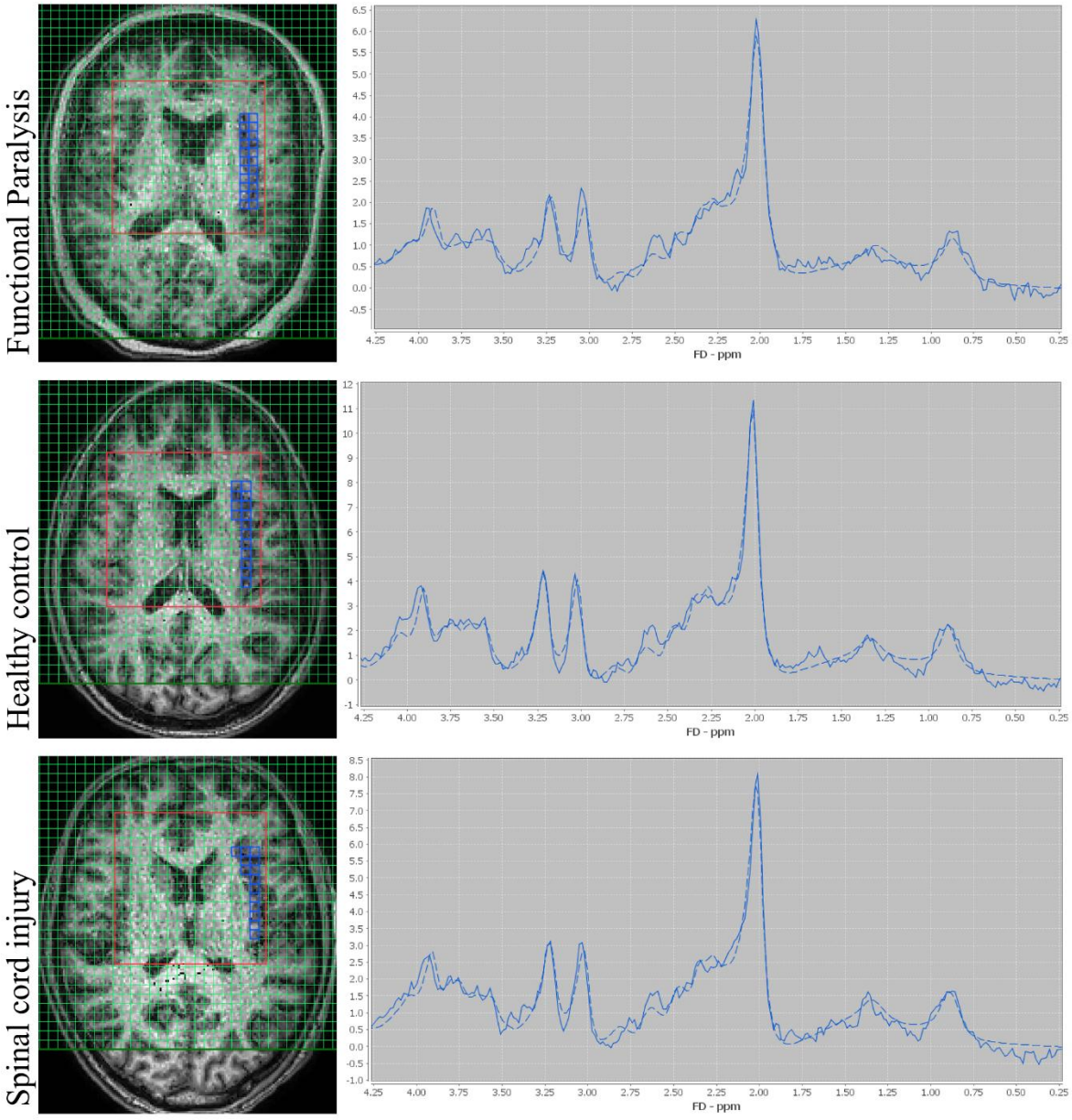

Note: On the left: MRSI planning for a representative participant of each group. The red square denotes the excited volume of interest, and blue squares highlight the analyzed voxels. Spectra correspond to the marked voxels.

On the right: Frequency-domain (FD) spectra from the selected region of interest (ROI), showing key metabolite peaks (total N-acetyl-aspartate [tNAA]: 2.01 parts per million [ppm], total creatine [tCr]: 3.03 ppm and 3.94 ppm, total choline [tCho]: 3.21 ppm, myo-inositol [mI]: 3.56 ppm, glutamate + glumatine [Glx]: 2.1–2.5 ppm). The dashed line represents the fitted model.

Supplementary Table 1.

	FP vs HC	FP vs SCI	SCI vs HC
Gray matter volume			
t-value	-0.41	-0.24	-0.15
p-value	0.68	0.813	0.881
White matter volume			
t-value	-0.84	-0.18	-0.63
p-value	0.406	0.858	0.53
Cerebrospinal fluid			
t-value	0.42	0.01	0.4
p-value	0.676	0.988	0.693

Note. Whole-brain gray matter, white matter, and cerebrospinal fluid volumes were compared between groups, controlling for age and sex. Statistical significance was assessed at two-tailed $p < 0.05$. No statistically significant group differences were observed.

Abbreviations: FP, functional paralysis group; HC, healthy controls; SCI, spinal cord injury group.

Supplementary Table 2.

	FP	HC	SCI
Anterior cingulate cortex			

Signal-to-noise ratio	31.91 ± 5.41	30.23 ± 5.19	36.58 ± 4.05
Linewidth	12.06	11.22	11.32
Left insula			
Signal-to-noise ratio	25.83 ± 6.38	27.75 ± 6.7	29.05 ± 6.54
Linewidth	15.22	10.77	10.97
Right insula			
Signal-to-noise ratio	15.56 ± 3.88	15.84 ± 3.6	19.72 ± 4.85
Linewidth	11.75	12.67	10.59

Note. Data were acquired from five randomly selected participants per group. The signal-to-noise ratio was calculated as the mean amplitude of the creatine peak divided by the standard deviation of noise. The linewidth was measured as the full-width at half-maximum (FWHM) of the creatine peak , converted from ppm to Hz using the scanner's Larmor frequency.

Abbreviations: FP, functional paralysis group; HC, healthy controls; SCI, spinal cord injury group.

Sensitivity Analyses

Supplementary Table 3.

Tested Relationship	Group	Controlled for	ρ	p-value
tNAA/tCr (ACC) ~ Motor strength	SCI	sex	0.56	0.01
tNAA/tCr (ACC) ~ Motor strength	SCI	sex + age	0.56	0.01
tNAA/tCr (ACC) ~ Motor strength	SCI	sex + TSS	0.52	0.03
tNAA/tCr (ACC) ~ Motor strength	SCI	sex + NRS	0.56	0.02
tNAA/tCr (ACC) ~ Motor strength	SCI	sex + HADS-D	0.56	0.02
tNAA/tCr (ACC) ~ Motor strength	SCI	sex + HADS-A	0.54	0.02

Abbreviations: Total N-acetyl-aspartate/total creatine, tNAA/tCr; anterior cingulate cortex, ACC; spinal cord injury, SCI; time since symptoms, TSS, numeric rating scale, NRS;

hospital anxiety and depression scale – depression, HADS-D; hospital anxiety and depression scale – anxiety, HADS-A.

Note: Sensitivity analyses testing the robustness of the association between tNAA/tCr in the ACC and motor strength score in the SCI group (n = 20). The primary association (adjusted for sex) remained significant ($\rho = 0.56$, $p = 0.01$) after additional adjustment for age, time since symptoms, current pain intensity (NRS), and depression/anxiety symptoms, supporting the stability of this finding. All correlations used partial Spearman's method.

3. Discussion

The aim of this thesis was to characterise the effects of paralysis on the brain in individuals with spinal cord injury (SCI) and functional paralysis (FP). To address this overarching aim, three studies were conducted. Study 1 aimed to characterise functional reorganisation processes in the brain during different phases following SCI. In studies 2 and 3, individuals with FP and SCI were compared in order to disentangle aberrant functional and metabolic correlates associated with the paralysis symptom itself from those arising from the underlying disorder. Study 2 focused on motor inhibition brain activity patterns, while study 3 investigated metabolic brain profiles in the bilateral anterior cingulate cortex and insula.

3.2 Summary of the findings

In study 1, resting-state functional connectivity (FC) and amplitude of low-frequency fluctuations (ALFF) — the latter reflecting spontaneous, slow oscillations in the blood-oxygen-level-dependent (BOLD) signal — were compared between individuals with subacute SCI (< 7 months), chronic SCI (> 24 months), and healthy controls (HC). Only those in the subacute SCI phase exhibited higher ALFF in the left thalamus ($p = 0.002$, false discovery rate (FDR) corrected, and Bonferroni corrected for the three-group comparison) compared with both the chronic SCI group and HC. The FC analysis revealed lower connectivity among the cerebellar vermis IX, the right superior frontal gyrus, and the right lateral occipital cortex in both SCI groups compared with HC ($p_{FDR} = 0.008$, and Bonferroni-post-hoc corrected). Individuals with chronic SCI also showed lower FC among the bilateral cerebellar Crus I and the left motor cortex compared with HC ($p_{FDR} = 0.001$, and Bonferroni post-hoc corrected), whereas a similar tendency in the subacute group was less pronounced. These findings support the hypothesis that functional reorganisation occurs after SCI and differs between the subacute and chronic phases. The higher ALFF of the left thalamus in subacute SCI aligns with the findings of Zhu et al. (2015), in which individuals examined within 30 days post-injury showed higher spontaneous brain activity, which was negatively correlated with the motor score. The thalamus is a key node of many afferent sensory pathways: it receives excitatory inputs from the cerebellum and is interconnected with pyramidal neurons in the cerebral cortex (Shine et al., 2023). These results indicate that disruption to afferent and efferent pathways after SCI goes through an adaptive process, whereby connectivity among motor-associated regions is reduced in the chronic phase.

Study 2, which investigated the task-based functional magnetic resonance imaging (fMRI) during motor inhibition, showed that individuals with FP and SCI exhibited higher FC between the right precentral gyrus and the left insula compared to HC ($p = 0.02$, family-wise error corrected, and Bonferroni post-hoc corrected for the three-group comparison). This increased FC was negatively associated with performance in the motor inhibition task ($\rho = -0.31$). Moreover, performance rates ($p = 0.115$) and response times ($p = 0.258$) in the motor inhibition task were intact in individuals with FP, comparable to those with SCI and HC, contrary to the initial hypothesis.

The dissociation between altered FC in inhibitory networks and intact behavioural performance in the inhibition task suggests these network changes in FP and SCI may reflect compensatory processes rather than dysfunction. This finding did not align with the results reported in other phenotypes of FND (Hamouda et al., 2021; van Wouwe et al., 2020; Voon et al., 2013) or in the same phenotype (Cojan et al., 2009; Hammond-Tooke et al., 2018) and indicates intact motor-inhibitory control in FP, unrelated to the disorder. A meta-analysis on neurocognitive performance in FND found inconsistent results depending on FND phenotype (Millman et al., 2025).

In functional neurological disorder (FND), there is a growing body of evidence that different symptom phenotypes show different functional networks in the brain: Mueller et al. (2022) found activation pattern differences between the negative motor symptom phenotype of FND (e.g. functional weakness) versus the positive motor symptom phenotype (e.g. functional tremor). This was also shown in different subtypes of functional dystonia (Piramide et al., 2022). Our FP vs SCI comparisons echo this principle by showing similar motor inhibition network alterations in both paralysis groups compared to HC. Although in the field of FND, it was often interpreted as an FND trait, this thesis provides evidence that this might simply be a symptom-related trait. A meta-analysis on neuroimaging found that activation of the insula was present in a wide range of psychiatric disorders suggesting its non-specificity (Nord et al., 2021).

The heterogeneity of neuroimaging findings in FND may stem from the fact that such studies often capture only the phenotypic manifestations of symptoms rather than their underlying mechanisms. As Bartl et al. (2020) note, many FND studies are often underpowered and in general fMRI is not useful on an individual basis; consequently, no single mechanism has been definitively established in FND.

Study 2 supports the idea that paralysis itself, as a motor symptom, alters brain connectivity. If immobility rather than lesion aetiology drives these changes, we would expect them to normalise when movement returns. Duggal et al. (2010) demonstrated that in spinal cord compression, the motor cortex over-activates to compensate for impairment, while the sensory cortex under-activates, likely due to disrupted sensory input. Using fMRI before and after surgical decompression, they found increased activation volume in the motor cortex post-surgery and partial restoration of sensory cortex activation. Before decompression surgery, regional homogeneity (local BOLD synchrony) in the sensorimotor cortex was reduced and normalised after surgery (Tan et al., 2015). This indicates that functional alterations in SCI and FP might only depict the persisting symptom at the current moment of the study perspective. Nonetheless, in these cases of spinal cord compression, the pathology differs yet still shows how sensorimotor networks rebound when movement is restored.

In study 3, the metabolic profile measured with proton magnetic resonance spectroscopy (^{1}H-MRS) showed normal metabolite ratios in the bilateral insula in individuals with FP, whereas the bilateral anterior cingulate cortex (ACC) exhibited reduced total N-acetyl-aspartate to total creatine (tNAA/tCr) ratios in both FP (p_{adj} = 0.042) and SCI (p_{adj} = 0.042) compared to HC. A low tNAA/tCr ratio is considered a marker of reduced neuronal viability. In SCI, lower tNAA/tCr in the ACC correlated with reduced motor strength scores (ρ = 0.49), indicating that neuronal integrity in this region scales with motor function. In FP, however, tNAA/tCr reductions were unrelated to motor strength (ρ = 0.07), suggesting a threshold-like dysfunction rather than a graded relationship. These are key regions associated with aberrant functional activation patterns in FP (Boeckle et al., 2016; Waugh et al., 2023; Weber et al., 2022), and these findings were contrary to the initial assumptions.

This work demonstrates that SCI not only affects the spine and the resulting functional symptoms but also brain activity patterns, which are already apparent in the subacute phase, as shown in study 1, in motor inhibitory networks, as shown in study 2, and neurochemical changes, as shown in study 3. In SCI — independent of phase (subacute or chronic) and also of completeness (incomplete vs. complete SCI) — grey matter atrophy has been reported in the anterior cingulate cortex, bilateral insular cortex as well as the bilateral orbitofrontal cortex and right superior temporal gyrus (Chen et al., 2017). Since tNAA is a marker of neuronal viability, this atrophy in that region might explain the lower levels of tNAA/tCr. Microstructural alterations such as lower fractional anisotropy, higher mean diffusivity and radial diffusivity were also reported in the cingulate gyrus in SCI, indicating

integrity loss in this region (Guo et al., 2019). The metabolic findings from study 3 further support the presence of biochemical alterations in the anterior cingulate cortex in SCI.

By contrast, in FP, the absence of a correlation between tNAA/tCr and motor strength argues against spinally mediated neuronal loss as the cause of the metabolic change. Instead, we suggest that the reduction may arise from dysfunctional higher-order networks involved in motor control, potentially reflecting a shared consequence of paralysis that is independent of aetiology.

3.3 Limitations and outlook

In addition to the study-specific limitations discussed earlier, several broader limitations should be acknowledged. Although study 1 compared two independent groups of individuals with SCI at different phases, its observational design means that between-group differences can only suggest temporal changes rather than prove them. A longitudinal design with paired samples would be required for causal inference. Nevertheless, these findings strongly support the need for future longitudinal studies to validate the observed effects. The recovery after an SCI is highly variable and difficult to predict. Knowing that the entire motor pathway including its connectivity and metabolic profile, is altered after SCI, might give the opportunity to further investigate whether there are correlates of good and poor recovery.

Studies 1 and 2 examined only FC, meaning they identified synchronised BOLD signals across hub regions — but not their directional origins or targets. To determine causal interactions, an effective-connectivity analysis would be required. However, effective connectivity analyses typically rely on predefined networks, often derived from prior FC studies that have replicated these patterns across multiple experiments. In this context, studies 1 and 2 fulfil their purpose by establishing foundational FC relationships for future causal investigations.

It must be emphasised that all fMRI studies share a fundamental limitation: the precise neurobiological meaning of BOLD signals remains incompletely understood (see Chapter 1.4.1). To truly unravel disorder mechanisms, a multimodal approach combining complementary techniques may be necessary to disentangle the brain's complex functional architecture and establish external validity.

Study 3 focused on a priori-selected regions of interest, the bilateral anterior cingulate and insular cortices, and specific metabolite types. Other brain regions may also show metabolic alterations that were not captured. Future studies could combine whole-brain MRS (targeting GABA, glucose, and other neurochemicals) with deuterated-glucose metabolic imaging, which can uniquely capture short-term metabolic fluxes via deuterated Glx production. Such approaches would offer a dynamic perspective on FP-related biochemical dysfunction. This initial broad approach in Study 3 provides an important foundation for such future work.

Across all three studies, we implemented strict inclusion criteria to ensure sample homogeneity, which, while methodologically rigorous, introduces important limitations. In study 1, we exclusively examined individuals with complete SCI to maximise clinical comparability by reducing variability in neurological impairment. While this approach strengthens internal validity for detecting consistent reorganisation patterns, it necessarily limits generalisability to incomplete SCI cases. This precision/generalisability trade-off reflects a fundamental tension in clinical neuroscience research between mechanistic clarity and clinical representativeness. Studies 2 and 3 included only chronic-phase FP cases to examine a stabilised manifestation of the disorder. While this increases comparability between participants, it means our findings may not extend to acute FP or other FND subtypes. The strict inclusion criteria also limited our sample sizes. Nevertheless, we found consistent effects despite these constraints, and all key results include effect sizes. Future studies with broader inclusion criteria could help establish the generalisability of these findings.

3.4 Conclusion

Study 1 indicates that, in the subacute phase of SCI, spontaneous brain activity is elevated, and that in the chronic SCI cohort large-scale resting-state FC remains altered, suggesting that early reorganisation persists into the long term. Study 2 reveals preserved motor inhibition in FP, yet shows an associated network alteration in both FP and SCI groups, likely a secondary adaptation to chronic motor dysfunction rather than its primary cause. Study 3 identified reduced tNAA/tCr, a marker of reduced neuronal viability, in the anterior cingulate cortex of both FP and SCI compared to HC. While paralysis, as a negative motor symptom, alters brain connectivity in both FP and SCI, the metabolic profile offers

subtle differentiation between the two: in SCI, neuronal dysfunction scales with motor impairment, whereas in FP it may reflect a threshold-like disruption within neural circuits for which gross structural damage has not yet been identified. This refines the ‘software vs. hardware’ analogy in FP: the motor dysfunction (‘software bug’) may involve dynamic biochemical dysregulation (‘faulty code execution’) within the system. Understanding why this biochemical dysregulation occurs, and how it contributes to symptom persistence, will be a critical focus for future research.

4. References

Aguilar, J., Humanes-Valera, D., Alonso-Calvino, E., Yague, J. G., Moxon, K. A., Oliviero, A., & Foffani, G. (2010). Spinal Cord Injury Immediately Changes the State of the Brain. *Journal of Neuroscience*, *30*(22), 7528–7537. https://doi.org/10.1523/JNEUROSCI.0379-10.2010

Ahuja, C. S., Nori, S., Tetreault, L., Wilson, J., Kwon, B., Harrop, J., Choi, D., & Fehlings, M. G. (2017). Traumatic Spinal Cord Injury—Repair and Regeneration. *Neurosurgery*, *80*(3S), S9–S22. https://doi.org/10.1093/neuros/nyw080

Alizadeh, A., Dyck, S. M., & Karimi-Abdolrezaee, S. (2019). Traumatic Spinal Cord Injury: An Overview of Pathophysiology, Models and Acute Injury Mechanisms. *Frontiers in Neurology*, *10*, 282. https://doi.org/10.3389/fneur.2019.00282

Anjum, A., Yazid, M. D., Daud, M. F., Idris, J., Ng, A. M. H., Naicker, A. S., Htwe, O., Ismail, R., Kumar, R. K. A., & Lokanathan, Y. (2020). Spinal Cord Injury: Pathophysiology, Multimolecular Interactions, and Underlying Recovery Mechanisms. *Int. J. Mol. Sci.*, 35.

Arnold, J. T., Dharmatti, S. S., & Packard, M. E. (1951). Chemical Effects on Nuclear Induction Signals from Organic Compounds. *The Journal of Chemical Physics*, *19*(4), 507–507. https://doi.org/10.1063/1.1748264

Atmaca, M., Aydin, A., Tezcan, E., Poyraz, A. K., & Kara, B. (2006). Volumetric investigation of brain regions in patients with conversion disorder. *Progress in Neuro-Psychopharmacology and Biological Psychiatry*, *30*(4), 708–713. https://doi.org/10.1016/j.pnpbp.2006.01.011

Aybek, S., Nicholson, T. R. J., Draganski, B., Daly, E., Murphy, D. G., David, A. S., & Kanaan, R. A. (2014). Grey matter changes in motor conversion disorder. *Journal of Neurology, Neurosurgery & Psychiatry*, *85*(2), 236–238. https://doi.org/10.1136/jnnp-2012-304158

Barbiellini Amidei, C., Salmaso, L., Bellio, S., & Saia, M. (2022). Epidemiology of traumatic spinal cord injury: A large population-based study. *Spinal Cord*, *60*(9), 812–819. https://doi.org/10.1038/s41393-022-00795-w

Bartl, M., Kewitsch, R., Hallett, M., Tegenthoff, M., & Paulus, W. (2020). Diagnosis and therapy of functional tremor a systematic review illustrated by a case report. *Neurological Research and Practice*, *2*(1), 35. https://doi.org/10.1186/s42466-020-00073-1

Bègue, I., Adams, C., Stone, J., & Perez, D. L. (2019). Structural alterations in functional neurological disorder and related conditions: A software and hardware problem? *NeuroImage: Clinical*, *22*, 101798. https://doi.org/10.1016/j.nicl.2019.101798

Benussi, A., Premi, E., Cantoni, V., Compostella, S., Magni, E., Gilberti, N., Vergani, V., Delrio, I., Gamba, M., Spezi, R., Costa, A., Tinazzi, M., Padovani, A., Borroni, B., & Magoni, M. (2020). Cortical inhibitory imbalance in functional paralysis. *Frontiers in Human Neuroscience*, *14*, 1–7. https://doi.org/10.3389/fnhum.2020.00153

Biswal, B., Zerrin Yetkin, F., Haughton, V. M., & Hyde, J. S. (1995). Functional connectivity in the motor cortex of resting human brain using echo-planar mri. *Magnetic Resonance in Medicine*, *34*(4), 537–541. https://doi.org/10.1002/mrm.1910340409

Blanco, S. R., Mitra, S., Howard, C. J., & Sumich, A. L. (2023). Psychological trauma, mood and social isolation do not explain elevated dissociation in functional neurological disorder (FND). *Personality and Individual Differences*, *202*, 111952. https://doi.org/10.1016/j.paid.2022.111952

Boeckle, M., Liegl, G., Jank, R., & Pieh, C. (2016). Neural correlates of conversion disorder: Overview and meta-analysis of neuroimaging studies on motor conversion disorder. *BMC Psychiatry*, *16*(1), 195. https://doi.org/10.1186/s12888-016-0890-x

Boulant, N., Mauconduit, F., Gras, V., Amadon, A., Le Ster, C., Luong, M., Massire, A., Pallier, C., Sabatier, L., Bottlaender, M., Vignaud, A., & Le Bihan, D. (2024). In vivo imaging of the human brain with the Iseult 11.7-T MRI scanner. *Nature Methods*, *21*(11), 2013–2016. https://doi.org/10.1038/s41592-024-02472-7

Broersma, M., Koops, E. A., Vroomen, P. C., Van der Hoeven, J. H., Aleman, A., Leenders, K. L., Maurits, N. M., & van Beilen, M. (2015). Can repetitive transcranial magnetic stimulation increase muscle strength in functional neurological paresis? A proof-of-principle study. *European Journal of Neurology*, *22*(5), 866–873. https://doi.org/10.1111/ene.12684

Calma, A. D., Heffernan, J., Farrell, N., Gelauff, J., O'Connell, N., Perez, D. L., Perriman, D., Smyth, L., Stone, J., & Lueck, C. J. (2023). The Impact of Depression, Anxiety and Personality Disorders on the Outcome of Patients with Functional Limb Weakness – Individual Patient Data Meta-Analysis. *Journal of Psychosomatic Research*, *175*, 111513. https://doi.org/10.1016/j.jpsychores.2023.111513

Carson, A., & Lehn, A. (2016). Epidemiology. In *Handbook of Clinical Neurology* (Vol. 139, pp. 47–60). Elsevier. https://doi.org/10.1016/B978-0-12-801772-2.00005-9

Chamberlain, J. D., Deriaz, O., Hund-Georgiadis, M., Meier, S., Scheel-Sailer, A., Schubert, M., Stucki, G., & Brinkhof, M. W. (2015). Epidemiology and contemporary risk profile of traumatic spinal cord injury in Switzerland. *Injury Epidemiology*, *2*(1), 28. https://doi.org/10.1186/s40621-015-0061-4

Chen, Q., Zheng, W., Chen, X., Wan, L., Qin, W., Qi, Z., Chen, N., & Li, K. (2017). Brain Gray Matter Atrophy after Spinal Cord Injury: A Voxel-Based Morphometry Study. *Frontiers in Human Neuroscience*, *11*, 211. https://doi.org/10.3389/fnhum.2017.00211

Cojan, Y., Waber, L., Carruzzo, A., & Vuilleumier, P. (2009). Motor inhibition in hysterical conversion paralysis. *NeuroImage*, *47*(3), 1026–1037. https://doi.org/10.1016/j.neuroimage.2009.05.023

Conejero, I., Collombier, L., Lopez-Castroman, J., Mura, T., Alonso, S., Olié, E., Boudousq, V., Boulet, F., Arquizan, C., Boulet, C., Wacongne, A., Heitz, C., Castelli, C., Mouchabac, S., Courtet, P., Abbar, M., & Thouvenot, E. (2022). Association between brain metabolism and clinical course of motor functional neurological disorders. *Brain*, *145*(9), 3264–3273. https://doi.org/10.1093/brain/awac146

Coupland, N. J., Ogilvie, C. J., Hegadoren, K. M., Seres, P., Hanstock, C. C., & Allen, P. S. (2005). Decreased Prefrontal Myo-Inositol in Major Depressive Disorder. *Biological Psychiatry*, *57*(12), 1526–1534. https://doi.org/10.1016/j.biopsych.2005.02.027

Crowe, M. J., Bresnahan, J. C., Shuman, S. L., Masters, J. N., & Beattie, M. S. (1997). Apoptosis and delayed degeneration after spinal cord injury in rats and monkeys. *Nature Medicine*, *3*(1), 73–76.

De Stefano, N., & Filippi, M. (2007). MR Spectroscopy in Multiple Sclerosis. *Journal of Neuroimaging*, *17*(s1). https://doi.org/10.1111/j.1552-6569.2007.00134.x

Demartini, B., Gambini, O., Uggetti, C., Cariati, M., Cadioli, M., Goeta, D., Marceglia, S., Ferrucci, R., & Priori, A. (2019). Limbic neurochemical changes in patients with functional motor symptoms. *Neurology*, *93*(1), e52–e58. https://doi.org/10.1212/WNL.0000000000007717

Demartini, B., Nisticò, V., Benayoun, C., Cigognini, A. C., Ferrucci, R., Vezzoli, A., Dellanoce, C., Gambini, O., Priori, A., & Mrakic-Sposta, S. (2023). Glutamatergic dysfunction, neuroplasticity, and redox status in the peripheral blood of patients with motor conversion disorders (functional movement disorders): A first step towards potential biomarkers discovery. *Translational Psychiatry*, *13*(1), 212. https://doi.org/10.1038/s41398-023-02500-8

DeVivo, M. J. (2012). Epidemiology of traumatic spinal cord injury: Trends and future implications. *Spinal Cord*, *50*(5), 365–372. https://doi.org/10.1038/sc.2011.178

Diez, I., Williams, B., Kubicki, M. R., Makris, N., & Perez, D. L. (2021). Reduced limbic microstructural integrity in functional neurological disorder. *Psychological Medicine*, *51*(3), 485–493. https://doi.org/10.1017/S0033291719003386

Duggal, N., Rabin, D., Bartha, R., Barry, R. L., Gati, J. S., Kowalczyk, I., & Fink, M. (2010). Brain reorganization in patients with spinal cord compression evaluated using fMRI. *Neurology*, *74*(13), 1048–1054. https://doi.org/10.1212/WNL.0b013e3181d6b0ea

Erschbamer, M., Öberg, J., Westman, E., Sitnikov, R., Olson, L., & Spenger, C. (2011). 1H-MRS in spinal cord injury: Acute and chronic metabolite alterations in rat brain and lumbar spinal cord: 1H-MRS in spinal cord injury. *European Journal of Neuroscience*, *33*(4), 678–688. https://doi.org/10.1111/j.1460-9568.2010.07562.x

Espay, A. J., Aybek, S., Carson, A., Edwards, M. J., Goldstein, L. H., Hallett, M., LaFaver, K., LaFrance, W. C., Lang, A. E., Nicholson, T., Nielsen, G., Reuber, M., Voon, V., Stone, J., & Morgante, F. (2018). Current Concepts in Diagnosis and Treatment of Functional Neurological Disorders. *JAMA Neurology*, *75*(9), 1132. https://doi.org/10.1001/jamaneurol.2018.1264

Fang, Z., Li, Y., Xie, L., Cheng, M., Ma, J., Li, T., Li, X., & Jiang, L. (2021). Characteristics and outcomes of children with dissociative (conversion) disorders in western China: A retrospective study. *BMC Psychiatry*, *21*(1), 31. https://doi.org/10.1186/s12888-021-03045-0

Fawcett, J. W., Curt, A., Steeves, J. D., Coleman, W. P., Tuszynski, M. H., Lammertse, D., Bartlett, P. F., Blight, A. R., Dietz, V., Ditunno, J., Dobkin, B. H., Havton, L. A., Ellaway, P. H., Fehlings, M. G., Privat, A., Grossman, R., Guest, J. D., Kleitman, N., Nakamura, M., … Short, D. (2007). Guidelines for the conduct of clinical trials for spinal cord injury as developed by the ICCP panel: Spontaneous recovery after spinal cord injury and statistical power needed for therapeutic clinical trials. *Spinal Cord*, *45*(3), 190–205. https://doi.org/10.1038/sj.sc.3102007

Finkelstein, S. A., Diamond, C., Carson, A., & Stone, J. (2024). Incidence and prevalence of functional neurological disorder: A systematic review. *Journal of Neurology, Neurosurgery & Psychiatry*, jnnp-2024-334767. https://doi.org/10.1136/jnnp-2024-334767

Fox, M. D., & Greicius, M. (2010). Clinical applications of resting state functional connectivity. *Frontiers in Systems Neuroscience*, *4*(19), 1–13. https://doi.org/10.3389/fnsys.2010.00019

Freund, P., Weiskopf, N., Ward, N. S., Hutton, C., Gall, A., Ciccarelli, O., Craggs, M., Friston, K., & Thompson, A. J. (2011). Disability, atrophy and cortical reorganization following spinal cord injury. *Brain*, *134*(6), 1610–1622. https://doi.org/10.1093/brain/awr093

Friston, K. J. (2011). Functional and Effective Connectivity: A Review. *Brain Connectivity*, *1*(1), 13–36. https://doi.org/10.1089/brain.2011.0008

Gazzaniga, M. S., Ivry, R. B., & Mangun, G. R. (2014). *Cognitive Neuroscience. The biology of the mind.* (4th ed.). W. W. Norton & Company.

Gelauff, J. M., Carson, A., Ludwig, L., Tijssen, M. A. J., & Stone, J. (2019). The prognosis of functional limb weakness: A 14-year case-control study. *Brain*, *142*(7), 2137–2148. https://doi.org/10.1093/brain/awz138

Ghosh, A., Haiss, F., Sydekum, E., Schneider, R., Gullo, M., Wyss, M. T., Mueggler, T., Baltes, C., Rudin, M., Weber, B., & Schwab, M. E. (2010). Rewiring of hindlimb corticospinal neurons after spinal cord injury. *Nature Neuroscience*, *13*(1), 97–104. https://doi.org/10.1038/nn.2448

Grover, V. P. B., Tognarelli, J. M., Crossey, M. M. E., Cox, I. J., Taylor-Robinson, S. D., & McPhail, M. J. W. (2015). Magnetic Resonance Imaging: Principles and Techniques: Lessons for Clinicians. *Journal of Clinical and Experimental Hepatology*, *5*(3), 246–255. https://doi.org/10.1016/j.jceh.2015.08.001

Guo, L., Tian, J., & Du, H. (2017). Mitochondrial Dysfunction and Synaptic Transmission Failure in Alzheimer's Disease. *Journal of Alzheimer's Disease*, *57*(4), 1071–1086. https://doi.org/10.3233/JAD-160702

Guo, Y., Gao, F., Liu, Y., Guo, H., Yu, W., Chen, Z., Yang, M., Du, L., Yang, D., & Li, J. (2019). White Matter Microstructure Alterations in Patients With Spinal Cord Injury Assessed by Diffusion Tensor Imaging. *Frontiers in Human Neuroscience*, *13*, 11. https://doi.org/10.3389/fnhum.2019.00011

Hahn, E. L., & Maxwell, D. E. (1952). Spin Echo Measurements of Nuclear Spin Coupling in Molecules. *Physical Review*, *88*(5), 1070–1084. https://doi.org/10.1103/PhysRev.88.1070

Hallett, M., Aybek, S., Dworetzky, B. A., McWhirter, L., Staab, J. P., & Stone, J. (2022). Functional neurological disorder: New subtypes and shared mechanisms. *The Lancet Neurology*, *21*(6), 537–550. https://doi.org/10.1016/S1474-4422(21)00422-1

Hammond-Tooke, G. D., Grajeda, F. T., Macrorie, H., & Franz, E. A. (2018). Response inhibition in patients with functional neurological symptom disorder. *Journal of Clinical Neuroscience*, *56*, 38–43. https://doi.org/10.1016/j.jocn.2018.08.005

Hamouda, K., Senf-Beckenbach, P. A., Gerhardt, C., Irorutola, F., Rose, M., & Hinkelmann, K. (2021). Executive Functions and Attention in Patients With Psychogenic Nonepileptic Seizures Compared With Healthy Controls: A Cross-Sectional Study. *Psychosomatic Medicine*, *83*(8), 880–886.

Haris, M., Cai, K., Singh, A., Hariharan, H., & Reddy, R. (2011). In vivo mapping of brain myo-inositol. *NeuroImage*, *54*(3), 2079–2085. https://doi.org/10.1016/j.neuroimage.2010.10.017

Hassa, T., de Jel, E., Tuescher, O., Schmidt, R., & Schoenfeld, M. A. (2016). Functional networks of motor inhibition in conversion disorder patients and feigning subjects. *NeuroImage: Clinical*, *11*, 719–727. https://doi.org/10.1016/j.nicl.2016.05.009

Hernando, K. A., Szaflarski, J. P., Ver Hoef, L. W., Lee, S., & Allendorfer, J. B. (2015). Uncinate fasciculus connectivity in patients with psychogenic nonepileptic seizures: A preliminary diffusion tensor tractography study. *Epilepsy & Behavior*, *45*, 68–73. https://doi.org/10.1016/j.yebeh.2015.02.022

Hill, C. E., Beattie, M. S., & Bresnahan, J. C. (2001). Degeneration and Sprouting of Identified Descending Supraspinal Axons after Contusive Spinal Cord Injury in the Rat. *Experimental Neurology*, *171*(1), 153–169. https://doi.org/10.1006/exnr.2001.7734

Horská, A., & Barker, P. B. (2010). Imaging of Brain Tumors: MR Spectroscopy and Metabolic Imaging. *Neuroimaging Clinics of North America*, *20*(3), 293–310. https://doi.org/10.1016/j.nic.2010.04.003

Hou, J., Xiang, Z., Yan, R., Zhao, M., Wu, Y., Zhong, J., Guo, L., Li, H., Wang, J., Wu, J., Sun, T., & Liu, H. (2016). Motor recovery at 6 months after admission is related to structural and functional reorganization of the spine and brain in patients with spinal cord injury: Neural Correlates of Motor Recovery After SCI. *Human Brain Mapping*, *37*(6), 2195–2209. https://doi.org/10.1002/hbm.23163

Hou, J.-M., Yan, R.-B., Xiang, Z.-M., Zhang, H., Liu, J., Wu, Y.-T., Zhao, M., Pan, Q.-Y., Song, L.-H., Zhang, W., Li, H.-T., Liu, H.-L., & Sun, T.-S. (2014). Brain

sensorimotor system atrophy during the early stage of spinal cord injury in humans. *Neuroscience*, *266*, 208–215. https://doi.org/10.1016/j.neuroscience.2014.02.013

Huettel, S. A. (2012). Event-related fMRI in cognition. *NeuroImage*, *62*(2), 1152–1156. https://doi.org/10.1016/j.neuroimage.2011.08.113

Huys, A.-C. M. L., Bhatia, K. P., Edwards, M. J., & Haggard, P. (2020). The Flip Side of Distractibility—Executive Dysfunction in Functional Movement Disorders. *Frontiers in Neurology*, *11*, 969. https://doi.org/10.3389/fneur.2020.00969

Iadecola, C. (2017). The Neurovascular Unit Coming of Age: A Journey through Neurovascular Coupling in Health and Disease. *Neuron*, *96*(1), 17–42. https://doi.org/10.1016/j.neuron.2017.07.030

Karlsson, A.-K. (2006). Overview: Autonomic dysfunction in spinal cord injury: clinical presentation of symptoms and signs. In *Progress in Brain Research* (Vol. 152, pp. 1–8). Elsevier. https://doi.org/10.1016/S0079-6123(05)52034-X

Kowalczyk, I., Duggal, N., & Bartha, R. (2012). Proton magnetic resonance spectroscopy of the motor cortex in cervical myelopathy. *Brain*, *135*(2), 461–468. https://doi.org/10.1093/brain/awr328

Kozlowska, K., Griffiths, K. R., Foster, S. L., Linton, J., Williams, L. M., & Korgaonkar, M. S. (2017). Grey matter abnormalities in children and adolescents with functional neurological symptom disorder. *NeuroImage: Clinical*, *15*, 306–314. https://doi.org/10.1016/j.nicl.2017.04.028

Kozlowska, K., Palmer, D. M., Brown, K. J., Scher, S., Chudleigh, C., Davies, F., & Williams, L. M. (2015). Conversion disorder in children and adolescents: A disorder of cognitive control. *Journal of Neuropsychology*, *9*(1), 87–108. https://doi.org/10.1111/jnp.12037

Lee, S., Allendorfer, J. B., Gaston, T. E., Griffis, J. C., Hernando, K. A., Knowlton, R. C., Szaflarski, J. P., & Ver Hoef, L. W. (2015). White matter diffusion abnormalities in patients with psychogenic non-epileptic seizures. *Brain Research*, *1620*, 169–176. https://doi.org/10.1016/j.brainres.2015.04.050

Li, S., & Stys, P. K. (2000). Mechanisms of Ionotropic Glutamate Receptor-Mediated Excitotoxicity in Isolated Spinal Cord White Matter. *The Journal of Neuroscience*, *20*(3), 1190–1198. https://doi.org/10.1523/JNEUROSCI.20-03-01190.2000

Lidstone, S. C., Costa-Parke, M., Robinson, E. J., Ercoli, T., & Stone, J. (2022). Functional movement disorder gender, age and phenotype study: A systematic review and

individual patient meta-analysis of 4905 cases. *Journal of Neurology, Neurosurgery & Psychiatry*, *93*(6), 609–616. https://doi.org/10.1136/jnnp-2021-328462

Logothetis, N. K. (2012). *What We Can and What We Can't Do with fMRI*. 8.

Logothetis, N. K., & Wandell, B. A. (2004). Interpreting the BOLD Signal. *Annual Review of Physiology*, *66*(1), 735–769. https://doi.org/10.1146/annurev.physiol.66.082602.092845

Ludwig, L., Pasman, J. A., Nicholson, T., Aybek, S., David, A. S., Tuck, S., Kanaan, R. A., Roelofs, K., Carson, A., & Stone, J. (2018). Stressful life events and maltreatment in conversion (functional neurological) disorder: Systematic review and meta-analysis of case-control studies. *The Lancet Psychiatry*, *5*(4), 307–320. https://doi.org/10.1016/S2215-0366(18)30051-8

McIntosh, R. D., McWhirter, L., Ludwig, L., Carson, A., & Stone, J. (2017). Attention and sensation in functional motor disorder. *Neuropsychologia*, *106*, 207–215. http://dx.doi.org/10.1016/j.neuropsychologia.2017.09.031

Mercimek-Andrews, S., & Salomons, G. S. (2022). Creatine Deficiency Disorders. In *GeneReviews*. University of Washington.

Millman, L. S. M., Williams, I. A., Jungilligens, J., & Pick, S. (2025). Neurocognitive performance in functional neurological disorder: A systematic review and meta-analysis. *European Journal of Neurology*, *32*(1), e16386. https://doi.org/10.1111/ene.16386

Moffett, J., Ross, B., Arun, P., Madhavarao, C., & Namboodiri, A. (2007). N-Acetylaspartate in the CNS: From neurodiagnostics to neurobiology. *Progress in Neurobiology*, *81*(2), 89–131. https://doi.org/10.1016/j.pneurobio.2006.12.003

Moon, H. S., Jiang, H., Vo, T. T., Jung, W. B., Vazquez, A. L., & Kim, S.-G. (2021). Contribution of Excitatory and Inhibitory Neuronal Activity to BOLD fMRI. *Cerebral Cortex*, *31*(9), 4053–4067. https://doi.org/10.1093/cercor/bhab068

Mueller, K., Růžička, F., Slovák, M., Forejtová, Z., Dušek, P., Dušek, P., Jech, R., & Serranová, T. (2022). Symptom-severity-related brain connectivity alterations in functional movement disorders. *NeuroImage: Clinical*, *34*, 102981. https://doi.org/10.1016/j.nicl.2022.102981

Murray, M. E., Przybelski, S. A., Lesnick, T. G., Liesinger, A. M., Spychalla, A., Zhang, B., Gunter, J. L., Parisi, J. E., Boeve, B. F., Knopman, D. S., Petersen, R. C., Jack, C. R., Dickson, D. W., & Kantarci, K. (2014). Early Alzheimer's Disease Neuropathology

Detected by Proton MR Spectroscopy. *The Journal of Neuroscience*, *34*(49), 16247–16255. https://doi.org/10.1523/JNEUROSCI.2027-14.2014

Nicholson, T. R., Aybek, S., Kempton, M. J., Daly, E. M., Murphy, D. G., David, A. S., & Kanaan, R. A. (2014). A structural MRI study of motor conversion disorder: Evidence of reduction in thalamic volume. *Journal of Neurology, Neurosurgery & Psychiatry*, *85*(2), 227–229. https://doi.org/10.1136/jnnp-2013-305012

Nord, C. L., Lawson, R. P., & Dalgleish, T. (2021). Disrupted Dorsal Mid-Insula Activation During Interoception Across Psychiatric Disorders. *American Journal of Psychiatry*, *178*(8), 761–770. https://doi.org/10.1176/appi.ajp.2020.20091340

O'Connell, N., Nicholson, T. R., Wessely, S., & David, A. S. (2020). Characteristics of patients with motor functional neurological disorder in a large UK mental health service: A case–control study. *Psychological Medicine*, *50*(3), 446–455. https://doi.org/10.1017/S0033291719000266

Ogawa, S., Lee, T. M., Kay, A. R., & Tank, D. W. (1990). Brain magnetic resonance imaging with contrast dependent on blood oxygenation. *Proceedings of the National Academy of Sciences*, *87*(24), 9868–9872. https://doi.org/10.1073/pnas.87.24.9868

Pan, Y., Dou, W., Wang, Y., Luo, H., Ge, Y., Yan, S., Xu, Q., Tu, Y., Xiao, Y., Wu, Q., Zheng, Z., & Zhao, H. (2017). Non-concomitant cortical structural and functional alterations in sensorimotor areas following incomplete spinal cord injury. *Neural Regeneration Research*, *12*(12), 2059. https://doi.org/10.4103/1673-5374.221165

Pedrosa De Barros, N., McKinley, R., Knecht, U., Wiest, R., & Slotboom, J. (2016). Automatic quality control in clinical 1H MRSI of brain cancer. *NMR in Biomedicine*, *29*(5), 563–575. https://doi.org/10.1002/nbm.3470

Perez, D. L., Williams, B., Matin, N., LaFrance, W. C., Costumero-Ramos, V., Fricchione, G. L., Sepulcre, J., Keshavan, M. S., & Dickerson, B. C. (2017). Corticolimbic structural alterations linked to health status and trait anxiety in functional neurological disorder. *Journal of Neurology, Neurosurgery & Psychiatry*, *88*(12), 1052–1059. https://doi.org/10.1136/jnnp-2017-316359

Piramide, N., Sarasso, E., Tomic, A., Canu, E., Petrovic, I. N., Svetel, M., Basaia, S., Dragasevic Miskovic, N., Kostic, V. S., Filippi, M., & Agosta, F. (2022). Functional MRI connectivity of the primary motor cortex in functional dystonia patients. *Journal of Neurology*, *269*(6), 2961–2971. https://doi.org/10.1007/s00415-021-10879-x

Proctor, W. G., & Yu, F. C. (1950). The Dependence of a Nuclear Magnetic Resonance Frequency upon Chemical Compound. *Physical Review*, *77*(5), 717–717. https://doi.org/10.1103/PhysRev.77.717

Qian, J., Herrera, J. J., & Narayana, P. A. (2010). Neuronal and Axonal Degeneration in Experimental Spinal Cord Injury: *In Vivo* Proton Magnetic Resonance Spectroscopy and Histology. *Journal of Neurotrauma*, *27*(3), 599–610. https://doi.org/10.1089/neu.2009.1145

Rae, C. D. (2014). A Guide to the Metabolic Pathways and Function of Metabolites Observed in Human Brain 1H Magnetic Resonance Spectra. *Neurochemical Research*, *39*(1), 1–36. https://doi.org/10.1007/s11064-013-1199-5

Ramadan, S., Lin, A., & Stanwell, P. (2013). Glutamate and glutamine: A review of *in vivo* MRS in the human brain. *NMR in Biomedicine*, *26*(12), 1630–1646. https://doi.org/10.1002/nbm.3045

Roelofs, K., van Galen, G. P., Eling, P., Keijsers, G. P. J., & Hoogduin, C. A. L. (2003). Endogenous and Exogenous Attention in Patients with Conversion Paresis. *Cognitive Neuropsychology*, *20*(8), 733–745. https://doi.org/10.1080/02643290342000069

Sarlo, G. L., & Holton, K. F. (2021). Brain concentrations of glutamate and GABA in human epilepsy: A review. *Seizure*, *91*, 213–227. https://doi.org/10.1016/j.seizure.2021.06.028

Schanne, F. A. X., Kane, A. B., Young, E. E., & Farber, J. L. (1979). Calcium Dependence of Toxic Cell Death: A Final Common Pathway. *Science*, *206*, 700–702.

Shannon, R. J., Van Der Heide, S., Carter, E. L., Jalloh, I., Menon, D. K., Hutchinson, P. J., & Carpenter, K. L. H. (2016). Extracellular *N* -Acetylaspartate in Human Traumatic Brain Injury. *Journal of Neurotrauma*, *33*(4), 319–329. https://doi.org/10.1089/neu.2015.3950

Shine, J. M., Lewis, L. D., Garrett, D. D., & Hwang, K. (2023). The impact of the human thalamus on brain-wide information processing. *Nature Reviews Neuroscience*, *24*(7), 416–430. https://doi.org/10.1038/s41583-023-00701-0

Silva, N. A., Sousa, N., Reis, R. L., & Salgado, A. J. (2014). From basics to clinical: A comprehensive review on spinal cord injury. *Progress in Neurobiology*, *114*, 25–57. https://doi.org/10.1016/j.pneurobio.2013.11.002

Slotboom, J., Boesch, C., & Kreis, R. (1998). Versatile frequency domain fitting using time domain models and prior knowledge. *Magnetic Resonance in Medicine*, *39*(6), 899–911. https://doi.org/10.1002/mrm.1910390607

Sojka, P., Diez, I., Bareš, M., & Perez, D. L. (2021). Individual differences in interoceptive accuracy and prediction error in motor functional neurological disorders: A DTI study. *Human Brain Mapping*, *42*(5), 1434–1445. https://doi.org/10.1002/hbm.25304

Sojka, P., Slovák, M., Věchetová, G., Jech, R., Perez, D. L., & Serranová, T. (2022). Bridging structural and functional biomarkers in functional movement disorder using network mapping. *Brain and Behavior*, *12*(5). https://doi.org/10.1002/brb3.2576

Stins, J. F., Kempe, C. (Lianne) A., Hagenaars, M. A., Beek, P. J., & Roelofs, K. (2015). Attention and postural control in patients with conversion paresis. *Journal of Psychosomatic Research*, *78*(3), 249–254. https://doi.org/10.1016/j.jpsychores.2014.11.009

Stone, J., & Aybek, S. (2016). Functional limb weakness and paralysis. In *Handbook of Clinical Neurology* (Vol. 139, pp. 213–228). Elsevier. https://doi.org/10.1016/B978-0-12-801772-2.00018-7

Stone, J., Hallett, M., Carson, A., Bergen, D., & Shakir, R. (2014). Functional disorders in the Neurology section of ICD-11: A landmark opportunity. *Neurology*, *83*(24), 2299–2301. https://doi.org/10.1212/WNL.0000000000001063

Stone, J., Warlow, C., Deary, I., & Sharpe, M. (2020). Predisposing Risk Factors for Functional Limb Weakness: A Case-Control Study. *The Journal of Neuropsychiatry and Clinical Neurosciences*, *32*(1), 50–57. https://doi.org/10.1176/appi.neuropsych.19050109

Stone, J., Warlow, C., & Sharpe, M. (2010). The symptom of functional weakness: A controlled study of 107 patients. *Brain*, *133*(5), 1537–1551. https://doi.org/10.1093/brain/awq068

Stone, J., Warlow, C., & Sharpe, M. (2012). Functional weakness: Clues to mechanism from the nature of onset. *Journal of Neurology, Neurosurgery & Psychiatry*, *83*(1), 67–69. https://doi.org/10.1136/jnnp-2011-300125

Tan, Y., Zhou, F., Wu, L., Liu, Z., Zeng, X., Gong, H., & He, L. (2015). Alteration of Regional Homogeneity within the Sensorimotor Network after Spinal Cord Decompression in Cervical Spondylotic Myelopathy: A Resting-State fMRI Study. *BioMed Research International*, *2015*, 1–6. https://doi.org/10.1155/2015/647958

Tomic, A., Agosta, F., Sarasso, E., Petrovic, I., Basaia, S., Pesic, D., Kostic, M., Fontana, A., Kostic, V. S., & Filippi, M. (2020). Are there two different forms of functional dystonia? A multimodal brain structural MRI study. *Molecular Psychiatry*, *25*(12), 3350–3359. https://doi.org/10.1038/s41380-018-0222-2

van Wouwe, N. C., Mohanty, D., Lingaiah, A., Wylie, S. A., & LaFaver, K. (2020). Impaired Action Control in Patients With Functional Movement Disorders. *The Journal of Neuropsychiatry and Clinical Neurosciences*, *32*(1), 73–78. https://doi.org/10.1176/appi.neuropsych.19030076

Voon, V., Ekanayake, V., Wiggs, E., Kranick, S., Ameli, R., Harrison, N. A., & Hallett, M. (2013). Response inhibition in motor conversion disorder: Response Inhibition in Conversion Disorder. *Movement Disorders*, *28*(5), 612–618. https://doi.org/10.1002/mds.25435

Voon, V., Gallea, C., Hattori, N., Bruno, M., Ekanayake, V., & Hallett, M. (2010). *The involuntary nature of conversion disorder*. 7.

Vroege, L., Koppenol, I., Kop, W. J., Riem, M. M. E., & Feltz-Cornelis, C. M. (2021). Neurocognitive functioning in patients with conversion disorder/functional neurological disorder. *Journal of Neuropsychology*, *15*(1), 69–87. https://doi.org/10.1111/jnp.12206

Wang, W., Xie, W., Zhang, Q., Liu, L., Liu, J., Zhou, S., Shi, J., Chen, J., & Ning, B. (2019). Reorganization of the brain in spinal cord injury: A meta-analysis of functional MRI studies. *Neuroradiology*, *61*(11), 1309–1318. https://doi.org/10.1007/s00234-019-02272-3

Waters, R. L., Adkins, R. H., & Yakura, J. S. (1991). Definition of complete spinal cord injury. *Spinal Cord*, *29*(9), 573–581. https://doi.org/10.1038/sc.1991.85

Waugh, R. E., Parker, J. A., Hallett, M., & Horovitz, S. G. (2023). Classification of Functional Movement Disorders with Resting-State Functional Magnetic Resonance Imaging. *Brain Connectivity*, *13*(1), 4–14. https://doi.org/10.1089/brain.2022.0001

Weber, S., Heim, S., Richiardi, J., Van De Ville, D., Serranová, T., Jech, R., Marapin, R. S., Tijssen, M. A. J., & Aybek, S. (2022). Multi-centre classification of functional neurological disorders based on resting-state functional connectivity. *NeuroImage: Clinical*, *35*, 103090. https://doi.org/10.1016/j.nicl.2022.103090

West, K. L., Zuppichini, M. D., Turner, M. P., Sivakolundu, D. K., Zhao, Y., Abdelkarim, D., Spence, J. S., & Rypma, B. (2019). BOLD hemodynamic response function changes significantly with healthy aging. *NeuroImage*, *188*, 198–207. https://doi.org/10.1016/j.neuroimage.2018.12.012

Witiw, C. D., & Fehlings, M. G. (2015). Acute Spinal Cord Injury. *Journal of Spinal Disorders and Techniques*, *28*(6), 202–210.

Wyss, P. O., Huber, E., Curt, A., Kollias, S., Freund, P., & Henning, A. (2019). MR Spectroscopy of the Cervical Spinal Cord in Chronic Spinal Cord Injury. *Radiology*, *291*(1), 131–138. https://doi.org/10.1148/radiol.2018181037

Yazigi Solis, M., De Salles Painelli, V., Giannini Artioli, G., Roschel, H., Concepción Otaduy, M., & Gualano, B. (2014). Brain creatine depletion in vegetarians? A cross-sectional^{1} H-magnetic resonance spectroscopy (^{1} H-MRS) study. *British Journal of Nutrition*, *111*(7), 1272–1274. https://doi.org/10.1017/S0007114513003802

Yousaf, T., Dervenoulas, G., & Politis, M. (2018). Advances in MRI Methodology. In *International Review of Neurobiology* (Vol. 141, pp. 31–76). Elsevier. https://doi.org/10.1016/bs.irn.2018.08.008

Zheng, J., Zhang, Y., Zhao, B., Wang, N., Gao, T., & Zhang, L. (2025). Metabolic changes of thalamus assessed by 1H-MRS spectroscopy in patients of cervical spondylotic myelopathy following decompression surgery. *Frontiers in Neurology*, *15*, 1513896. https://doi.org/10.3389/fneur.2024.1513896

Zhu, L., Wu, G., Zhou, X., Li, J., Wen, Z., & Lin, F. (2015). Altered spontaneous brain activity in patients with acute spinal cord injury revealed by resting-state functional MRI. *PLOS ONE*, *10*(3), 1–11. https://doi.org/10.1371/journal.pone.0118816

Declaration of originality

Last name, first name: Vallesi, Vanessa

Matriculation number: 13-759-055

I hereby declare that this thesis represents my original work and that I have used no other sources except as noted by citations. All data, tables, figures and text citations which have been reproduced from any other source, including the internet, have been explicitly acknowledged as such. I am aware that in case of non-compliance, the Senate is entitled to withdraw the doctorate degree awarded to me on the basis of the present thesis, in accordance with the "Statut der Universität Bern (Universitätsstatut; UniSt)", Art. 69, of 7 June 2011.

Place, date

Signature